Swiss J Palaeontol (2013) 132:141–219
DOI 10.1007/s13358-013-0058-y

Smithian ammonoid faunas from Utah: implications for Early Triassic biostratigraphy, correlation and basinal paleogeography

Arnaud Brayard · Kevin G. Bylund · James F. Jenks · Daniel A. Stephen · Nicolas Olivier · Gilles Escarguel · Emmanuel Fara · Emmanuelle Vennin

Received: 14 March 2013 / Accepted: 4 July 2013 / Published online: 30 August 2013

Abstract Intensive sampling of the lower portion of the Thaynes and Moenkopi Groups (Lower Triassic) at separate localities within the Confusion Range, Pahvant Range, Mineral Mountains, Star Range, Kanarraville, Cedar City, Torrey and San Rafael Swell areas (mainly central and southern Utah, USA) leads to the recognition of a new key regional Smithian ammonoid succession. The new biostratigraphical sequence, which is more precise than the long-recognized *Meekoceras gracilitatis* and *Anasibirites kingianus* Zones, comprises twelve subdivisions, thus resulting in a sequence with much higher resolution that can be correlated not only with other western USA sites, but also with major worldwide localities as well. Middle and late Smithian faunas contain many taxa with wide geographic distribution, thus enabling long-distance correlation with faunal successions from other regions (e.g., British Columbia, Canadian Arctic, South China, Spiti and Oman). New assemblages from the lowermost beds are the least diversified and poorest preserved; they represent the earliest early/middle Smithian ammonoid faunas reported from the western North American basin. They highlight (a) the sudden Smithian advancement of the marine transgression within this epicontinental sea, (b) that this event is diachronous, and (c) that the paleotopography of the basin most likely was highly irregular. The newly obtained ammonoid succession also allows us to date and follow the transgression from the northern and central part of the basin to the southwesternmost and southeasternmost parts, which were reached during the late Smithian (*Anasibirites kingianus* beds). In addition, we briefly discuss the now-limited previous regional biozonation in the light of these new results. One new genus (*Minersvillites*) and nine new species (*Kashmirites utahensis*, *Kashmirites confusionensis*, *Kashmirites stepheni*, *?Xiaoqiaoceras americanum*, *Minersvillites farai*, *Inyoites beaverensis*, *Meekoceras olivieri*, *Meekoceras millardense*, *Vercherites undulatus*) are also described.

Keywords Ammonoids · Early Triassic · Smithian · Utah · Biostratigraphy · Paleogeography · New genus and species

A. Brayard (✉) · E. Fara · E. Vennin
UMR CNRS 6282 Biogéosciences, Université de Bourgogne,
6 Boulevard Gabriel, 21000 Dijon, France
e-mail: arnaud.brayard@u-bourgogne.fr

K. G. Bylund
140 South 700 East, Spanish Fork, UT 84660, USA

J. F. Jenks
1134 Johnson Ridge Lane, West Jordan, UT 84084, USA

D. A. Stephen
Department of Earth Science, Utah Valley University,
800 West University Parkway, Orem, UT 84058, USA

N. Olivier · G. Escarguel
Laboratoire de Géologie de Lyon: Terre, Planètes,
Environnement, UMR CNRS 5276, Université Claude Bernard
Lyon 1, 27-43 Boulevard du 11 novembre 1918,
69622 Villeurbanne Cedex, France

Introduction

The aftermath of the Permian–Triassic mass extinction is receiving more and more attention from the earth science community. However, biostratigraphically controlled paleontological data are often lacking and insufficient on a global scale to produce realistic models for the Early Triassic recovery. Significant progress at a large temporal and spatial scale is obtained using new databases grounded on primary data from the field and carefully revised taxonomy combined with recently published radiometric ages (e.g., Brayard et al. 2009c; Romano et al. 2013). Parallel to the global-scale approach, the pace of the recovery and underlying evolutionary mechanisms also need to be precisely studied on a more detailed regional scale. However, highly resolved temporal data remain rare for the Early Triassic. For instance, the taxonomic revision and detailed biostratigraphy of new ammonoid faunas from the Northern Indian Margin yield an unprecedented high resolution zonation that demonstrates surprisingly high evolutionary rates and thus confirms the explosive rediversification and high level of diversity attained by these cephalopods during the Smithian (Brayard et al. 2009c; Brühwiler et al. 2010a). Indeed, this time-interval is crucial since it records on a worldwide scale the main rediversification of several marine organisms only 1–2 myr after the mass extinction (e.g., Brayard et al. 2006, 2009c, 2011b; Orchard 2007), the reappearance of many Lazarus taxa among bivalves, gastropods and ammonoids (Brayard et al. 2007a; Kaim et al. 2010; Hautmann and Nützel 2005; Nützel 2005), and the return of some large-size taxa (Brayard et al. 2010, 2011a). Thus, an understanding of the mechanisms underlying the Early Triassic biotic recovery requires an accurate and robust Smithian regional biostratigraphical framework that may have worldwide correlation. Our recent field investigations of the Lower Triassic Thaynes and Moenkopi Groups in western, central and southern Utah have led to the recognition of several new Smithian ammonoid assemblages; they allow the construction of a new detailed biostratigraphical scheme for the low latitudes in eastern Panthalassa. In this paper, we mainly focus on the taxonomy, biostratigraphy and correlation of these new ammonoid assemblages. Paleo(bio)geographical and phylogenetic implications as well as correlation across latitudes and Panthalassa are also discussed.

Geological settings

The Sonoma Foreland Basin of western USA represents a unique key study area located at a near-equatorial position in eastern Panthalassa during the Early Triassic (Fig. 1). Smithian marine deposits are widely distributed within a large area covering Wyoming, Idaho, Utah and Nevada. These deposits generally contain abundant fossils, but a detailed regional biostratigraphical zonation has never been proposed for this substage (Silberling and Tozer 1968).

The alternating limestones and shales of the Lower Triassic Thaynes Group (sensu Lucas et al. 2007b) reflect deposition within the relatively shallow Sonoma Foreland Basin. Outcrops with different lithologies of these rocks can be widely seen from Idaho to Utah. These marine sedimentary deposits thin from the northwest to southeast across Utah, where they interfinger with the terrestrial sediments of the Moenkopi Group (sensu Lucas et al. 2007b). Deposits of the Thaynes Group roughly include both the Smithian and the Spathian substages. They are mostly renowned for mass occurrence or exceptional preservation of ammonoids (e.g., Brayard et al. 2009a; Gardner and Mapes 2000; Guex et al. 2010; Jenks 2007;

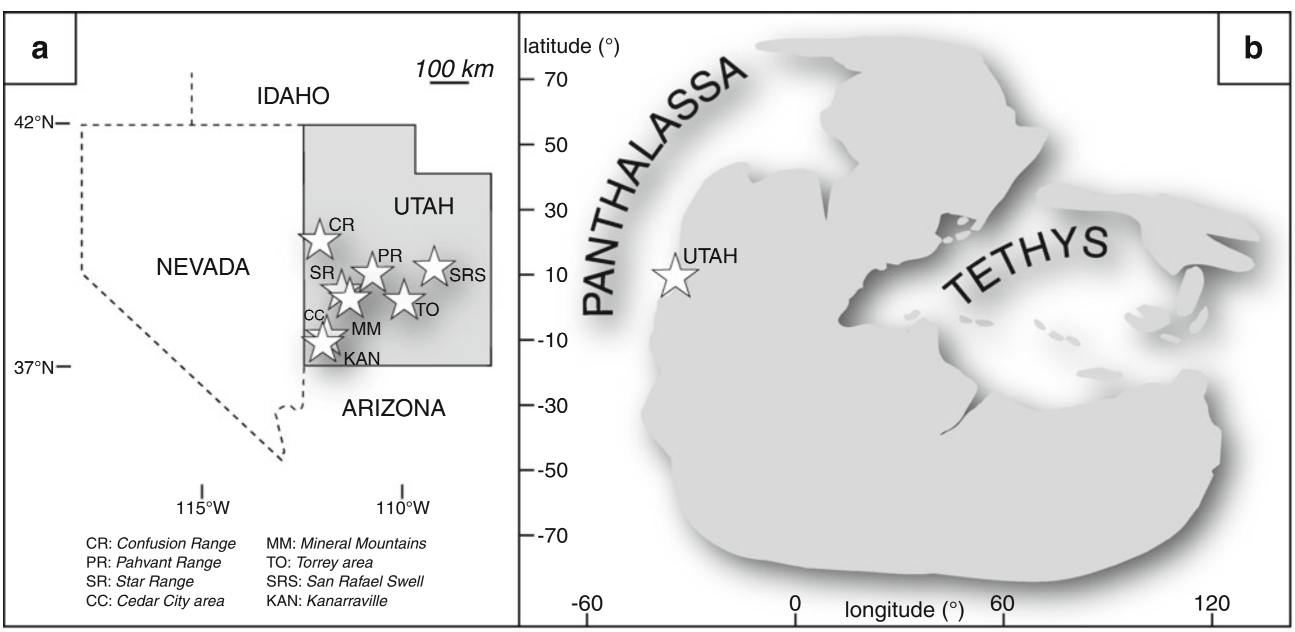

Fig. 1 Present-day (**a**) and Early Triassic (**b**) locations of the western USA basin and sampled sections in Utah

Jenks et al. 2010, 2013; Kummel and Steele 1962; Silberling and Tozer 1968; Stephen et al. 2010). In this work, we focus on Smithian sedimentary successions from western, central and southern Utah in the Confusion Range, Pahvant Range, Star Range, Mineral Mountains, Kanarraville, Cedar City, Torrey and San Rafael Swell areas (Fig. 1).

Some of these Lower Triassic exposures and their ammonoid faunas such as within the Confusion Range have already been described in a very general sense, but the Smithian and especially its lowermost part have never been detailed (Bacon 1948; Collinson et al. 1976; Guex et al. 2010; Hose and Repenning 1959; Newell 1948; Silberling and Tozer 1968). Accurate Smithian biostratigraphical data regarding the other localities are much scarcer and often diluted or repeated among different studies (Baetcke 1969; Blakey 1973, 1974, 1977, 1979; Crosby 1959; Davis 1983; Dean 1981; Gilluly and Reeside 1928; Hintze and Davis 2003; Lucas et al. 2007a, b; Nielson 1991; Smith et al. 1963; Stewart et al. 1972).

All sections were measured within the lower portion of the Thaynes or Moenkopi Groups and nearly all contain numerous fossiliferous beds (Figs. 2, 3, 4, 5, 6, 7, 8, 9, 10, 11, 12, 13). These sections are rather similar in their upper parts in terms of lithological succession although deposits are slightly diachronous, thus highlighting the southward transgression of the sea within the basin during the Smithian (e.g., Paull and Paull 1993). All sections are relatively thick, indicating high sedimentation rates, but thickness also varies considerably from section to section. This variation probably represents deposition of sediments on a complex paleo-relief formed during the Late Permian–earliest Triassic transition (Collinson et al. 1976; Dean 1981). Ammonoids were systematically collected bed by bed, and though generally poorly preserved and often not measurable in the lowermost Smithian beds, they are abundant in the upper beds of all measured sections. Not all studied sections are depicted here, but each illustrated section log corresponds to the best biostratigraphical succession of the region.

Classical regional Smithian biostratigraphy

The *Meekoceras gracilitatis* Zone

The most famous ammonoid beds of the Early Triassic and of the Thaynes Group are probably the *Meekoceras gracilitatis* Zone. This long-recognized zone, originally described from southeastern Idaho [Peale in White (1879)], is commonly used as a regional Smithian time-marker. It also represents the most diversified Smithian ammonoid fauna within the eastern Panthalassic low-paleolatitudes (Kummel and Steele 1962; Silberling and Tozer 1968; Smith 1932). In the USA, older fossiliferous Lower Triassic outcrops are rare (e.g., Candelaria and Dinwoody Formations) and often not well dated (Ware et al. 2011). Triassic deposits are also often considered to unconformably overlie Permian rocks with a major sedimentary hiatus (e.g., Hose and Repenning 1959). Within this scheme, the *M. gracilitatis* Zone is essential because it serves as one of the first, easily accessible macrofossil time-markers for the Early Triassic. However, this well-known index species displays a tabulate, relatively involute and compressed geometry that is frequent among Smithian ammonoids. A major problem, therefore, is to correctly identify true occurrences of *M. gracilitatis*. For instance, reports of several successive beds with *Meekoceras* sp. or *M. gracilitatis* throughout a thick outcrop are not rare (e.g., Crosby 1959; Davis 1983; Dean 1981, Hintze and Davis 2003), and these discrepancies must be clarified to obtain precise age calibration of the considered section.

Based on ammonoid faunas from California (e.g., Union Wash), Nevada (Phelan Ranch), SE Idaho and the work of Mathews (1929) in Utah, Smith (1932) proposed subdivisions for this regional biostratigraphical interval as follows in ascending order: the *Pseudosageceras* subzone, *Owenites* subzone and *Anasibirites* subzone. This biostratigraphical terminology was customarily accepted until the work of Kummel and Steele (1962), who suggested the use of the twofold subdivision consisting of the *M. gracilitatis* and *Anasibirites kingianus* Zones, in ascending order.

Recent biostratigraphical improvements

Despite a few studies of the *M. gracilitatis* Zone (Kummel and Steele 1962; Silberling and Tozer 1968), ammonoid workers have only recently suggested that this zone (a) represents only the middle/late Smithian; and (b) can be subdivided into supplementary different subzones and beds that have exact trans-Panthalassic correlatives (Brayard et al. 2009a; Jenks et al. 2010; Stephen et al. 2010). For instance, Jenks et al. (2010) recently highlighted that the *M. gracilitatis* Zone is essential for reasonably precise correlation between eastern and western Panthalassa (e.g., South China), and between low and high latitudes (British Columbia and the Canadian Arctic). The co-occurrence of several ammonoid genera on opposite sides of Panthalassa at that time indicates significant faunal exchange during the Smithian (Brayard et al. 2007b, 2009b; Jenks et al. 2010).

Brayard et al. (2009a) and Stephen et al. (2010) recently discussed cephalopod occurrences within the uppermost Smithian beds of the Confusion Range. They refined the previous local zonation proposed by Hose and Repenning (1959), and identified within the upper part of the *M. gracilitatis* Zone in ascending order, the *Inyoites oweni*

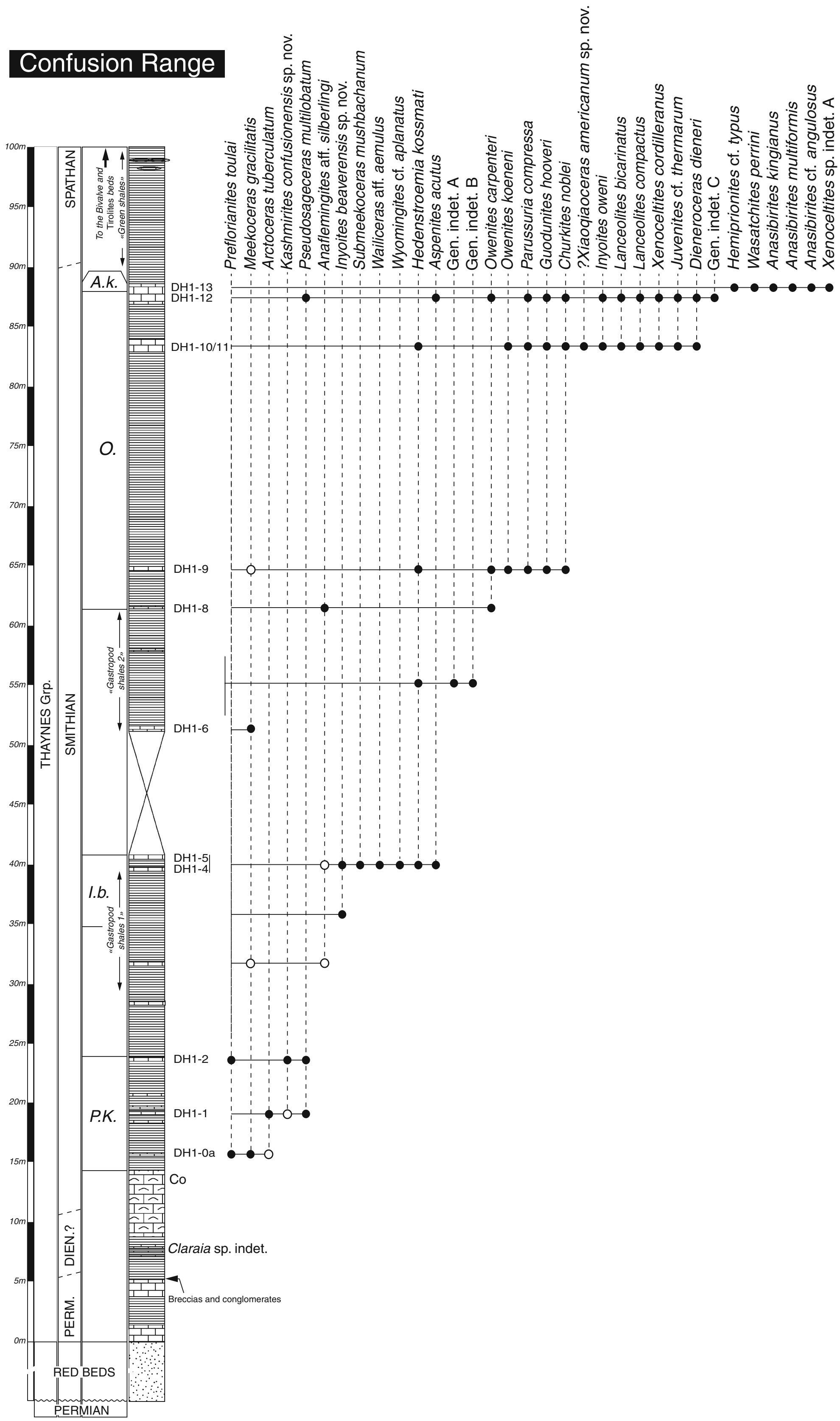
Confusion Range
Preflorianites toulai
Meekoceras gracilitatis
Arctoceras tuberculatum
Kashmirites confusionensis sp. nov.
Pseudosageceras multilobatum
Anaflemingites aff. silberlingi
Inyoites beaverensis sp. nov.
Submeekoceras mushbachanum
Wailiceras aff. aemulus
Wyomingites cf. aplanatus
Hedenstroemia kossmati
Aspenites acutus
Gen. indet. A
Gen. indet. B
Owenites carpenteri
Owenites koeneni
Parussuria compressa
Guodunites hooveri
Churkites noblei
?Xiaoqiaoceras americanum sp. nov.
Inyoites oweni
Lanceolites bicarinatus
Lanceolites compactus
Xenoceltites cordilleranus
Juvenites cf. thermarum
Dieneroceras dieneri
Gen. indet. C
Hemiprionites cf. typus
Wasatchites perrini
Anasibirites kingianus
Anasibirites multiformis
Anasibirites cf. angulosus
Xenoceltites sp. indet. A
100m
95m
90m
85m
80m
75m
70m
65m
60m
55m
50m
45m
40m
35m
30m
25m
20m
15m
10m
5m
0m
THAYNES Grp.
SPATHAN
SMITHIAN
DIEN.?
PERM.
RED BEDS
PERMIAN
To the Bivalve and Tirolites beds «Green shales»
A.k.
O.
«Gastropod shales 2»
I.b.
«Gastropod shales 1»
P.K.
DH1-13
DH1-12
DH1-10/11
DH1-9
DH1-8
DH1-6
DH1-5
DH1-4
DH1-2
DH1-1
DH1-0a
Co
Claraia sp. indet.
Breccias and conglomerates

◀ **Fig. 2** Distribution of ammonoid taxa in the Confusion Range section (CR in Fig. 1). *Open dots* indicate occurrences based only on fragmentary or poorly preserved material. *Perm.* Permian, *Dien.* Dienerian, *P.K. Preflorianites–Kashmirites* beds, *I.b. Inyoites beaverensis* sp. nov. beds, *O. Owenites* beds, *A.k. Anasibirites kingianus* beds, *Co* oldest Smithian conodont occurrence within the section

beds, and the *Anasibirites kingianus* beds. In particular, they reported characteristic occurrences of *A. kingianus*, *Wasatchites perrini* and *Xenoceltites* sp. at the top of the section (bed 13), and more diverse assemblages below (beds 9–12) including *I. oweni*, *Wyomingites arnoldi*, *Churkites noblei*, *Guodunites hooveri*, *Owenites koeneni*, *Pseudosageceras multilobatum, Aspenites acutus*, *Lanceolites bicarinatus*, *Juvenites septentrionalis*, ?*Kashmirites intermontanus*, an ussuriid, and an unidentified proptychitid. Based on the occurrence of *O. koeneni* and *I. oweni*, Brayard et al. (2009a) and Stephen et al. (2010) defined the late–middle Smithian *I. oweni* beds in the uppermost part of the *Owenites koeneni* subzone and also recognized that: (a) the uppermost part of the *M. gracilitatis* beds and *I. oweni* beds correlate with the *Owenites* beds (middle Smithian) of the Tethyan paleoequatorial zonation; and (b) the *I. oweni* beds correlate with the *Inyoites* horizon in South China (Brayard and Bucher 2008).

The initial in-depth study of the Confusion Range by Hose and Repenning (1959) did not report ammonoid faunas from the lowermost Smithian levels. Several additional beds with ammonoids are herein described that characterize the early (but not earliest) and middle Smithian. Griesbachian or Dienerian ammonoid faunas have not been discovered. However, marine late Griesbachian?/Dienerian deposits do occur a few meters above Late Permian beds as shown by the occurrence of the bivalve *Claraia* (Fig. 2, R. Hofmann ongoing work; see McRoberts 2010 for temporal distributions of Early Triassic bivalves). These beds were deposited on an inherited complex Permian topography as suggested by the presence of breccias, conglomerates and normal faults underlying the Lower Triassic deposits. This emersion and erosion phase is overlain by microbialites characterized by small stromatolitic structures. Younger ammonoid faunas of early Spathian age also occur within this area at Cowboy Pass, and were included in a recent revision by Guex et al. (2010).

This work also complements recent reports of the occurrence of the late Smithian *Anasibirites* fauna at several sites in southwestern and southeastern Utah (e.g., Lucas et al. 2007a, b). For instance, ammonoid assemblages from the Pahvant Range and Mineral Mountains described herein provide a significant geographic link between localities to the east and south and to the west and north. Interestingly, ammonoids typical of the middle Smithian *Meekoceras* fauna have usually been assumed to be absent in the correlative Timpoweap and Sinbad

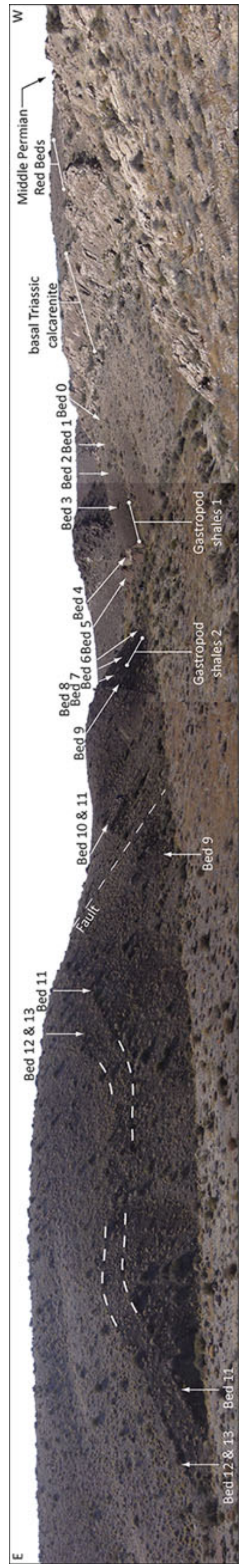

Fig. 3 Panorama of the main Confusion Range section showing ammonoid bed locations

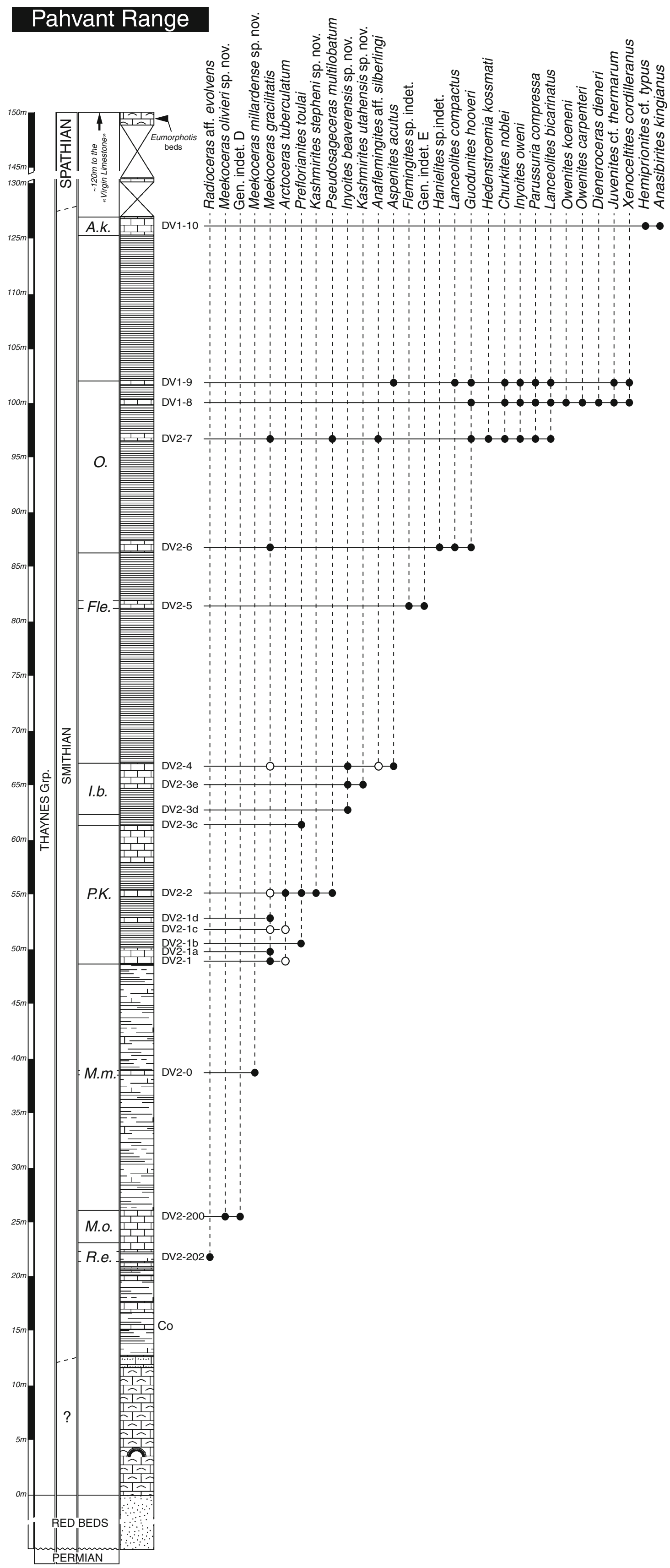

Fig. 4 Distribution of ammonoid taxa in the Pahvant Range section (PR in Fig. 1). *Open dots* indicate occurrence based only on fragmentary or poorly preserved material. Abbreviations as in Fig. 2. *Fle. Flemingites* sp. indet. bed, *M.m. Meekoceras millardense* sp. nov. bed, *M.o. Meekoceras olivieri* sp. nov. beds, *R.e. Radioceras* aff. *evolvens* beds

Fig. 5 Panorama showing the location of part of the lower ammonoid beds within the main Pahvant Range section

Limestone localities to the southwest and southeast, respectively. Therefore, the occurrence of the *Meekoceras* fauna in the Pahvant Range until now has been the farthest southeast that this fauna has been reported in Utah. However, we newly report herein the occurrence of several taxa of the *Meekoceras* fauna (*M. gracilitatis*, *Juvenites* aff. *spathi*, *Guodunites hooveri*, *Churkites noblei*, *Xenoceltites* sp. indet.) within the lower and middle units of the Sinbad Limestone in the Torrey area, indicating that near-maximum extent of the Smithian sea in the southeastern part of the basin was reached earlier than previously thought (middle Smithian instead of late Smithian).

New biostratigraphical subdivisions

We provide here for the first time a comprehensive distribution of ammonoid faunas throughout the Smithian of the Thaynes and Moenkopi Groups in Utah, thus expanding and refining previous biozonations. No formal zone names are introduced since we currently prefer to use the terms "beds" or "assemblages" to describe the local faunal sequence. Eight new early–middle Smithian ammonoid assemblages are described; the new Smithian succession encompasses 12 subdivisions (Fig. 14). In furtherance of the work of Brayard et al. (2009a) and Stephen et al. (2010), we herein report the occurrence of several new species from the middle and late Smithian. A synthetic range chart of genera is given in Fig. 15.

Vercherites undulatus sp. nov. bed

This assemblage is found only in the Mineral Mountains. It is probably the oldest known Smithian ammonoid fauna of the Thaynes Group. It is characterized by the unique occurrence of *Vercherites undulatus* sp. nov., which has not been found elsewhere. An exact correlation with other Panthalassic or Tethyan localities is uncertain (Figs. 12, 14, 15), but our specimens are similar to some late Dienerian/early Smithian proptychitids from the Salt Range (Pakistan) such as *Vercherites* (Brühwiler et al. 2012c), and thus are provisionally considered to be the oldest assemblage found in the studied area. A diagnostic Smithian conodont species (*Furnishius triserratus*) was discovered in the same bed confirming the Smithian age of the rocks.

Radioceras aff. *evolvens* beds

These beds are characterized by the unique occurrence of the rare involute taxon: *Radioceras* aff. *evolvens*. This subdivision was observed only within the Pahvant Range. It is probably younger than the *Vercherites undulatus* sp.

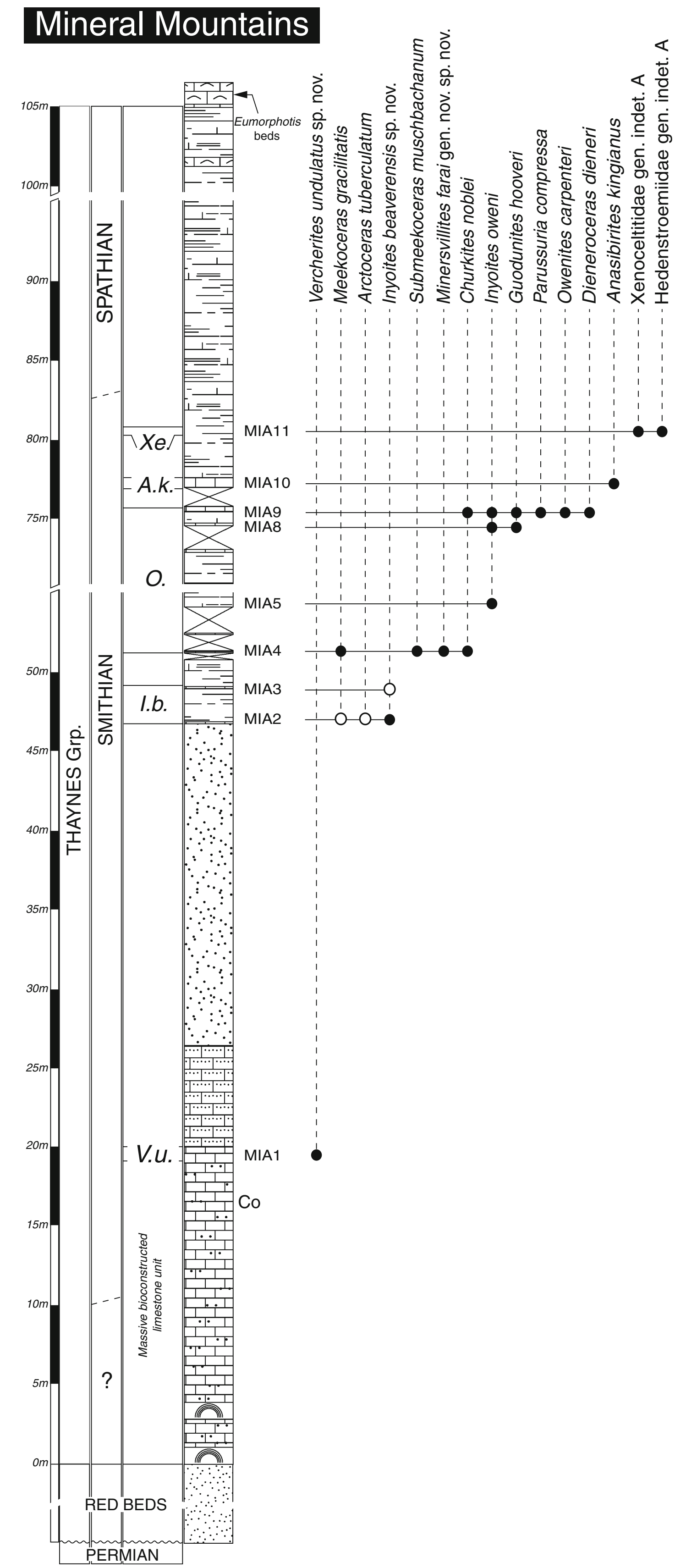

Fig. 6 Distribution of ammonoid taxa in the Mineral Mountain section (MM in Fig. 1). *Open dots* indicate occurrence based only on fragmentary or poorly preserved material. Abbreviations as in Figs. 2 and 4. *Xe* Xenoceltitidae gen. indet. A beds, *V.u.* *Vercherites undulatus* sp. nov. bed

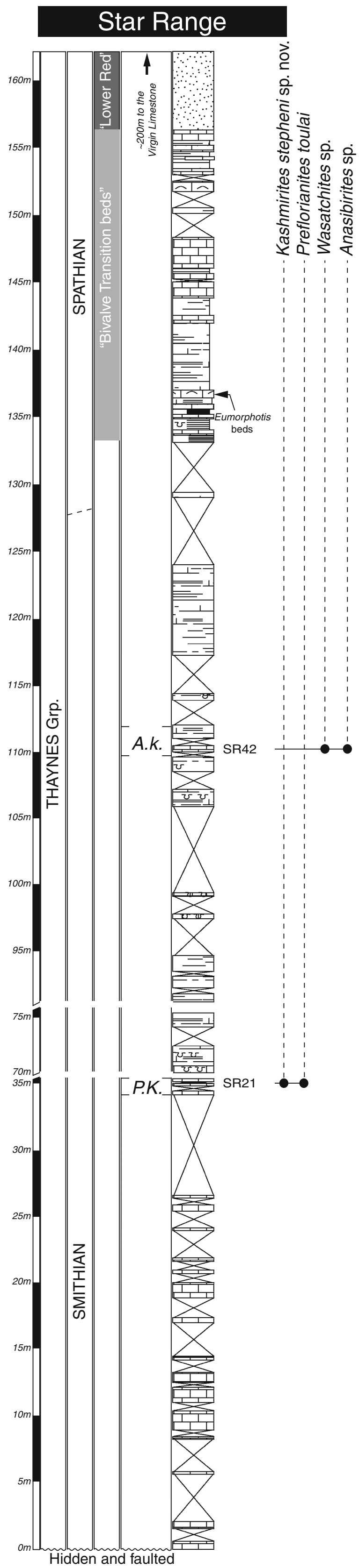

Fig. 7 Distribution of ammonoid taxa in the Star Range section (SR in Fig. 1). Abbreviations as in Figs. 2, 4 and 6

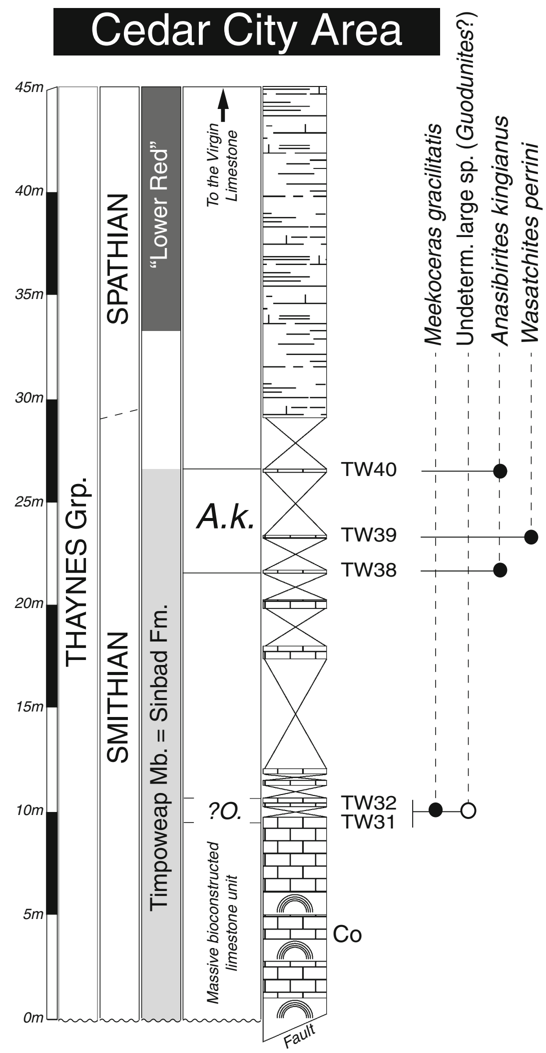

Fig. 8 Distribution of ammonoid taxa in the Cedar City area (CC in Fig. 1). *Open dots* indicate occurrence based only on fragmentary or poorly preserved material. Abbreviations as in Figs. 2, 4 and 6

nov. bed, when compared with ammonoid successions found in the North Indian Margin (Brühwiler et al. 2010a). It also has no exact worldwide correlative.

Meekoceras olivieri sp. nov. beds

These beds are characterized by the association of the prionitid *Meekoceras olivieri* sp. nov. with a possible flemingitid. This assemblage, documented only in the Pahvant Range, may be a correlative of early Smithian flemingitid faunas from the Salt Range (Brühwiler et al. 2012c).

Meekoceras millardense sp. nov. bed

This subdivision from the Pahvant Range contains only the rare involute taxon *Meekoceras millardense* sp. nov. This bed has no exact worldwide correlative.

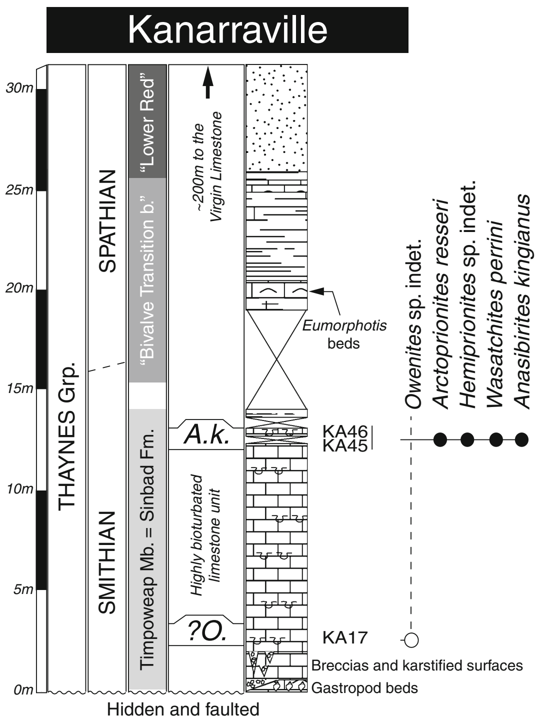

Fig. 9 Distribution of ammonoid taxa in the Kanarraville section (KAN in Fig. 1). *Open dots* indicate occurrence based only on fragmentary or poorly preserved material. Abbreviations as in Figs. 2, 4 and 6

Preflorianites–Kashmirites beds

This assemblage is relatively well documented and contains a rather diverse Smithian fauna with *Kashmirites* sp., *Preflorianites toulai*, *Arctoceras tuberculatum*, and *Pseudosageceras multilobatum*. The fauna is also marked by the first occurrence of true *Meekoceras gracilitatis*. This subdivision is probably located near the early/middle Smithian boundary (Figs. 14, 15). Indeed, it may correlate with

- the early Smithian *Kashmirites kapila* beds of South China (Brayard and Bucher 2008) and *Kashmirites* sp. indet. beds of South Tibet (Brühwiler et al. 2010b), as it corresponds to the first regional appearance of *Kashmirites*,
- and possibly also to the lowermost part of the *Flemingites rursiradiatus* beds of South China (Brayard and Bucher 2008), Oman (Brühwiler et al. 2012a) and the Salt Range (Brühwiler et al. 2012c), because it contains *Arctoceras* and *Preflorianites*.

Inyoites beaverensis sp. nov. beds

This assemblage, present in the Pahvant Range, Confusion Range and Mineral Mountains, is characterized by the occurrence of *Inyoites beaverensis* sp. nov., *Kashmirites*

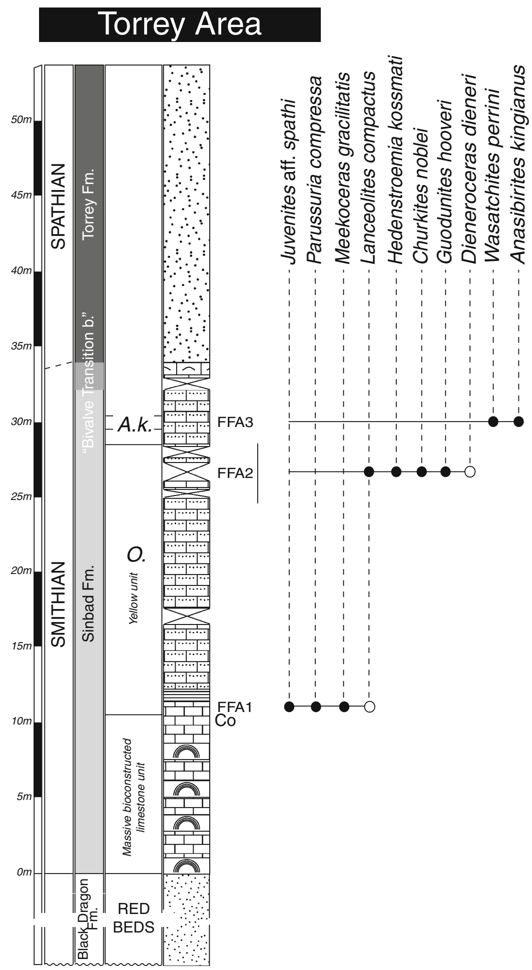

Fig. 10 Distribution of ammonoid taxa in the Torrey area (TO in Fig. 1). *Open dots* indicate occurrence based only on fragmentary or poorly preserved material. Abbreviations as in Figs. 2, 4 and 6

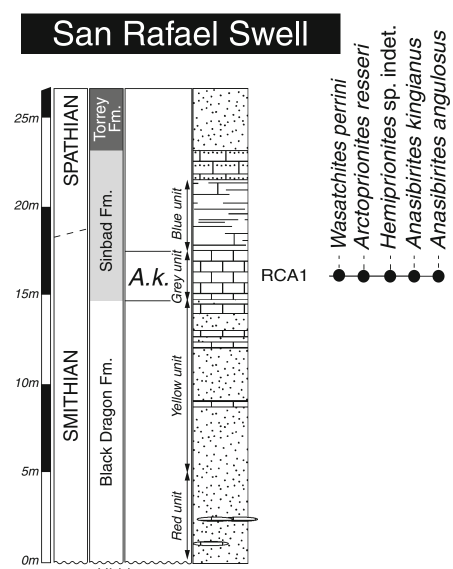

Fig. 11 Distribution of ammonoid taxa in the San Rafael Swell (SRS in Fig. 1). Abbreviations as in Figs. 2, 4 and 6

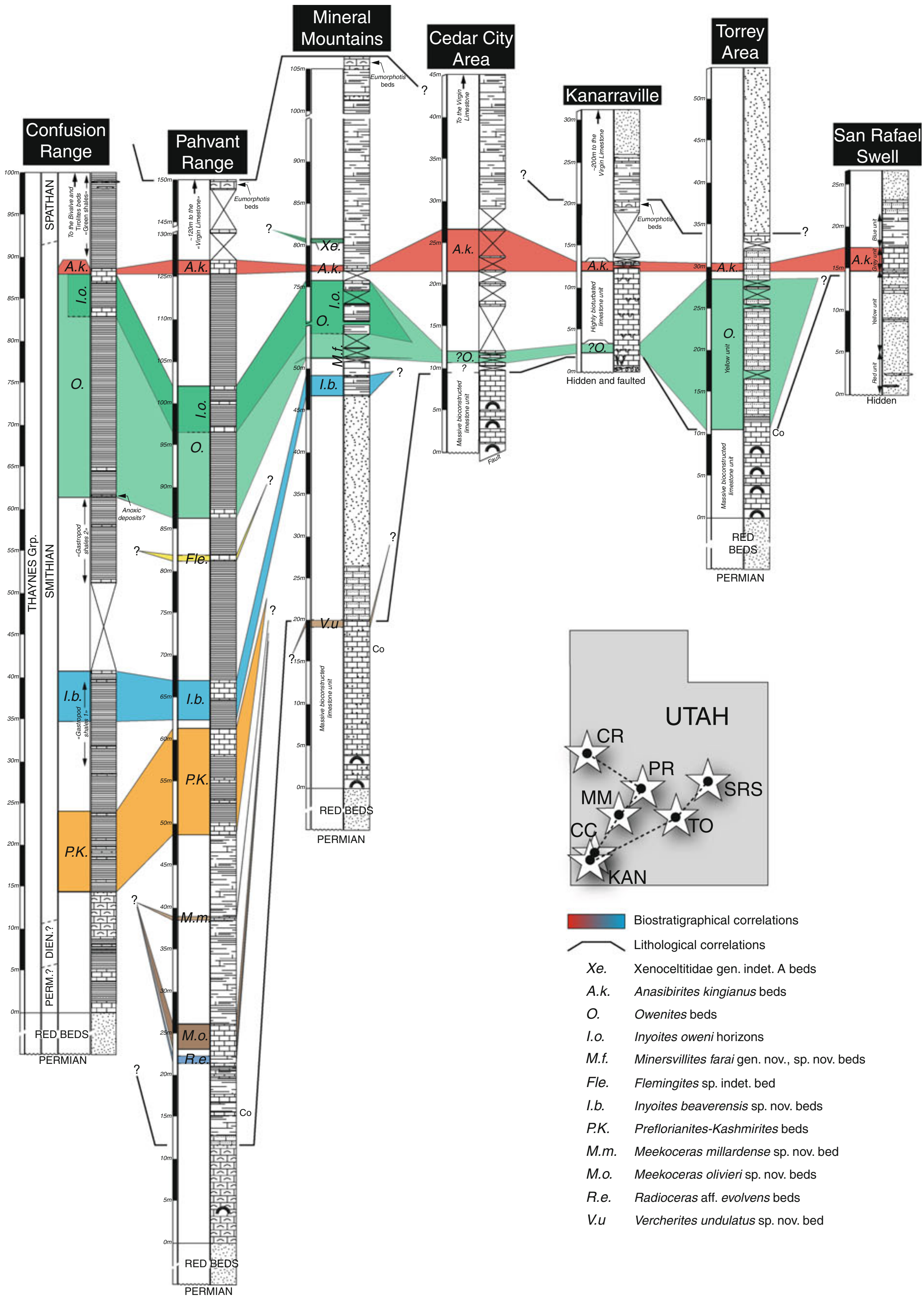

Fig. 12 Biostratigraphical correlation between the studied sections illustrating the diachronism of sedimentary deposits

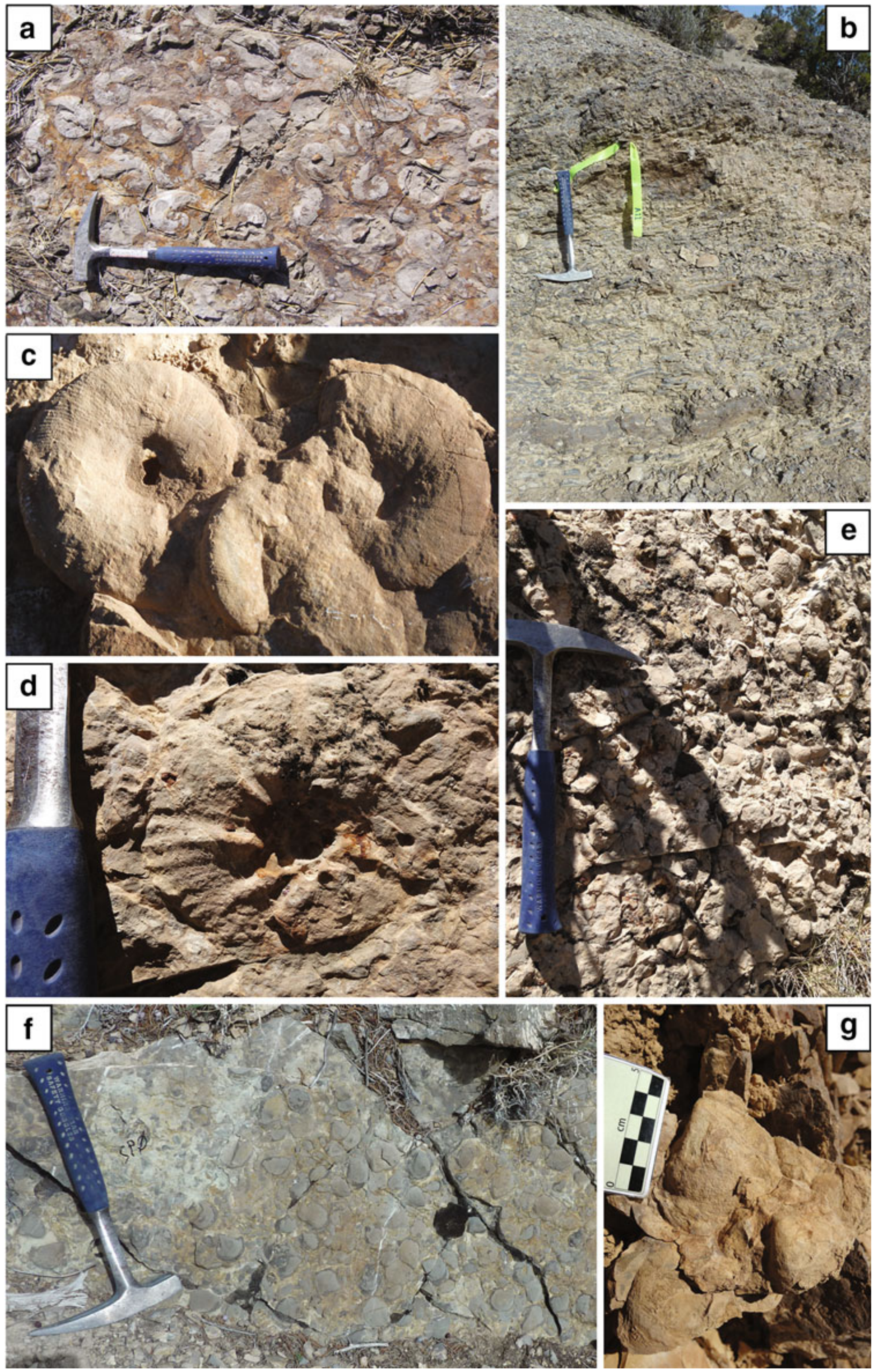

Fig. 13 Late Smithian deposits of the *Anasibirites kingianus* beds at different studied localities. **a** Confusion Range; **b** Mineral Mountains; **c** Torrey area (left *A. kingianus* is ~10 cm in diameter); **d**, **e** Kanarraville section (*Wasatchites perrini* is illustrated in **d**); **f**, **g** *Eumorphotis* beds representing the Smithian–Spathian transition in the Mineral Mountains (**f**) and Kanarraville sections (**g**)

utahensis sp. nov., *Anaflemingites* sp. indet., *Aspenites acutus* and *Meekoceras gracilitatis*. This fauna may correlate in part with the *Flemingites rursiradiatus* beds from South China, Oman and the Salt Range (op. cit.). This is the oldest known occurrence of the genus *Inyoites* in the world.

Flemingites sp. indet. bed

This bed is characterized by the occurrence of an undetermined species of *Flemingites*. Since it is found just below the first occurrence of *Owenites* in the Pahvant Range, it may correspond to the uppermost part of the

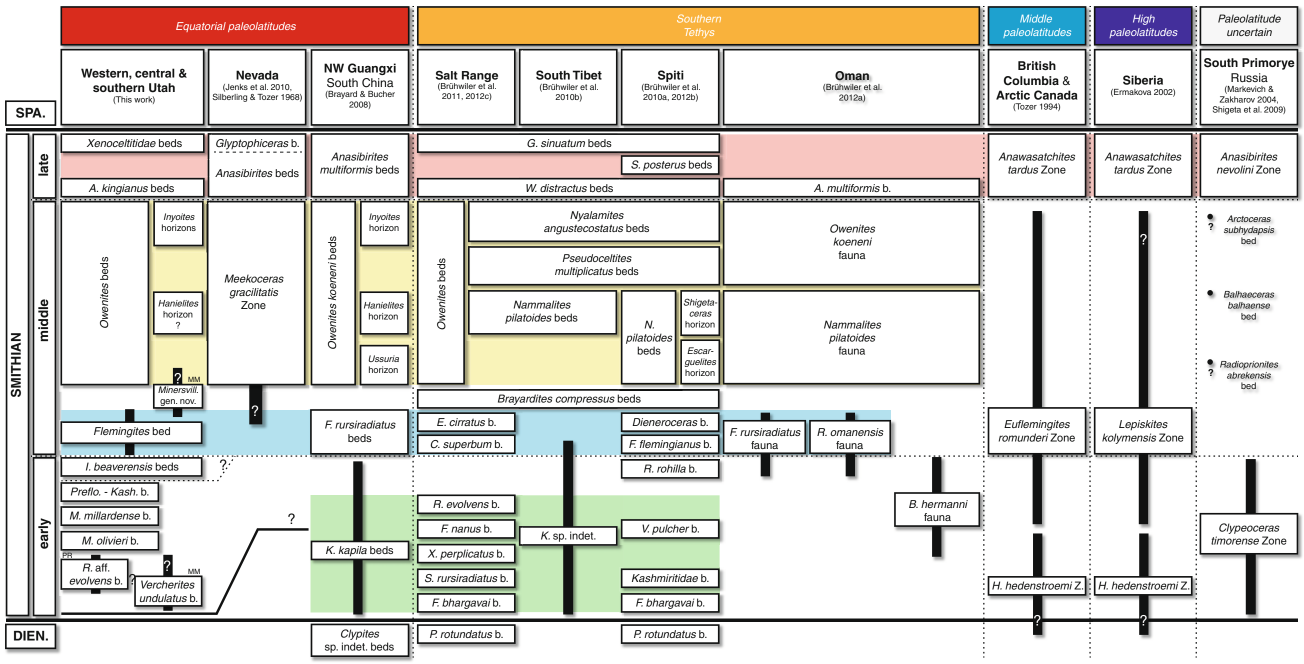

Fig. 14 Central and Southern Utah ammonoid zonation and correlation with other Smithian successions. *Spa.* Spathian, *Dien.* Dienerian, *PR* Pahvant Range, *MM* Mineral Mountains

Flemingites rursiradiatus beds from South China, Oman and the Salt Range (op. cit.).

Owenites beds

These beds, characterized by the occurrence of several *Owenites* species, are documented from all studied sections, except the San Rafael Swell area. These assemblages, previously described by Brayard et al. (2009a) and Stephen et al. (2010), are probably the most diverse within Utah, and our extensive collections allow us to augment previous occurrence lists. These beds commonly contain *O.* cf. *koeneni*, *O. carpenteri*, *Meekoceras gracilitatis*, *Churkites noblei*, *Guodunites hooveri*, *Inyoites oweni*, *Juvenites* cf. *thermarum*, *Aspenites acutus*, *Pseudosageceras multilobatum*, *Hedenstroemia kossmati*, *Lanceolites compactus*, *L. bicarinatus*, *Dieneroceras dieneri*, *Xenoceltites cordilleranus*, *Parussuria compressa* and an indeterminate prionitid. *Wyomingites arnoldi*, a taxon previously reported from these beds (Stephen et al. 2010), is herein newly assigned to *Dieneroceras dieneri*. A major portion of this fauna consists of widely occurring taxa known from several localities within the paleoequatorial belt: South China (Brayard and Bucher 2008), South Tibet (Brühwiler et al. 2010b), Salt Range (Brühwiler et al. 2012c), and Oman (Brühwiler et al. 2012a). This characteristic middle Smithian assemblage can be subdivided into different successive faunas. The co-occurrence of *Inyoites oweni* and *O. carpenteri* distinguishes the uppermost fauna and defines the *I. oweni* horizons (Brayard et al. 2009a; Stephen et al. 2010), which can be correlated with the *Inyoites* horizon from South China (Brayard and Bucher 2008) and the *Nyalamites angustecostatus* beds from Spiti, Salt range, and Oman (Brühwiler et al. 2012a, b, c). In the Pahvant Range, *Hanielites* (*H.* sp. indet.) is probably present but restricted to a single bed, thus suggesting the existence of a lower eponymous subdivision. The same applies in the Mineral Mountains where a new arctoceratid, *Minersvillites farai* gen. nov., sp. nov. co-occurs with *Submeekoceras muschbachanum* and *Churkites noblei* at the base of the *Owenites* beds. If the occurrence of *Hanielites* is confirmed, this bed can be correlated with the *Hanielites* horizon of South China and the upper part of the *Nammalites pilatoides* beds of South Tibet (Brühwiler et al. 2010b). *Minersvillites farai* gen. nov., sp. nov. is closely related to *Brayardites*, which is known from the Salt Range, South Tibet and Spiti, and thus could constitute an approximated correlative bed. It should also be noted that ussuriids such as *Parussuria*, which occur earlier in South China than in Utah, define the first subdivision of the *Owenites koeneni* beds (Brayard and Bucher 2008).

Anasibirites kingianus beds

These late Smithian beds are characterized by *Anasibirites kingianus* associated with *Wasatchites perrini*, and several species of *Arctoprionites*, *Hemiprionites* and *Xenoceltites*. This low-diversity fauna is recognized worldwide and

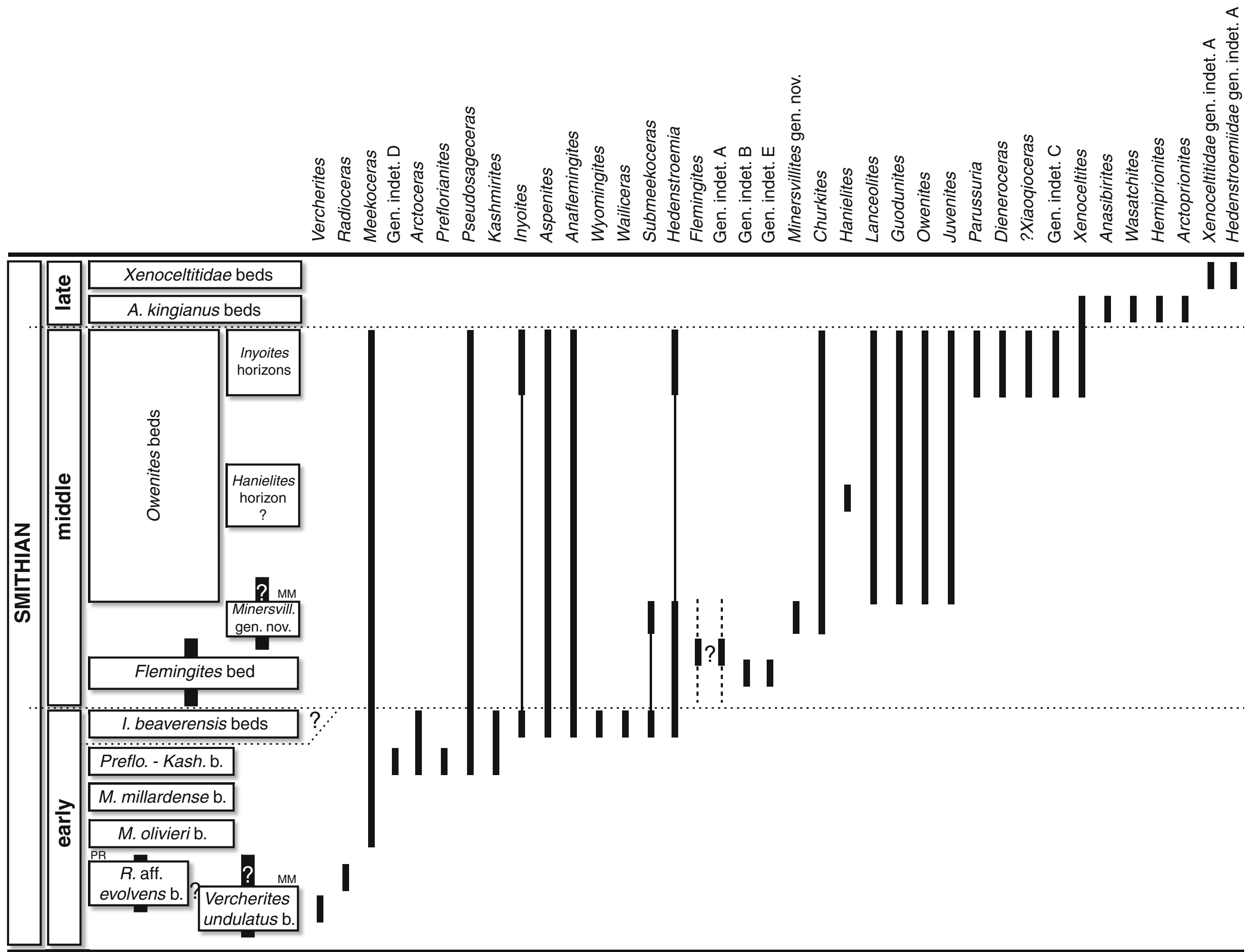

Fig. 15 Synthetic range chart of Smithian ammonoid genera from central and southern Utah

corresponds to a major global ammonoid extinction event (Brayard et al. 2006, 2009c), coinciding with the onset of marked events in the geochemical, sedimentological, palynological and climate records (Galfetti et al. 2007a, b, c; Hermann et al. 2011; Romano et al. 2013). All studied localities display different facies (Fig. 13a–e) for this short time-interval, but they also exhibit significant sedimentological evidence (e.g., shallow and proximal facies such as red beds) indicating an extremely rapid regression spanning the Smithian/Spathian boundary after the deposition of the *Anasibirites kingianus* beds.

Xenoceltitidae gen. indet. A beds

These beds commonly contain common specimens of Xenoceltitidae gen. indet. A. They represent the latest Smithian and probably correlate with the *Glyptophiceras sinuatum* beds from South Tibet and the Salt Range (Brühwiler et al. 2010b, 2012c), which generally contain an abundant xenoceltitid fauna with *Glyptophiceras* and *Xenoceltites* species. This zone is here reported for the first time from Utah, but it also has previously been reported from Crittenden Springs, Nevada (Jenks et al. 2010). However, the extremely poor preservation of our specimens precludes any definitive assignment to these taxa. *Pseudosageceras augustum*, another latest Smithian diagnostic taxon, has not been documented from the studied area. However, Hedenstroemiidae gen. indet. A, an ammonoid somewhat similar to *P. augustum*, also occurs within these beds.

Discussion

Global and basinal biostratigraphical correlations

This work shows that the ammonoid succession in western Utah is quite uniform for the late–middle and late Smithian. The updated biozonation for this interval is to a certain extent also recognized worldwide, thus allowing for more precise correlation than previously achieved. In contrast, many of the sections were found to contain new but different assemblages in the early and early–middle Smithian transition. On the one hand, this sometimes precludes precise correlation within the western USA Basin and with other basins of different paleolatitudes for this time-interval. On the other hand, it supports previous works that suggested early–middle Smithian ammonoids were more endemic and latitudinally restricted than during the late Smithian (Brayard et al. 2006, 2007b, 2009b; Jenks 2007; Jenks et al. 2010). Long-distance correlation across latitudes is only possible during the late Smithian, when genera such as *Anasibirites*, *Wasatchites* or *Xenoceltites* are fully cosmopolitan (Fig. 14), concomitant with a marked extinction probably linked to major oceanographic and/or climate changes (e.g., Brayard et al. 2009c; Galfetti et al. 2007c; Romano et al. 2013).

After extensive fieldwork, it has become apparent to the authors that beds with very abundant bivalves above the *Anasibirites kingianus* beds usually mark the Smithian–Spathian transition in central and southern Utah. In numerous places, this regional bloom is characterized by large *Eumorphotis* (e.g., *E. virginensis*, *E. ericius*, *E. multiformis*; Fig. 13f, g). Although they may be marginally diachronous, these deposits ("bivalve transition beds" or "*Eumorphotis* beds" in Figs. 2, 4, 6, 7, 8, 9, 10, 11) probably reflect a significant faunal event within the basin and may serve as a regional time-marker for the earliest Spathian. A formal link between this regional bivalve bloom and the end-Smithian extinction has not yet been determined, but this study is beyond the scope of the present paper.

On the use of *Meekoceras gracilitatis* for regional biozonation

M. gracilitatis appears to be a relatively long-ranging species that occurs mainly in the early/middle Smithian and thus, it is not very useful for precise biostratigraphical zonation and correlation. Early Triassic ammonoid workers are well aware that the Smithian contains numerous homeomorph taxa (e.g., Kummel and Steele 1962). We illustrate herein several taxa exhibiting a close resemblance to *M. gracilitatis* that characterize the regional lowermost Smithian, thus questioning some previous taxonomic assignments and zonations. Also, weathered specimens of such taxa as *Anasibirites*, *Wailiceras*, *Hedenstroemia* or *Radioceras* may easily be confused with *M. gracilitatis*. This species is therefore not well suited to characterize the entire time-interval as is usually the case. Thus, whenever possible, it is recommended not to use *M. gracilitatis* as a time-marker, but instead, we suggest the use of more abundant and short-ranging taxa with specific and easily recognizable morphologies (e.g., *Inyoites oweni* or *Preflorianites toulai*) to obtain precise ages for the Smithian in Utah.

On the age and correlation of Smithian formations in Utah

According to the newly obtained ammonoid succession, it appears obvious that sedimentary deposits of established stratigraphic units usually assumed to be time-equivalent within central and southern Utah are diachronous (Fig. 12), which modifies previously suggested correlative schemes such as that by Goodspeed and Lucas (2007). Thus, caution should be taken when using formation names to designate a specific time-interval, especially when it applies to regional and worldwide correlation.

Within Utah, the best known and most widely used Smithian formation is the "Sinbad Limestone". It was defined in the San Rafael Swell area (Gilluly and Reeside 1928; Fig. 1) and then extrapolated to southwestern Utah. This formation has been often considered as entirely of Smithian age in many recent studies (e.g., Fraiser and Bottjer 2004). However, ammonoid occurrences clearly indicate that only the lower $\sim 1/4$ of this thick unit at the type-locality is actually end-Smithian (*Anasibirites kingianus* beds, Fig. 11), and that the rest of the unit is likely earliest Spathian (see also Goodspeed and Lucas 2007). The "Sinbad Limestone" is also widely found in the Torrey area (Dean 1981; Fig. 1). However, although sedimentary successions are rather similar to those of the San Rafael Swell area, ammonoids indicate a middle-to-late Smithian age for this unit in the Torrey area (Fig. 10). In southwestern Utah (Cedar City, Kanarraville and Virgin areas), the "Timpoweap Member" is usually considered as a time-equivalent and junior synonym of the "Sinbad Limestone" (Lucas et al. 2007b). Nevertheless, ammonoids indicate a middle-to-late Smithian age for this unit. Thus, it can only be correlated with the "Sinbad Limestone" of the Torrey area, and not (or only partly) with its type-locality in the San Rafael Swell area. Depending on the studied area in Utah, authors should therefore clearly specify the age of the section by means of ammonoids or conodonts, if possible, and not refer to just the "Sinbad Limestone" designation, which may either be middle-to-late Smithian or span the end-Smithian/Spathian transition.

Dating and monitoring of the Smithian transgression within Utah

The newly obtained ammonoid succession allows us to closely follow the advancing sea during the Smithian. Our scenario fits well with the global Smithian reconstruction previously proposed by, e.g., Carr and Paull (1983), Collinson et al. (1976), Collinson and Hasenmueller (1978) and

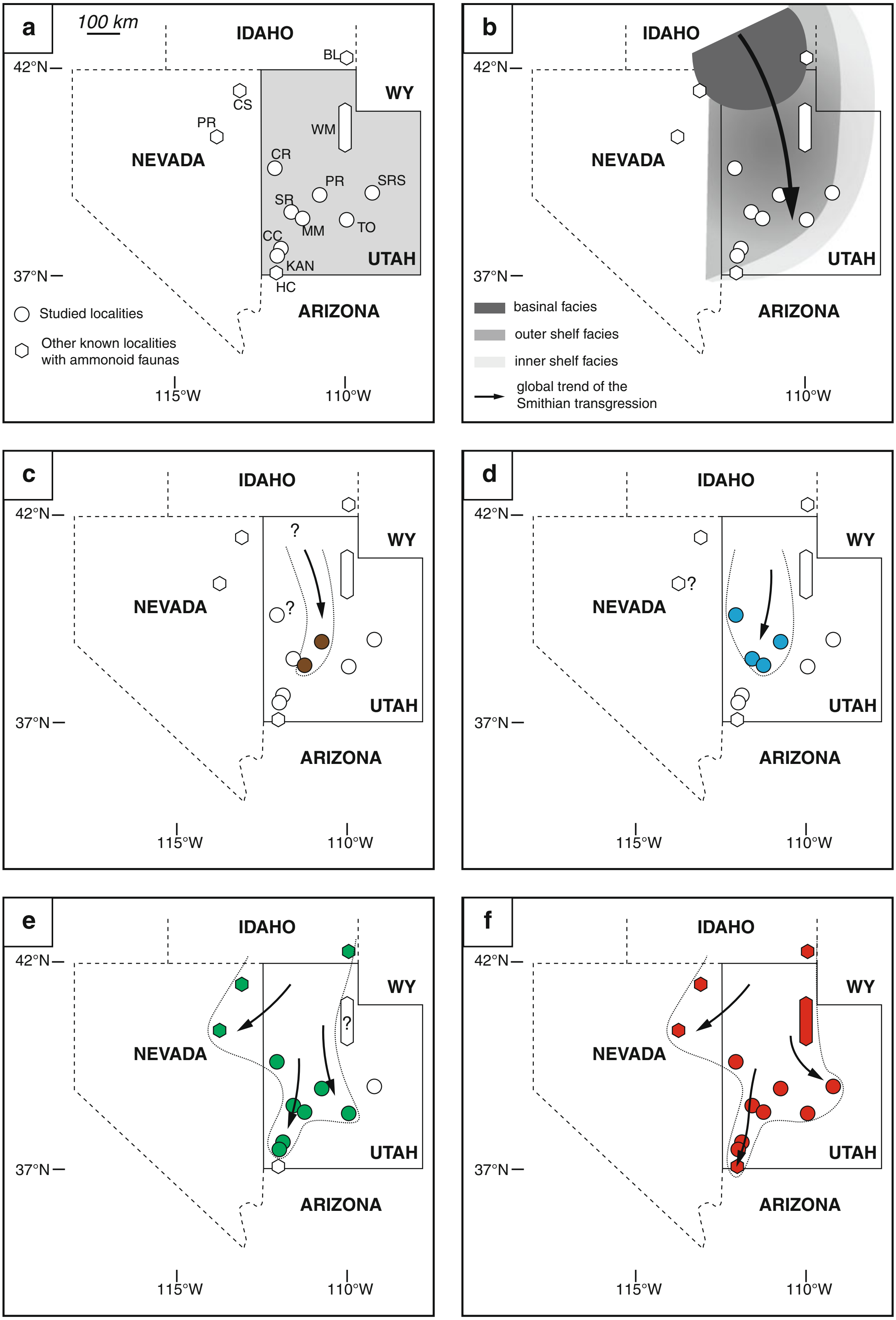
a
100 km
IDAHO
42°N
37°N
BL
CS
PR
WM
WY
NEVADA
CR
PR
SRS
SR
MM
TO
CC
KAN
UTAH
HC
ARIZONA
Studied localities
Other known localities with ammonoid faunas
115°W
110°W
b
IDAHO
NEVADA
UTAH
ARIZONA
basinal facies
outer shelf facies
inner shelf facies
global trend of the Smithian transgression
110°W
c
IDAHO
WY
NEVADA
UTAH
ARIZONA
?
?
115°W
110°W
d
IDAHO
WY
NEVADA
UTAH
ARIZONA
?
115°W
110°W
e
IDAHO
WY
NEVADA
UTAH
ARIZONA
?
115°W
110°W
f
IDAHO
WY
NEVADA
UTAH
ARIZONA
115°W
110°W

◀ **Fig. 16** Schematic advance of the sea within Utah during the Smithian, based on ammonoid data. **a** Localities used for the reconstruction (same sites and abbreviations as in Fig. 1, with the addition of other known outcrops where ammonoids were collected; *BL* Bear Lake area, *CS* Crittenden Springs, *PR* Phelan Ranch, *WM* Wasatch Mountains, *HC* Hurricane Cliffs; e.g., Hofmann et al. 2013; Hyatt and Smith 1905; Jenks 2007; Jenks et al. 2010; Kummel and Steele 1962; Smith 1932). **b** Schematic extent of the Smithian open marine depositional facies (based on Carr and Paull 1983; Collinson and Hasenmueller 1978; Paull and Paull 1993). Detailed evolution of the transgression: **c** from the *Vercherites undulatus* sp. nov. bed up to the *Preflorianites–Kashmirites* beds; **d** during deposition of the *Preflorianites–Kashmirites* beds and *Inyoites beaverensis* sp. nov. beds; **e** during deposition of the *Owenites* beds; **f** during deposition of the *Anasibirites kingianus* beds

Paull and Paull (1993) based on conodont zonation and sedimentological evidence. However, our data provide a scenario with a greater time resolution for the Smithian. We thus define the five following main steps (Fig. 16):

1. Earliest Smithian ammonoid faunas are apparently absent from Utah. However, supposedly time-equivalent deposits corresponding to shallow environments and occasional microbial-sponge reefs (Figs. 2, 4, 6, 10; Brayard et al. 2011b) represent the very beginning of the Smithian transgression within the basin. These early Smithian deposits are mainly found in central Utah (Pahvant Range, Mineral Mountains). This area is also the first to record the presence of ammonoid faunas (*Vercherites undulatus* sp. nov. bed up to the *Preflorianites–Kashmirites* beds); hence, we interpret it as corresponding to true open marine conditions. Following this hypothesis, the transgression appears to proceed southward along a central corridor within Utah, rather than spreading out from the basin depocenter in all directions. In particular, the transgression seems not to have reached some neighboring localities such as Crittenden Springs in Nevada, the Confusion Range or the Wasatch Mountains in Utah. This indicates that these localities may have been part of a complex basinal paleogeography with an irregular shoreline inherited from the Permian topography. Furthermore, it suggests that the pathway of the early Smithian transgression may have also resulted from a combination of (a) the subsidence of the foreland basin with the deeper parts (down through central Utah) possibly marking the axis of the foreland basin (the location of which is often estimated with great uncertainty; see Dickinson 2006); and (b) paleotopographic highs on each side of the basin;
2. The transgression reached the Confusion Range during the time of deposition of the *Preflorianites–Kashmirites* beds and *Inyoites beaverensis* sp. nov. beds. However, during this time, the open sea was restricted to the previous flooded area and did not move further South enough to record ammonoids and true open marine facies in this area. The accommodation space in this part of the basin was already sufficient to sustain thick deposits. Areas in southern Utah may have been partly isolated from the transgression by the existence of a wide epeiric platform that dampened incoming waves, or by being positioned behind a barrier, or within a restricted embayment. Incidentally, such a fragmented paleogeographic setting may well have led to the development of relatively isolated paleobiogeographic areas with island-like features such as the local occurrence of unbalanced benthic faunas with some remarkably small-sized species. This hypothesis, which remains to be further tested, would offer an interesting alternative scenario to the henceforth refuted global Early Triassic "Lilliput effect" (Brayard et al. 2010, 2011a);
3. The *Owenites* beds probably represent a new advancing phase of the transgression within the basin, reaching previously discussed western and southern areas. Almost all parts of the basin are thus inundated slightly earlier than previously thought (middle Smithian instead of late Smithian);
4. The maximum extent of the transgression was reached during deposition of the *Anasibirites kingianus* beds (late Smithian) when all localities were characterized by this assemblage, especially the southwesternmost and southeasternmost parts of the basin. All studied localities display sedimentological evidence (e.g., shallow and proximal deposits such as red beds) of an extremely rapid regression spanning the Smithian/Spathian boundary after deposition of the *Anasibirites kingianus* beds;
5. Following this event, a new early Spathian marine transgression is marked by marine faunas such as *Tirolites* or nautiloid occurrences within well-known deposits such as the Virgin limestone in southwestern Utah (e.g., Hofmann et al. 2013). However, in Utah this Spathian transgression did not reach the maximum extent of the Smithian sea, since it is not recorded on the eastern side of the basin (Carr and Paull 1983; Collinson and Hasenmueller 1978; Paull and Paull 1993).

Conclusion

Intensive sampling within central and southern Utah has led to the recognition of 10 new Smithian ammonoid taxa (one new genus and nine species) and 12 successive associations. The resulting new biostratigraphical succession is therefore more precise than the previous twofold subdivision suggested by Kummel and Steele (1962). This new faunal sequence can be correlated in detail with several worldwide localities (Fig. 14) thanks to the presence of many trans-Panthalassic (middle Smithian) and cosmopolitan (late Smithian) taxa. However, a detailed correlation for the early–middle Smithian transition remains hampered by poor ammonoid preservation and a high degree of endemism, as well as an insufficient knowledge of ammonoid faunas collected from the western USA basin. Earliest Smithian ammonoid faunas are apparently absent. *Meekoceras gracilitatis*, the commonly used Smithian ammonoid index, is here shown to be a long-ranging genus and a rather good indication of the middle Smithian interval. However, this species can be easily confused with other taxa such as the prionitid genera *Anasibirites* or *Hemiprionites*, especially in the case of poor preservation. Therefore, we call for the use of more abundant, short-ranging taxa with specific and easily recognizable morphologies (e.g., *Inyoites oweni* or *Preflorianites toulai*) to precisely characterize ages of the various Smithian sedimentary successions in Utah.

This new biostratigraphical scheme draws attention to the highly irregular nature of the Smithian basinal paleogeography that most probably is due to an inherited complex Permian topography. It also allows us to closely follow the southward Smithian open sea transgression within Utah. The transgression reached its maximum extent during the late Smithian (*Anasibirites kingianus* beds of the Cedar City, Kanarraville and San Rafael Swell areas), but arrived earlier than previously thought in most studied localities (e.g., *Radioceras* aff. *evolvens* beds in the Pahvant Range, and base of the *Owenites* beds in the Torrey area).

Systematic paleontology (Brayard, Bylund and Jenks)

Systematic descriptions follow the ammonoid classification of Tozer (1981, 1994) and Brayard and Bucher (2008), and then further refined by Brühwiler et al. (2012a, b, c). The

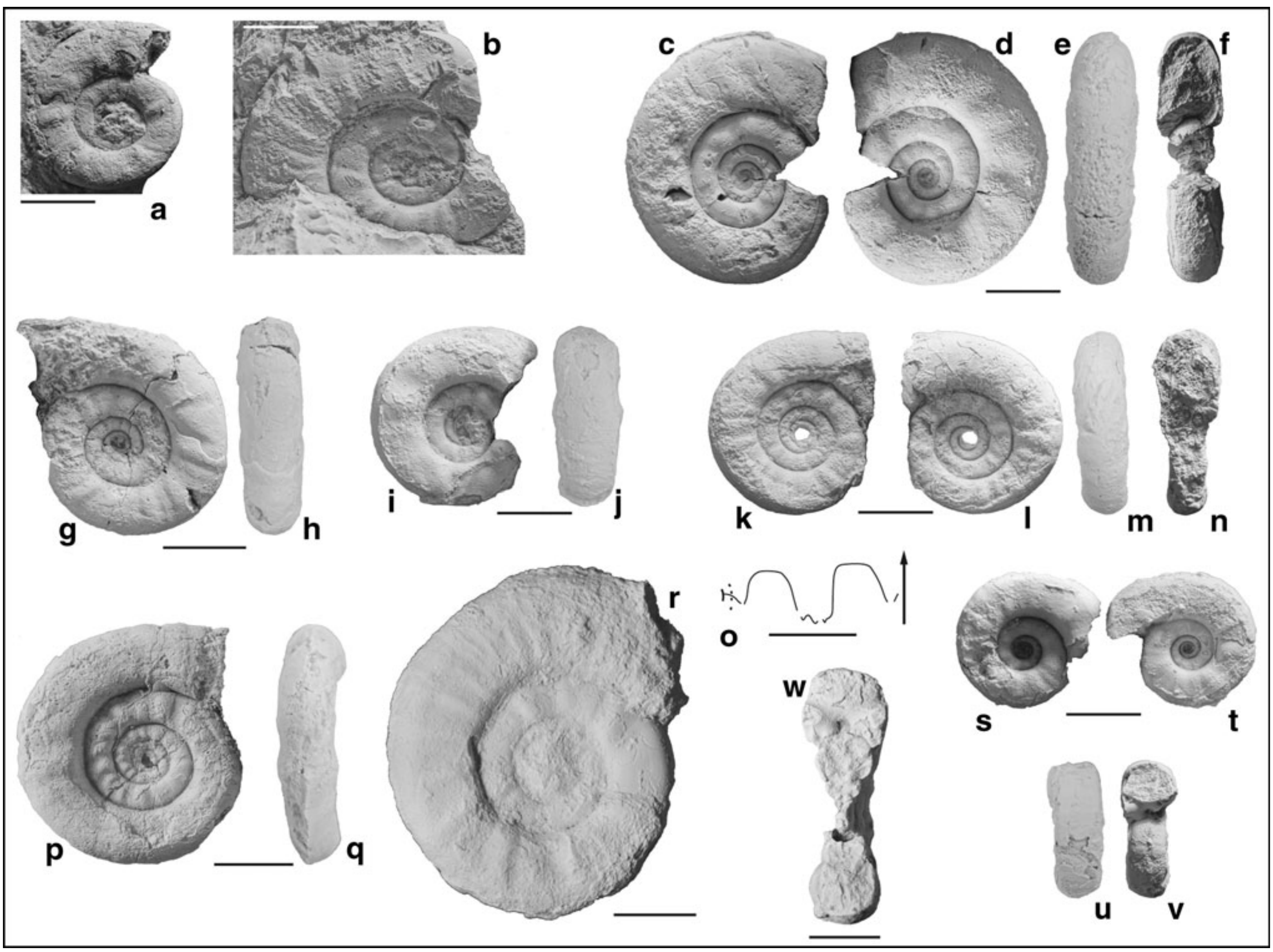

Fig. 17 *Xenoceltites cordilleranus* (Smith 1932). All from the *Owenites* beds, *Inyoites oweni* horizons, Smithian; **a**, **b** UBGD 275000, UBGD 275001, respectively, loc. DV1-9, Pahvant Range; **c–f** UBGD 275002, loc. DH1-12, Confusion Range; **g**, **h** UBGD 275003, Loc. DH1-12, Confusion Range; **i**, **j** UBGD 275004, loc. DH1-11, Confusion Range; **k–o** UBGD 275005, loc. DH1-12, Confusion Range; **o** *scale bar* is 5 mm ($H = 7.5$ mm); **p**, **q** UBGD 275006, loc. DH1-12, Confusion Range; **r** UBGD 275007, loc. DH1-11, Confusion Range; **s–v** UBGD 275008, loc. DH1-11, Confusion Range; **w** UBGD 275009, loc. DH1-11, Confusion Range

quantitative morphological ranges for each species are described (when permitted by preservation) using the four classical geometrical parameters of the ammonoid shell: diameter (*D*), whorl height (*H*), whorl width (*W*) and umbilical diameter (*U*). *H*, *W* and *U* are plotted in absolute values and ratios (*H*/*D*, *W*/*D* and *U*/*D*). Repository of figured and measured specimens is abbreviated UBGD (Université de Bourgogne, Géologie Dijon). Scale bar on illustrated specimens is 10 mm unless otherwise indicated.

Order Ammonoidea Zittel, 1884
Suborder Ceratitina Hyatt, 1884
Family Xenoceltitidae Spath, 1930
Genus ***Xenoceltites*** Spath, 1930
Type species Xenoceltites subevolutus = *Xenodiscus* cf. *comptoni* (non Diener) Frebold, 1930

Xenoceltites cordilleranus (Smith, 1932)
Fig. 17a–x

1932 *Xenodiscus cordilleranus*; Smith, p. 43, pl. 24, figs. 21-29.
1932 *Xenodiscus intermontanus*; Smith, p. 44, pl. 24, figs. 10-20.
p 1932 *Xenodiscus nivalis*; Smith, p. 44, pl. 56, figs. 6-9 [only].
? 1979 *Dieneroceras knechti*; Nichols and Silberling, pl. 1, figs. 22-26.
2010 ?*Kashmirites intermontanus*; Stephen et al., figs. 5e, f, h.

Occurrence Common in the Confusion Range [DH1-12, DH1-10/11] and Pahvant Range [DV1-9, DV1-8], *Owenites* beds, *Inyoites oweni* horizons. Not documented from the other studied sections.

Description Evolute, compressed platycone with a large intraspecific variation. Venter rounded or broadly arched with rounded shoulders forming rectangular to subquadratic whorl sections. Flanks almost parallel. Umbilicus wide, with moderately deep, perpendicular (inner whorls) to oblique (outer whorls) wall and rounded shoulders. Ornamentation varies from regularly distant, marked and slightly rursiradiate ribs on inner whorls to dense, rursiradiate and more variable strength ribs at maturity. Suture line ceratitic, with broad ventral saddle and a smaller umbilical saddle.

Measurements See Fig. 18. Estimated maximal size: ~5 cm.

Discussion See Brayard and Bucher (2008) for a discussion on *Xenoceltites* species assignments based on main morphological characteristics. *X. cordilleranus* is one of the older reported xenoceltitids since most of them occur worldwide within the *Anasibirites kingianus* beds. *Xenodiscus hannai* Mathews (1929) displays a similar coiling geometry and a similar coarse ornamentation type (Mathews' specimens were reported as *Xenodiscus nivalis* in Smith 1932, pl. 79, figs. 1, 2). However, its ribs were described and illustrated as "nearly straight, slightly flexuous, radial" (Mathews 1929, p. 5). This species thus appears rather distinct from *X. cordilleranus* with its rursiradiate ornamentation. Moreover, an exact temporal occurrence of *Xenodiscus hannai* was not reported by Mathews.

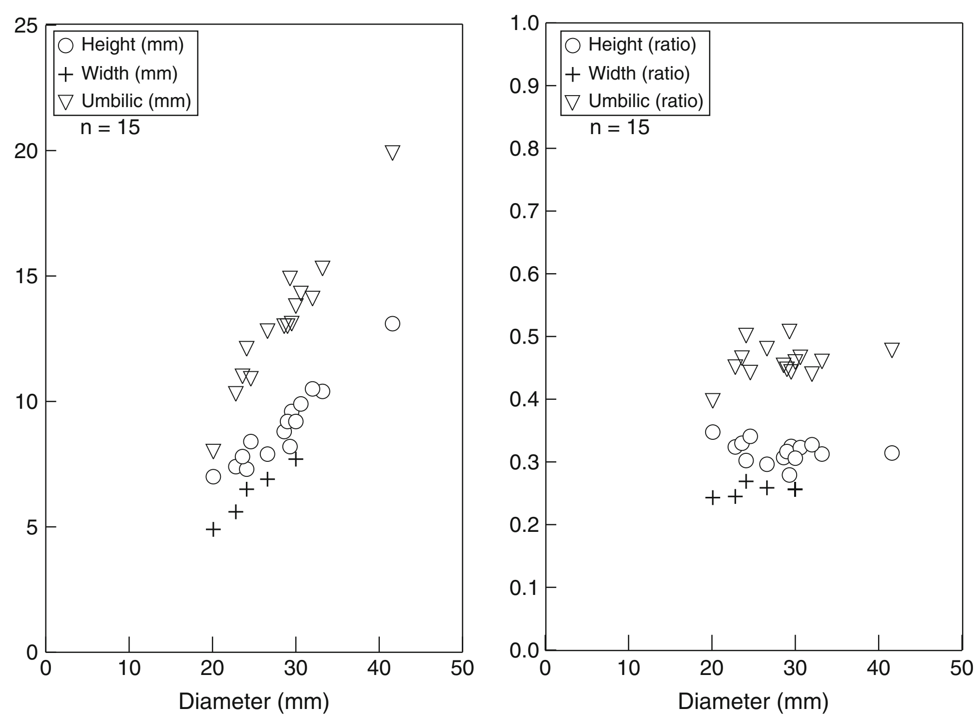

Fig. 18 Scatter diagrams of *H*, *W* and *U*, and *H*/*D*, *W*/*D* and *U*/*D* for *Xenoceltites cordilleranus* (all specimens from the Confusion Range, *Owenites* beds, *Inyoites oweni* horizon)

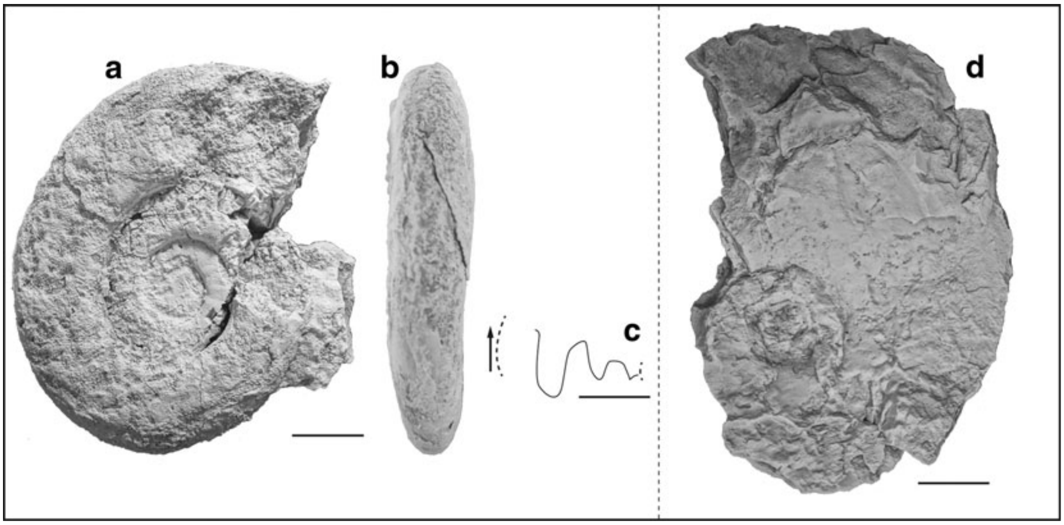

Fig. 19 **a–c** *Xenoceltites* sp. indet. A., UBGD 275010, loc. DH1-13, Confusion Range, *Anasibirites kingianus* beds, Smithian; **c** *scale bar* is 5 mm ($H = 10.6$ mm); **d** Xenoceltitidae gen. indet. A., UBGD 275011, loc. MIA11, Mineral Mountains, Xenoceltitidae gen. indet. A beds, Smithian

***Xenoceltites* sp. indet. A**
Fig. 19a–c

? 2010 *Xenoceltites* sp.; Stephen et al., fig. 7d.

Occurrence Extremely rare in the Confusion Range, *Anasibirites kingianus* beds [$n = 2$; DH1-13]. Not documented from the other studied sections.

Description Shell geometry typical of the xenoceltitidae: evolute, compressed platycone with rounded venter, rounded ventral shoulders, and almost parallel flanks, becoming gently convergent on ventral shoulder. Umbilicus wide, with moderately deep, oblique wall and rounded shoulders. No ornamentation visible on our unique specimen at maturity. Very weak folds appear to be present on juvenile stages. Suture line apparently ceratitic, with a broad, deep lateral lobe and very small umbilical saddle.

Measurements See Table 1.

Table 1 Measurements of some Smithian ammonoids from Utah

Genus	Species	Specimen number	*D*	*H*	*W*	*U*	Remarks
Xenoceltites	sp. indet. A	UBGD 275010	53.4	17	11.4	21.7	Slightly deformed
Kashmirites	*confusionensis* sp. nov.	UBGD 275018	50.2	13.7	–	26.6	Holotype
?Xiaoqiaoceras	*americanum* sp. nov.	UBGD 275042	21.6	9.5	8.4[a]	5.2[a]	Holotype, phragmocone only
Wyomingites	cf. *aplanatus*	UBGD 275053	35.5	13.1	7.5[a]	12.5	
Wyomingites	cf. *aplanatus*	UBGD 275052	28.5[a]	9.5	5.8	11.4	
Flemingites	sp. indet.	UBGD 275054	76[a]	28	13.6[a]	28	
Submeekoceras	*mushbachanum*	–	72.6	31	20.1	18.5	K. G. Bylund pers. collection
Minervillites	*farai*	UBGD 275061	68[a]	25.7[a]	14.7	26.7	Paratype
Hemiprionites	cf. *typus*	UBGD 275110	45.7	24.3	11.8[a]	–	
Arctoprionites	*resseri*	UBGD 275112	115[a]	54[a]	30.1	23.5	
Meekoceras	*millardense* sp. nov.	UBGD 275121	37.7	20.3	–	–	Holotype
Owenites	*koeneni*	UBGD 275123	36.5	18.1	8.9	4.4	
Gen. indet. A		UBGD 275149	30	10.9	6.7	11.6	
Gen. indet. A		UBGD 275150	22.7	9	5.6	7	
Gen. indet. B		UBGD 275158	25.2	9.5	6.7	9.6	
Gen. indet. C		UBGD 275161	41.2	23.4	–	–	
Gen. indet. D		UBGD 275162	50	19.7	9.5	14.7	

D diameter, *H* whorl height, *W* whorl width, *U* umbilical diameter

[a] Estimated

Discussion The poor preservation of our specimen unfortunately prevents its attribution to a species. However, our specimen does not display distinctive marked ornamentation (ribs, bulges, constrictions) at maturity, thus differing from the other known species from late Smithian correlative beds of Guangxi, Salt Range, Spiti (*X. variocostatus*; see Brayard and Bucher 2008, Brühwiler et al. 2012b, c) or Spitsbergen (*X. spitsbergensis*; see Weitschat and Lehmann 1978). Although apparently slightly more evolute, the overall shape of our specimen invites more of a comparison with *X. subevolutus* from correlative beds of Spitsbergen (see Weitschat and Lehmann 1978) and Siberia (see Dagys and Ermakova 1990).

Xenoceltitidae gen. indet. A
Fig. 19d

Occurrence Common in the Mineral Mountains, Xenoceltitidae gen. indet. beds [$n = 12$; MIA11]. Not documented from the other studied sections.

Description Sampled specimens are all very poorly preserved, but coiling is moderately evolute with rounded venter and rounded ventral shoulders. Flanks probably parallel. Umbilicus often crushed, but with moderately deep, oblique wall and rounded shoulders. Ornamentation and suture line not preserved.

Measurements Not possible due to poor preservation. Estimated maximum size: ~7 cm.

Discussion The poor preservation of our specimens precludes any taxonomic assignment. However, they roughly resemble latest Smithian *Xenoceltites* or *Glyptophiceras* species such as *X. variocostatus* from South China or *G. sinuatum* from the Salt Range (e.g., Brayard and Bucher 2008; Brühwiler et al. 2012c). Another indirect indication of affiliation with the xenoceltitid group is its stratigraphic position above the *Anasibirites kingianus* beds, which elsewhere corresponds to the *Glyptophiceras sinuatum* beds and its xenoceltitid fauna.

Family Kashmiritidae Spath, 1934
Genus ***Preflorianites*** Spath, 1930
Type species Danubites strongi Hyatt and Smith, 1905

Preflorianites toulai (Smith, 1932)
Fig. 20a–h

? 1922 *Xenodiscus bittneri*; Welter, p. 106, pl. 4, figs. 7, 8; 1932 *Xenodiscus toulai*; Smith, p. 45, pl. 25, figs. 1-3; pl. 53, figs. 9–12.

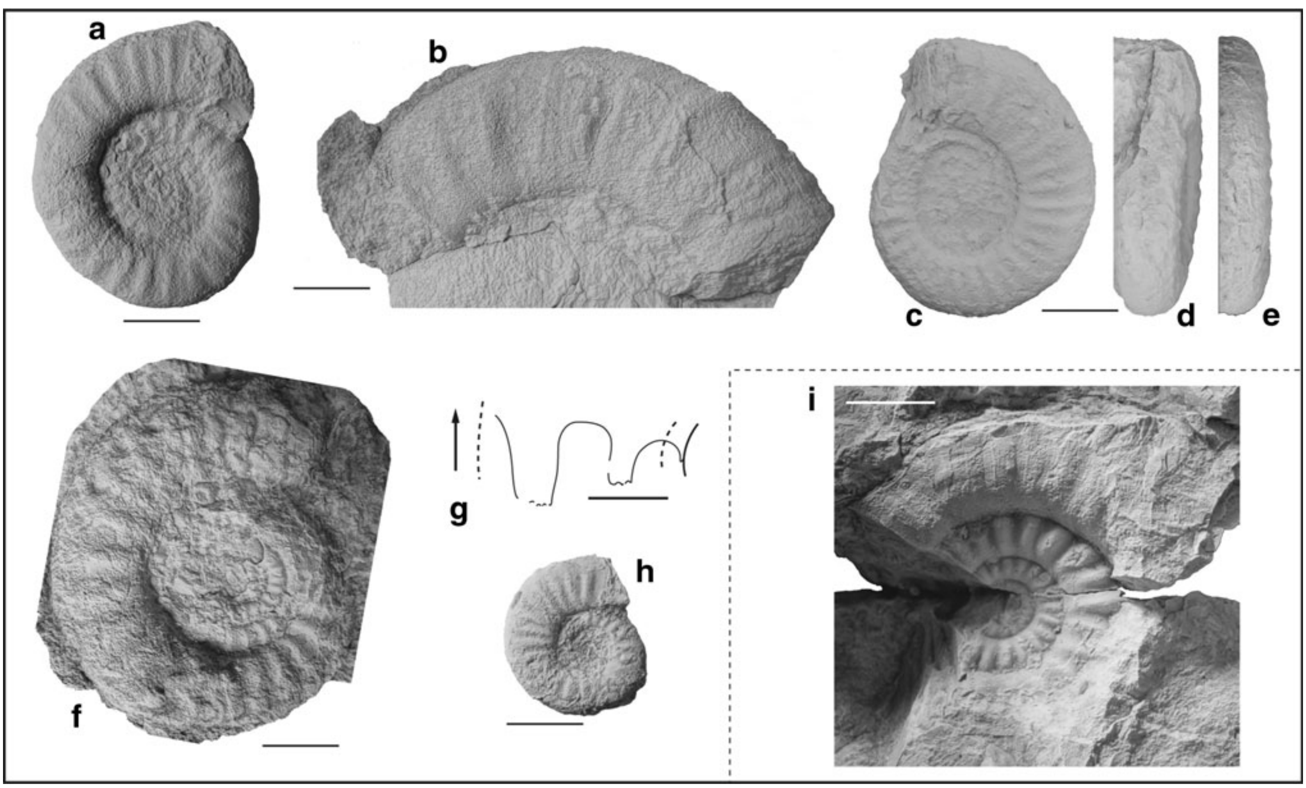

Fig. 20 *Preflorianites toulai* (Smith 1932). All from the *Preflorianites–Kashmirites* beds, Smithian; **a** UBGD 275012, loc. DV2-3C, Pahvant Range; **b** UBGD 275013, loc. DH1-2, Confusion Range; **c–e** UBGD 275014, loc. DH1-2, Confusion Range; **f–g** UBGD 275015, loc. DH1-2, Confusion Range; **g** *scale bar* is 5 mm ($H = 13.4$ mm); **h** UBGD 275016, loc. DH1-2, Confusion Range; **i** *Kashmirites utahensis* sp. nov., UBGD 275017, loc. DV2-3E, Pahvant Range, *Preflorianites–Kashmirites* beds, Smithian, holotype

1932 *Proteusites rotundus*; Smith, p. 103, pl. 53, figs. 5–8.
1959 *Preflorianites radians*; Chao, p. 196, pl. 3, figs. 6–8.
1962 *Preflorianites toulai*; Kummel and Steele, p. 669, pl. 100, figs. 18–20; pl. 102,fig. 5.
? 1968 *Preflorianites* cf. *radians*; Zakharov, p. 137, pl. 27, figs. 5, 6.
1995 *Preflorianites toulai*; Shevyrev, p. 26, pl. 2, fig. 4.
2008 *Pseudoceltites*? *angustecostatus*; Brayard and Bucher, p. 18; pl. 3, figs. 1–7;text-fig. 19.
2012a *Preflorianites radians*; Brühwiler and Bucher, p. 15, pl. 1, figs. 8, 9; pl. 2, figs.1–7.

Occurrence Rather common in the Confusion Range [DH1-0] and rare in the Pahvant Range [DV2-2, DV2-3], *Preflorianites–Kashmirites* beds. Not documented from the other studied sections.

Description Evolute conch with a compressed whorl section, but showing a wide range of intraspecific variation. Venter broadly to highly arched with rounded shoulders forming near-rectangular to ovoid whorl sections. Flanks slightly convex. Large, shallow umbilicus with an oblique wall and rounded shoulders. Ornamentation consists of regularly spaced, marked and radial ribs fading out towards the venter. Faintly sinuous, fine growth lines are sometimes barely perceptible. Suture line ceratitic, with deep lateral lobes, well-rounded saddles and very small umbilical saddle.

Measurements See Fig. 21. Estimated maximal size: ~9 cm.

Discussion The type species apparently differs from *Preflorianites toulai* by its angular venter that is seen only on the holotype (see Hyatt and Smith 1905). Its coiling features and ornamentation do not show any other divergence. Although specimens from beds that contain the type specimens of *P. strongi* at Union Wash are abundant, additional individuals presenting an angular venter were not illustrated or subsequently collected (A.B. personal observation). This therefore suggests that the original illustration of the type specimen entails a false characteristic. In this case, *P. toulai* should be synonymized with the type species. However, we prefer to retain the two erected species as we have not yet examined the holotype to check its diagnostic angular venter.

It has been commonly assumed that *P. strongi* and *P. toulai* differ from *P. radians* from South China (Chao 1959; see Brayard and Bucher 2008) and Oman (Brühwiler et al. 2012a) only by its slightly more involute coiling and an apparently smaller mature size. However, based on the new specimens from Utah, which exhibit a wide range of intraspecific variation and near identical measurements (Fig. 22), we hypothesize that these taxa are conspecific because we presently do not see any major difference that would justify erection of dissimilar species. *P.* cf. *radians* described from South China by Brayard and Bucher (2008) exhibits a weaker and slightly more sinuous ornamentation as well as a venter that may be more tabulate. However, its other shell characteristics fit well with the *Preflorianites* diagnosis. The wide range of variation of *P. toulai* in Utah may be partly explained by the Buckman's first law of

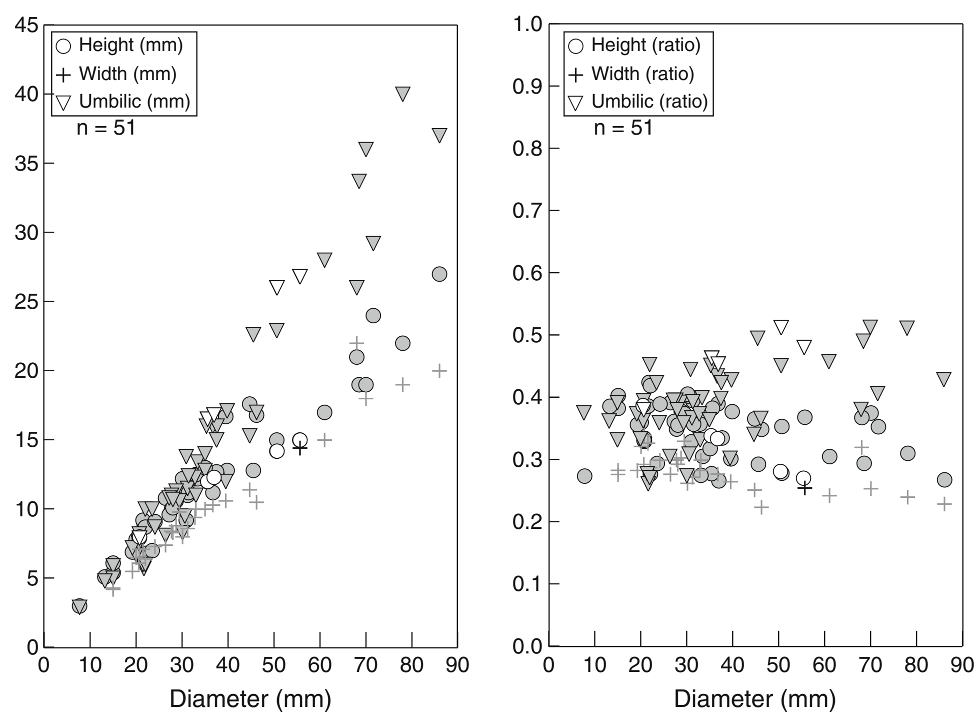

Fig. 21 Scatter diagrams of *H*, *W* and *U*, and *H*/*D*, *W*/*D* and *U*/*D* for *Preflorianites toulai* (*open symbols* indicate measurable specimens from the Confusion Range and Pahvant Range, *Preflorianites–Kashmirites* beds [$n = 5$]; *grey symbols* indicate specimens from Nevada [$n = 12$], Caucausus [$n = 2$], Primorye [$n = 4$], South China [$n = 21$] and Oman [$n = 7$]; data respectively from Kummel and Steele 1962, Shevyrev 1995, Zakharov 1968, Brayard and Bucher 2008 and Brühwiler et al. 2012a)

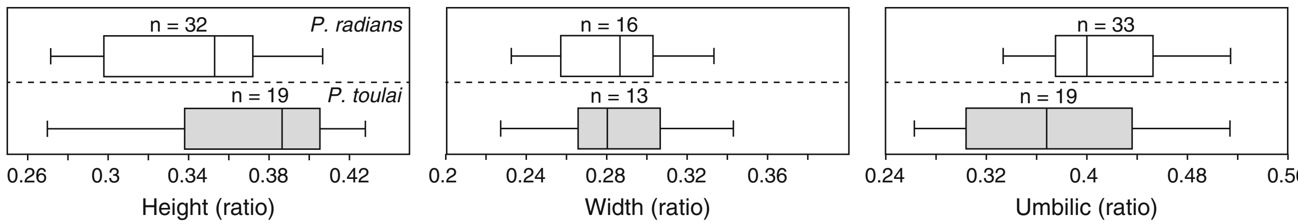

Fig. 22 Box plots of *H/D*, *W/D* and *U/D* for *Preflorianites toulai* from Utah, Nevada and the Caucasus (this work, Kummel and Steele 1962 and Shevyrev 1995, respectively) and *P. radians* from Primorye, South China and Oman (Zakharov 1968, Brayard and Bucher 2008 and Brühwiler et al. 2012a, respectively)

covariation, which Westermann (1966) coined to account for the varying degrees of intraspecific variation commonly observed in coiled ammonoids (e.g., Dagys and Weitschat 1993; Kennedy and Cobban 1976; Monnet and Bucher 2005; Monnet et al. 2010; Weitschat 2008).

Genus ***Kashmirites*** Diener, 1913
Type species Celtites armatus Waagen, 1895

Kashmirites utahensis **sp. nov.**
Fig. 20i

Holotype UBGD 275017 (Fig. 20i), loc. DV2-3E, Pahvant Range, *Inyoites beaverensis* sp. nov. beds, Smithian.

Derivation of name Species name refers to the State of Utah.

Diagnosis Rather thick, evolute and markedly ornamented kashmiritid differing from the type species by a shallower umbilicus and dense ribs on inner whorls becoming distant fold-like ribs on outer whorls.

Occurrence Extremely rare. One incomplete specimen found in the Pahvant Range within the *Inyoites beaverensis* sp. nov. beds [DV2-3E].

Description Evolute and rather thick shell with an apparent subtabulate or slightly arched venter. Ventral shoulders not well preserved, but flanks appear almost parallel. Umbilicus rather shallow with an inclined wall and rounded margins. Our unique specimen exhibits conspicuous, radial and dense ribs on inner whorls that are transformed on outer whorls into large, regularly spaced folds. Suture line unknown.

Measurements Not possible. Estimated maximum size: ~5 cm.

Discussion The overall shape of this species is close to most *Kashmirites* species, but mainly differs by its inclined umbilical wall and ornamentation that fades on outer whorls. This type of ornamentation resembles that of *Kashmirites guangxiense* described from South China (Brayard and Bucher 2008).

Kashmirites confusionensis **sp. nov.**
Fig. 23a–f

Holotype UBGD 275018 (Fig. 23a–c), loc. DH1-2, Confusion Range, *Preflorianites–Kashmirites* beds, Smithian.

Derivation of name Species name refers to the Confusion Range.

Diagnosis Large, evolute kashmiritid with a simplified suture line, an apparent arched venter and dense, regularly spaced ribs that do not fade away on outer whorls.

Occurrence Rather common in the *Preflorianites–Kashmirites* beds of the Confusion Range, but often only body chambers are preserved.

Description Large, evolute discoidal shell with an apparent arched venter. Venter appears more subtabulate on robust variant. Ventral shoulders rounded, with almost parallel flanks. Umbilicus large and moderately shallow with a vertical wall and rounded margins. Ornamentation consists of conspicuous, radial and regularly spaced ribs that do not fade on outer whorls. Ribs apparently do not cross the venter. Simplified ceratitic suture line with only two large lateral saddles.

Measurements See Table 1. Estimated maximum size: ~7 cm.

Discussion This species can be distinguished from other *Kashmirites* species by its simplified suture line architecture. It also mainly differs from *K. utahensis* sp. nov. by its regularly spaced ornamentation that does not fade on outer whorls. *K. confusionensis* sp. nov. may be easily confused with *Preflorianites toulai* if specimens are weathered.

Kashmirites stepheni **sp. nov.**
Fig. 23g–j

Holotype UBGD 275020 (Fig. 23g, h), loc. DV2-2, Pahvant Range, *Preflorianites–Kashmirites* beds, Smithian.

Derivation of name Species named after Daniel A. Stephen (Utah Valley University).

Diagnosis Rather compressed kashmiritid with an arched venter, an apparent egressively coiled final portion of mature body chambers and variable, conspicuous ribbing.

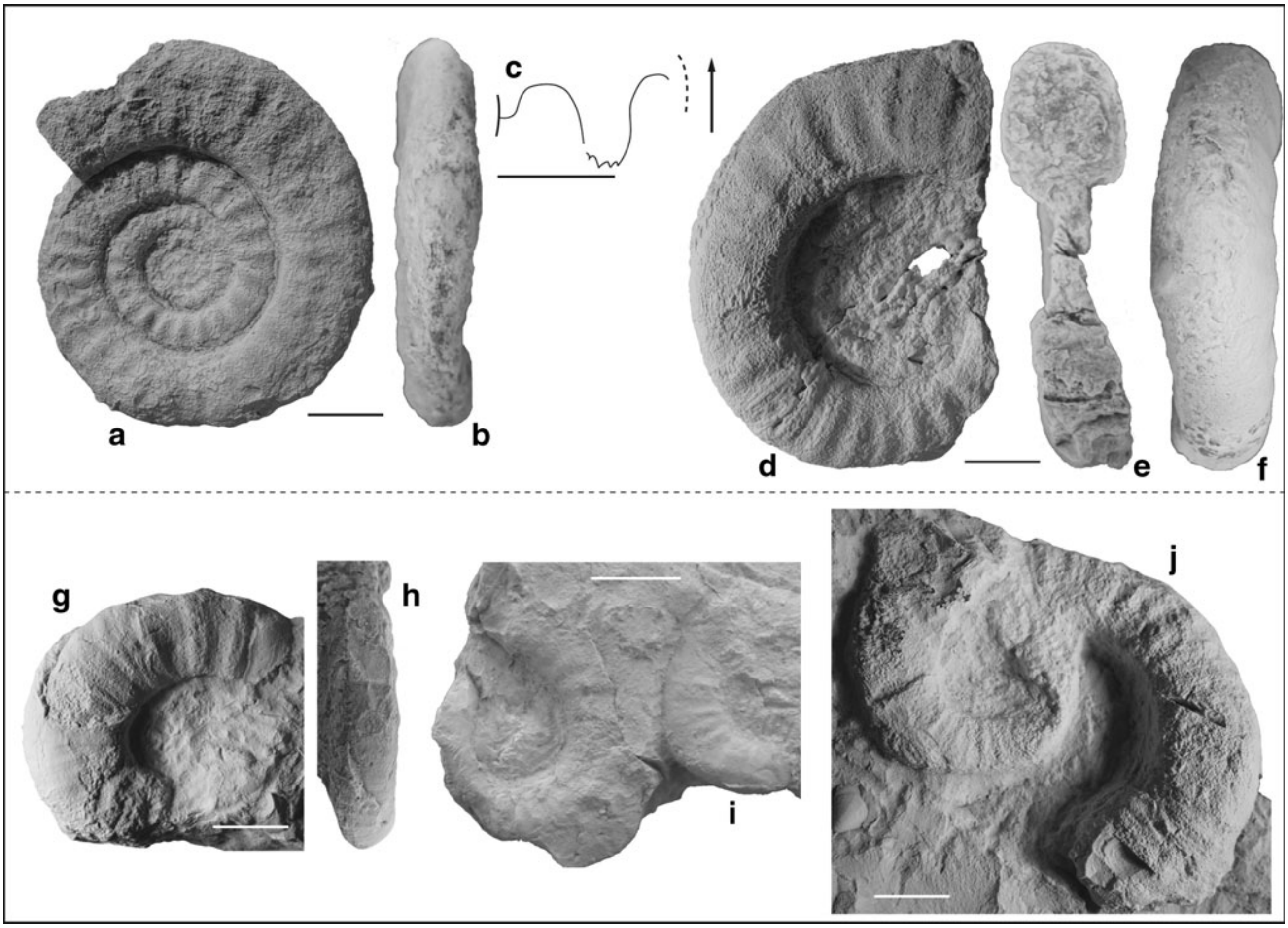

Fig. 23 **a–f** *Kashmirites confusionensis* sp. nov. All from loc. DH1-2, Confusion Range. *Preflorianites–Kashmirites* beds, Smithian; **a–c** UBGD 275018, holotype; **c** *scale bar* is 5 mm ($H = 10$ mm); **d–f** UBGD 275019, paratype. **g–j** *Kashmirites stepheni* sp. nov. All from the *Preflorianites–Kashmirites* beds, Smithian; **g**, **h** UBGD 275020, holotype, loc. DV2-2, Pahvant Range; **i** UBGD 275021, paratype, loc. DV2-2, Pahvant Range; **j** UBGD 275022, paratype, loc. SR21, Star Range

Occurrences Body chambers are common in the Pahvant Range [DV2-2] and Star Range [SR21] within the *Preflorianites–Kashmirites* beds.

Description Moderately evolute shell exhibiting apparent egression, that becomes less curved and straighter on body chambers. Whorl section rather rectangular with an apparent arched venter. Flanks almost parallel and gradually converging toward venter, whose ventral shoulders are indistinct. Umbilicus unknown as inner whorls are not preserved on our specimens. Umbilical wall appears high and slightly oblique with rounded shoulders. Ornamentation consists of conspicuous, radial and unevenly spaced ribs and plications fading on ventral margins. Rib strength changes during ontogeny with stronger ribs at maturity. Suture line unknown.

Measurements Not possible. Estimated maximum size: $\sim$6 cm.

Discussion This new species mainly differs from other kashmiritid taxa by its arched venter, its irregular ornamentation and its unique apparent egressively coiled ending on large body chambers.

Genus ***Hanielites*** Welter, 1922
Type species Hanielites elegans Welter, 1922.

Hanielites **sp. indet.**
Fig. 24a–c

Occurrence Extremely rare. One incomplete specimen found in the Pahvant Range within the *Owenites* beds [DV2-6].

Description Moderately involute, compressed shell with an apparent arched venter. Ventral shoulders are rounded and flanks are parallel. Umbilicus shallow with a gently sloping wall and rounded margins. Ornamentation consists of slightly sinuous, radial ribs alternating with rare thin plications. Some ribs are projected forward near the ventral margin and may cross the venter. Other ribs fade before reaching the venter. Suture line unknown.

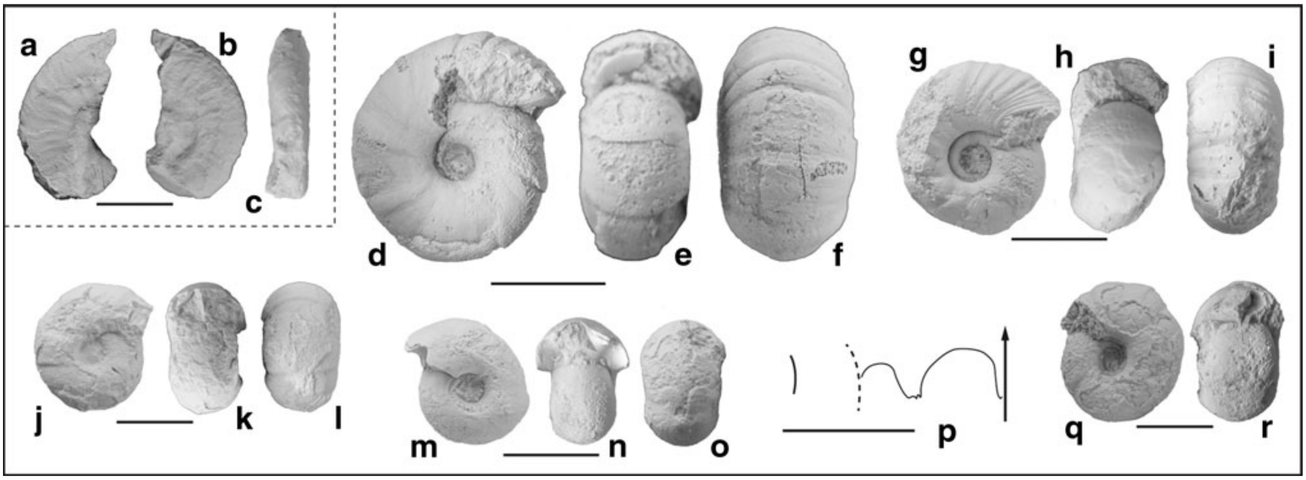

Fig. 24 **a–c** *Hanielites* sp. indet., UBGD 275023, loc. DV2-6, Pahvant Range, *Owenites* beds, Smithian; **d–r** *Juvenites* cf. *thermarum* (Smith 1927). All from the *Owenites* beds, *Inyoites oweni* horizons, Smithian; **d–f** UBGD 275024, loc. DH1-11, Confusion Range; **g–i** UBGD 275025, loc. DH1-11, Confusion Range; **j–l** UBGD 275026, loc. DH1-12, Confusion Range; **m–p** UBGD 275027, loc. DH1-11, Confusion Range; **p** *scale bar* is 5 mm ($H = 5$ mm); **q**, **r** UBGD 275028, loc. DH1-12, Confusion Range

Measurements Not possible. Estimated maximum size: ~2.5 cm.

Discussion Our specimen exhibits a few characters reminiscent of *Hanielites* species from South China (see Brayard and Bucher 2008) such as the compressed shell and alternation of ribs and plications. However, it apparently differs from these species by the absence of a keeled or triangular venter, thus preventing a specific taxonomic assignment. The occurrence of *Hanielites* species is also rare in South China, but they are probably present in Utah within time-correlative horizons of the *Owenites* beds.

Family Melagathiceratidae Waagen, 1895
Genus ***Juvenites*** Smith, 1927
Type species Juvenites kraffti Smith, 1927

Juvenites* cf. *thermarum (Smith, 1927)
Fig. 24d–r

1927 *Thermalites thermarum*; Smith, p. 24, pl. 21, figs. 11–20.
1932 *Prenkites depressus*; Smith, p. 110, pl. 31, figs. 16–18.
1932 *Thermalites thermarum*; Smith, p. 111, pl. 21, figs. 11–20.
? 1962 *Juvenites thermarum*; Kummel and Steele, p. 689, pl. 100, figs. 12, 13.
? 1973 *Arnautoceltites thermarum*; Collignon, p.17, pl. 4, fig. 10.
v 2007 *Paranannites* sp. indet.; Klug et al., p. 1467, text-fig. 4A–E.
2010 *Juvenites septentrionalis*; Stephen et al., fig. 5k-, l.
2012a *Juvenites* cf. *thermarum*; Brühwiler et al., p. 40, pl. 22, figs. 1–9.

Occurrence Present but not abundant in the Confusion Range [$n = 7$; DH1-12, DH1-10/11], Pahvant Range [$n = 3$; DV1-9, DV1-8] and Torrey area [$n = 2$; FFA1], *Owenites* beds, *Inyoites oweni* beds. Not documented from other studied sections.

Description Globose and involute shell with a slightly evolute coiling. Venter rounded. Umbilicus relatively deep with perpendicular wall and broadly rounded shoulders. Ornamentation consists of distant, forward projected constrictions that cross the venter in varying strength. Suture line ceratitic and very simple with two broad, asymmetrical saddles.

Measurements See Figs. 25 and 26. Estimated maximal size: ~4 cm.

Discussion Species included within *Juvenites* are often extremely hard to distinguish, especially at small juvenile sizes. Moreover, these taxa also display a wide range of intraspecific variation and consequently, their species diagnoses sometimes overlap. Pending a thorough revision of *Juvenites* species based on the robust statistics of coiling geometry of a sufficient number of specimens, we follow here the species definition of Smith (1932) and the rare measurements published by, e.g., Kummel and Steele (1962) for American species.

J. cf. *thermarum* differs from the type species and *J. septentrionalis* (Smith, 1927) by its more involute coiling and more depressed whorl section (Fig. 26). A comparison with measurements published by Brühwiler et al. (2012a) for *J.* cf. *thermarum* yield rather similar results, but the

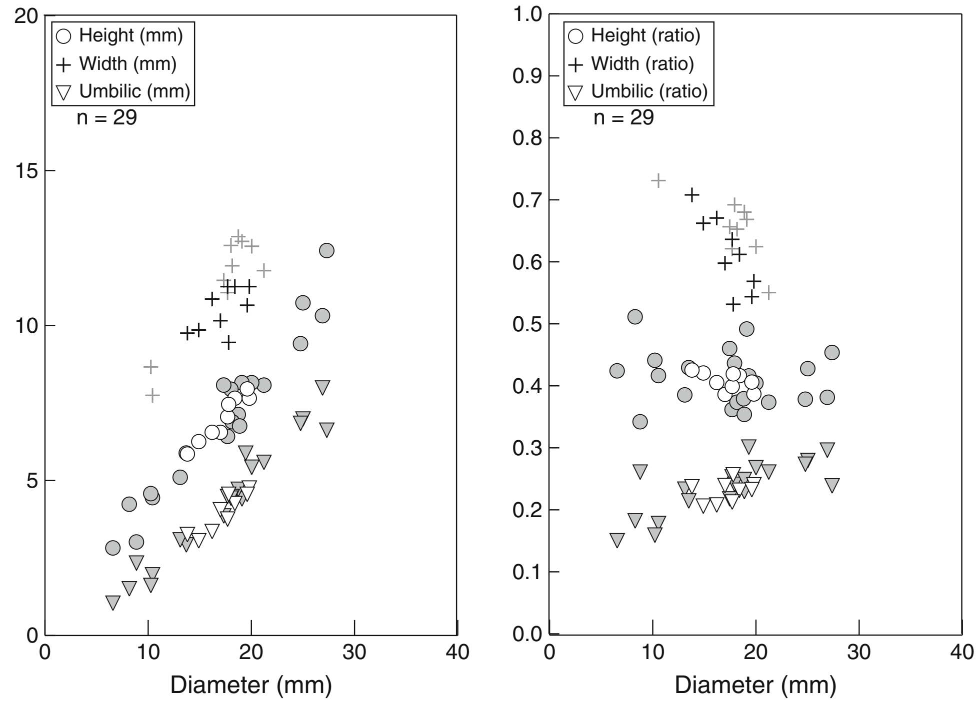

Fig. 25 Scatter diagrams of *H*, *W* and *U*, and *H*/*D*, *W*/*D* and *U*/*D* for *Juvenites* cf. *thermarum* (*open symbols* indicate specimens from the Confusion Range and Pahvant Range, *Owenites* beds, *Inyoites oweni* horizons [$n = 9$]; *grey symbols* indicate specimens from Oman; data from Brühwiler et al. 2012a [$n = 20$])

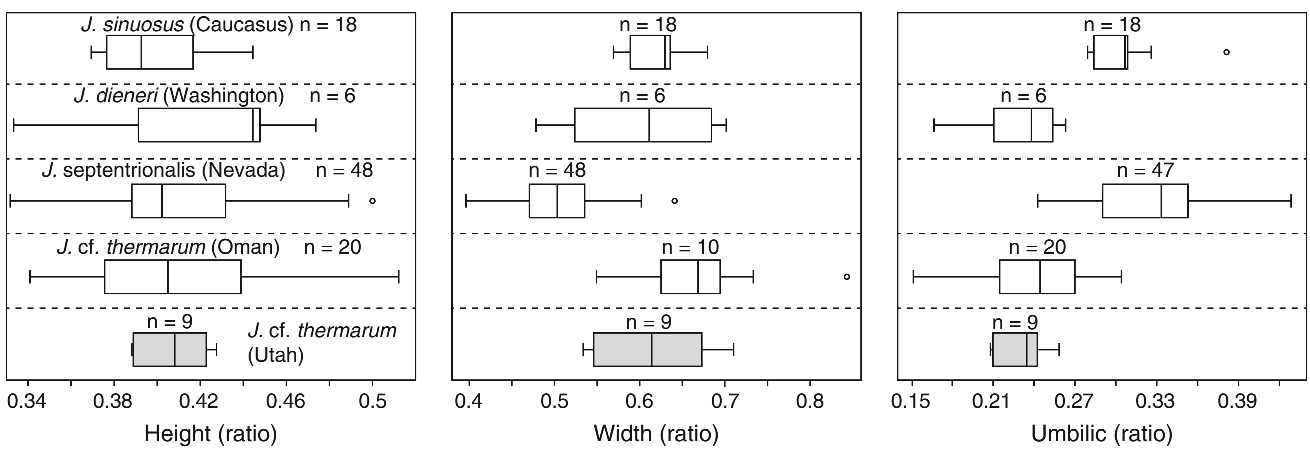

Fig. 26 Box plots of *H*/*D*, *W*/*D* and *U*/*D* for *Juvenites sinuosus* from the Caucasus (Shevyrev 1995), *J. dieneri* from the State of Washington (USA; Kuenzi 1965), *J. septentrionalis* from Nevada (Kummel and Steele 1962) and *J. thermarum* from Oman and Utah (Brühwiler et al. 2012a and this work, respectively)

American specimens are probably slightly more depressed. The relatively few measurements of Kummel and Steele (1962) for *J. thermarum* are more disparate with more extreme variants preventing a strict a comparison of the three collections.

Juvenites spathi (Frebold 1930) and *J. procurvus* Brayard and Bucher (2008) differ respectively from other species included in the genus by a triangular venter and much stronger, more closely spaced constrictions (see Brayard and Bucher 2008 and Brühwiler et al. 2012a).

J. sinuosus Shevyrev (1995) documented from the Caucasus displays a depressed conch similar to *J. thermarum*, but its coiling involution is closer to *J. septentrionalis* (Fig. 26).

Based on their more or less depressed coiling and their involution, *J. dieneri* (Hyatt and Smith 1905) may be conspecific with *J. thermarum* (Fig. 26), and *J. sanctorum* Smith (1932) with *J. septentrionalis*. This partly agrees with the discussion of Kummel and Steele (1962) regarding the distinction of American *Juvenites* species. However, without additional measurements from the original material, this hypothesis must remain uncorroborated.

Juvenites* aff. *spathi (Frebold, 1930)
Fig. 27a–c

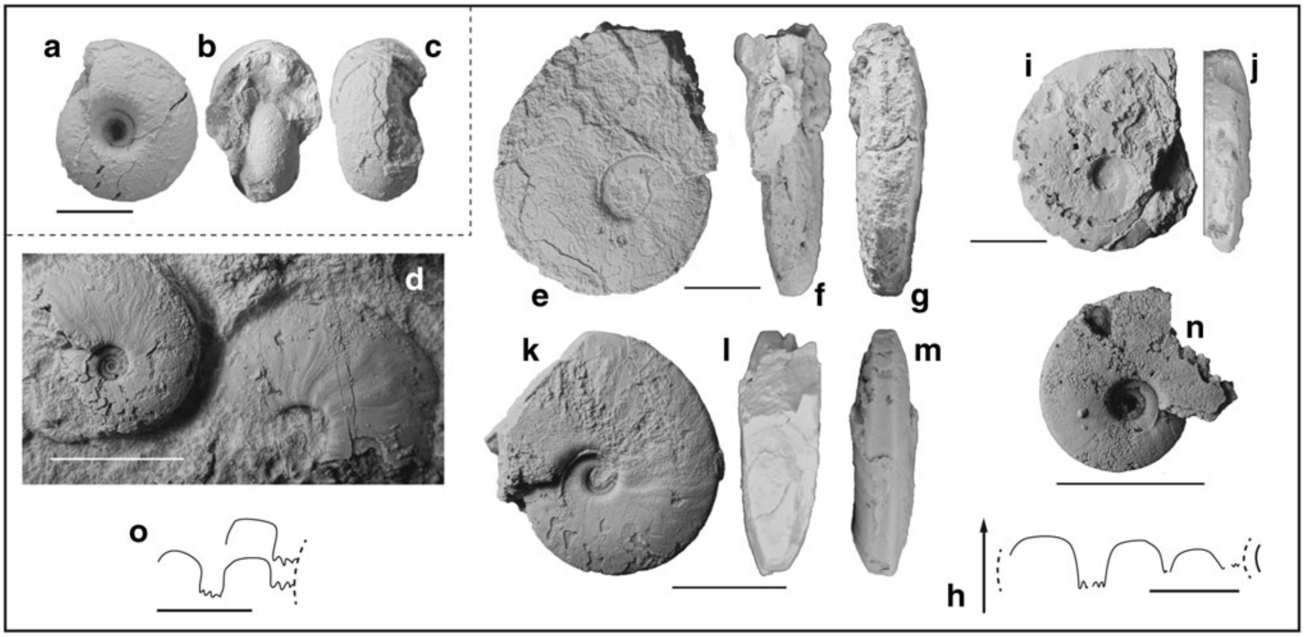

Fig. 27 **a–c** *Juvenites* aff. *spathi* (Frebold 1930), UBGD 275029, Loc. FFA1, Torrey area, *Owenites* beds, below the *Inyoites oweni* horizons, Smithian. **d–o** *Vercherites undulatus* sp. nov. All from loc. MIA1, Mineral Mountains, *Vercherites undulatus* sp. nov. beds, Smithian; **d** UBGD 275030, paratype; **e–g** UBGD 275031, holotype; **h** *scale bar* is 5 mm ($H = 14.6$ mm); **i, j** UBGD 275032, paratype; **k–m** UBGD 275033, paratype; **n** UBGD 275034, paratype; **o** suture line of UBGD 275035, paratype, *scale bar* is 5 mm ($H = 13.3$ mm)

1930 *Prosphingites spathi*; Frebold, p. 20, pl. 4, figs. 2, 3, 3a.
1934 *Prosphingites spathi*; Spath, p. 195, pl. 13, figs. 1, 2.
p? 1959 *Prosphingites kwangsianus*; Chao, p. 296, pl. 28, figs. 17, 18.
p? 1959 *Prosphingites sinensis*; Chao, p. 297, pl. 27, figs. 14–17, text-fig. 40a.
? 1961 *Prosphingites spathi*; Tozer, p. 58, pl. 13, figs. 1, 2.
? 1982 *Prosphingites spathi*; Korchinskaya, pl. 5, fig. 2.
? 1994 *Paranannites spathi*; Tozer, p. 77, pl. 36, figs. 1, 2.
v. 2008 *Paranannites spathi*; Brayard and Bucher, p. 63, pl. 35, figs. 10–19.
v. 2010b *Paranannites spathi*; Brühwiler et al., p. 426, fig. 16(1, 2).
v. 2012a *Juvenites spathi*; Brühwiler and Bucher, p. 38, pl. 22, figs. 12–17.
v. 2012b *Juvenites* cf. *spathi*; Brühwiler et al., p. 161, figs. 37A–O.

Occurrence Present within the Torrey area [$n = 8$; only 3 measurable], *Owenites* beds, below the *Inyoites oweni* beds. Not documented from other studied sections.

Description Globose and moderately evolute shell with an arched venter. Flanks gradually converge to venter from abruptly rounded umbilical shoulder. Deep, funnel-like umbilicus with high, perpendicular wall and broadly rounded shoulders. Ornamentation barely visible but consists of very weak, dense, forward projected folds (constrictions?) that are more evident on umbilical margins of largest specimens. Suture line ceratitic, with two main, broad saddles, but too poorly preserved to be illustrated.

Measurements See Figs. 28 and 29. Estimated maximal size: ~3 cm (Utah specimens).

Discussion Typical large-size specimens of *Juvenites* (*Paranannites*) *spathi* display a triangular whorl section and a marked crateriform umbilicus (see Frebold 1930 and discussion in Brayard and Bucher 2008). However, Korchinskaya (1982), Brühwiler et al. (2010b, 2012b) and Tozer (1994) illustrated more compressed variants with only an arched venter and attribute them to the species. Our specimens from the Torrey area also exhibit a large rounded venter but the coiling is very similar to the species features, especially the funnel-like umbilicus. Although the ornamentation is not well visible compared to other known specimens, which is probably due to their poor preservation, we tentatively assign our specimens to *J. spathi*. Specimens from Oman (Brühwiler et al. 2012a) also appear slightly more involute than South Chinese specimens (Brayard and Bucher 2008) (Fig. 29).

Kummel and Steele (1962) defined a "*Prosphingites*" *slossi* species (*Prosphingites* is normally considered as a Spathian taxon) displaying at first sight characteristics close to *J. spathi*, the main difference apparently being a slightly more evolute and compressed coiling (Fig. 29).

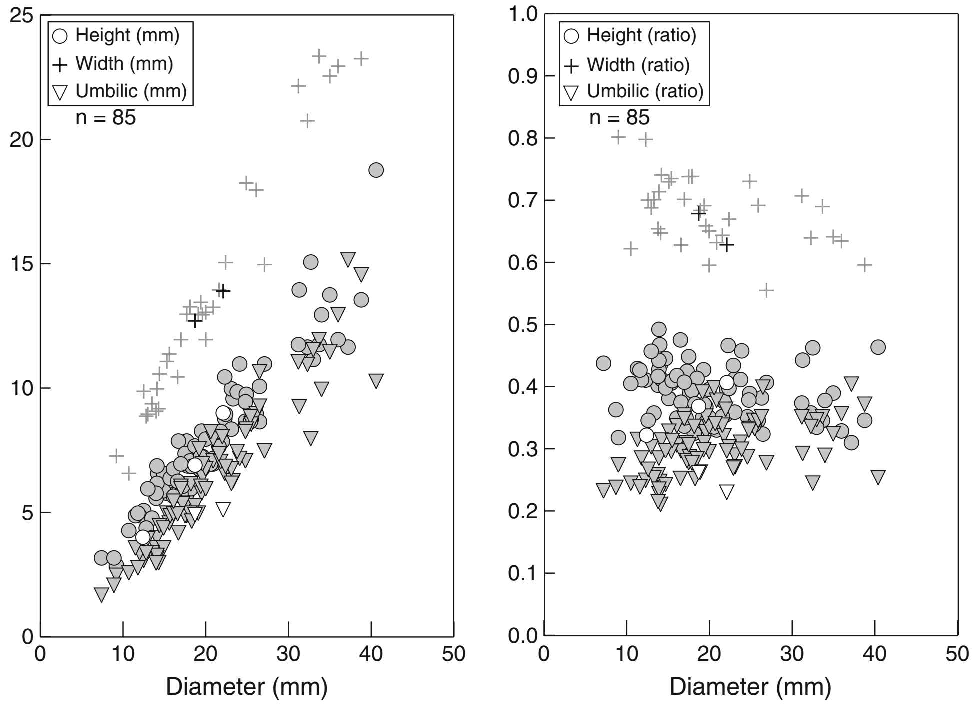

Fig. 28 Scatter diagrams of *H*, *W* and *U*, and *H*/*D*, *W*/*D* and *U*/*D* for *Juvenites* aff. *spathi* (*open symbols* indicate specimens from the Torrey area, base of the *Owenites* beds, below *Churkites* and *Guodunites* occurrences [$n = 3$]; *grey symbols* indicate specimens from South China and Oman; data respectively from Brayard and Bucher 2008 and Brühwiler et al. 2012a [$n = 82$])

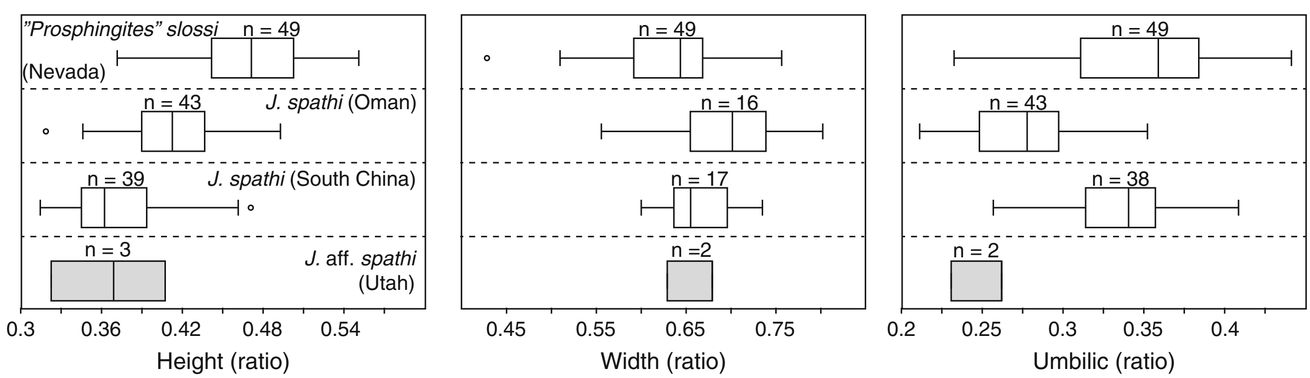

Fig. 29 Box plots of *H*/*D*, *W*/*D* and *U*/*D* for *Juvenites* aff. *spathi* from Utah (this work), *J. spathi* from South China (Brayard and Bucher 2008) and Oman (Brühwiler et al. 2012a) and the morphologically close taxon *"Prosphingites" slossi* from Nevada (Kummel and Steele 1962)

Juvenites spathi is found worldwide near the base of the *Owenites* beds (e.g., *Brayardites compressus* and *Nammalites pilatoides* beds in Spiti; Brühwiler et al. 2012b), which is apparently the same for Utah (below occurrence of *Churkites* and *Guodunites*).

Family Galfettitidae Brühwiler and Bucher in Brühwiler et al. 2012a

Genus ***Vercherites*** Brühwiler et al. 2010c

Type species Koninckites vercherei Waagen, 1895

Vercherites undulatus **sp. nov.**

Fig. 27d–o

Holotype UBGD 275031 (Fig. 27e–h), loc. MIA1, Mineral Mountains, *Vercherites undulatus* sp. nov. beds, Smithian.

Derivation of name Species name refers to its folded ornamentation.

Diagnosis Moderately involute *Vercherites* species, similar to *V. pulchrum*, but with a simplified auxiliary series in the suture line and exhibiting weak folds on flanks.

Occurrence Abundant in the Mineral Mountains within the *Vercherites undulatus* sp. nov. beds [MIA1].

Description Moderately involute, compressed shell with an almost triangular whorl section. Inner whorls are tightly coiled and umbilicus gradually opens during ontogeny. Venter tabulate with nearly angular shoulders. Flanks convex with maximum curvature at mid-flank. Umbilicus moderately deep with a high vertical wall and rounded margins. Ornamentation consists of regularly spaced, weak

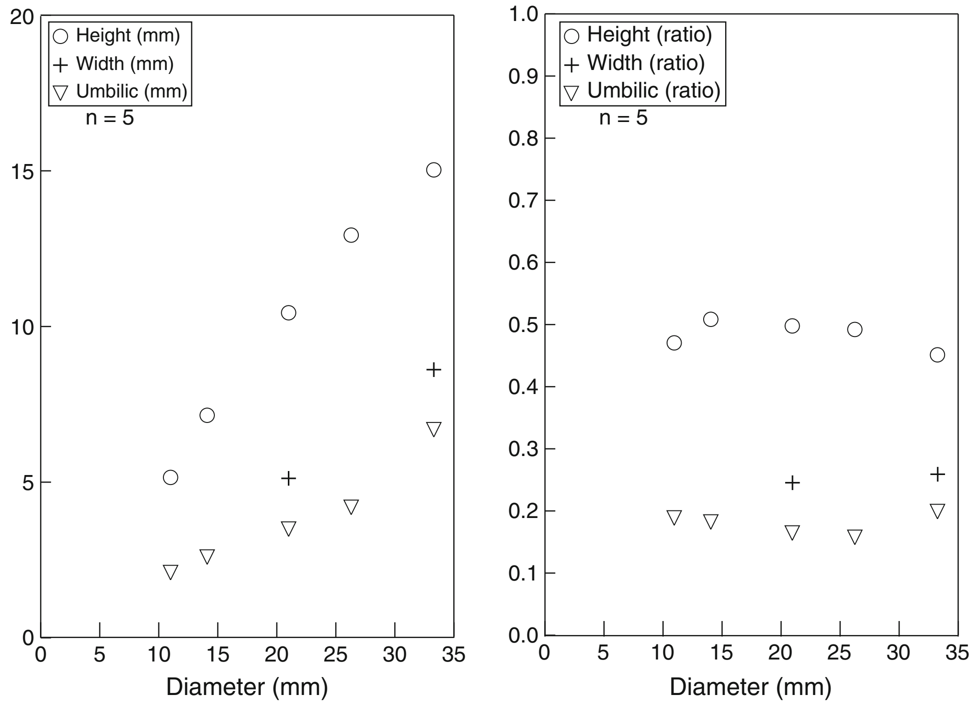

Fig. 30 Scatter diagrams of *H*, *W* and *U*, and *H*/*D*, *W*/*D* and *U*/*D* for *Vercherites undulatus* sp. nov. (all specimens from Mineral Mountains, *Vercherites undulatus* bed)

sinuous folds. Surface apparently smoother at small size. Suture line ceratitic with broad second and third lateral saddles and finely indented lobes. A very small auxiliary series is present.

Measurements See Fig. 30. Estimated maximal size: ~7 cm.

Discussion Our specimens show strong similarities with *V. pulchrum* from the North Indian Margin (Brühwiler et al. 2010c, 2012c) such as the involute coiling at the juvenile stages. However, they mainly differ by their weak folds on flanks, thus justifying the erection of a new species. Moreover, the auxiliary series of the suture line appears very simplified (rest of suture line is rather similar). It differs from the type species by its more involute coiling. *Vercherites vercherei* and *V. pulchrum* also ostensibly reached much larger sizes (>10 cm; e.g., Brühwiler et al. 2012c).

In comparison with ammonoid assemblages from the North Indian Margin (e.g., Brühwiler et al. 2012c), the occurrence of *V. undulatus* sp. nov. probably represents the oldest Smithian ammonoid fauna found in Utah.

Family Gyronitidae Waagen, 1895
Genus ***Radioceras*** Waterhouse, 1996
Type species Meekoceras radiosum Waagen, 1895

Radioceras* aff. *evolvens (Waagen, 1895)
Fig. 31a–k

1895 *Aspidites evolvens*; Waagen, p. 223, pl. 25, figs. 1.
1895 *Aspidites discus*; Waagen, p. 228, pl. 25, figs. 2.
1895 *Meekoceras radiosum*; Waagen, p. 257, pl. 36, fig. 2a–d.
2012c *Radioceras evolvens*; Brühwiler and Bucher, p. 51, figs. 30A–G, 31A–P.

Occurrence Common in the Pahvant Range, within the *Radioceras* aff. *evolvens* beds [DV2-202]. Not found in other studied sections.

Description Involute and compressed shell exhibiting convex, convergent flanks. Venter is tabulate with angular shoulders at small size. Ventral margins and venter become more subtabulate to rounded at large size. Umbilicus rarely preserved and often crushed on our specimens but appears very narrow with rounded shoulders. Surface apparently smooth. Suture line typical with deeply indented lobes and a well-individualized auxiliary series. Second lateral saddle slightly elongated toward the umbilicus.

Measurements Not possible. Estimated maximum size: ~15 cm.

Discussion The overall shape of our specimens and their suture lines closely resemble *Radioceras evolvens* from the Salt Range (see Brühwiler et al. 2012c). However, since most of our specimens consist of crushed fragments with imperfect preservation, a definitive assignment to *R. evolvens* is not possible. *R. evolvens* is very similar *to R. kraffti*, but apparently differs by its more egressive coiling and a well-individualized auxiliary series (Brühwiler et al. 2012c). *R.* aff. *evolvens* represents one of the oldest Smithian ammonoid assemblage found in Utah and by

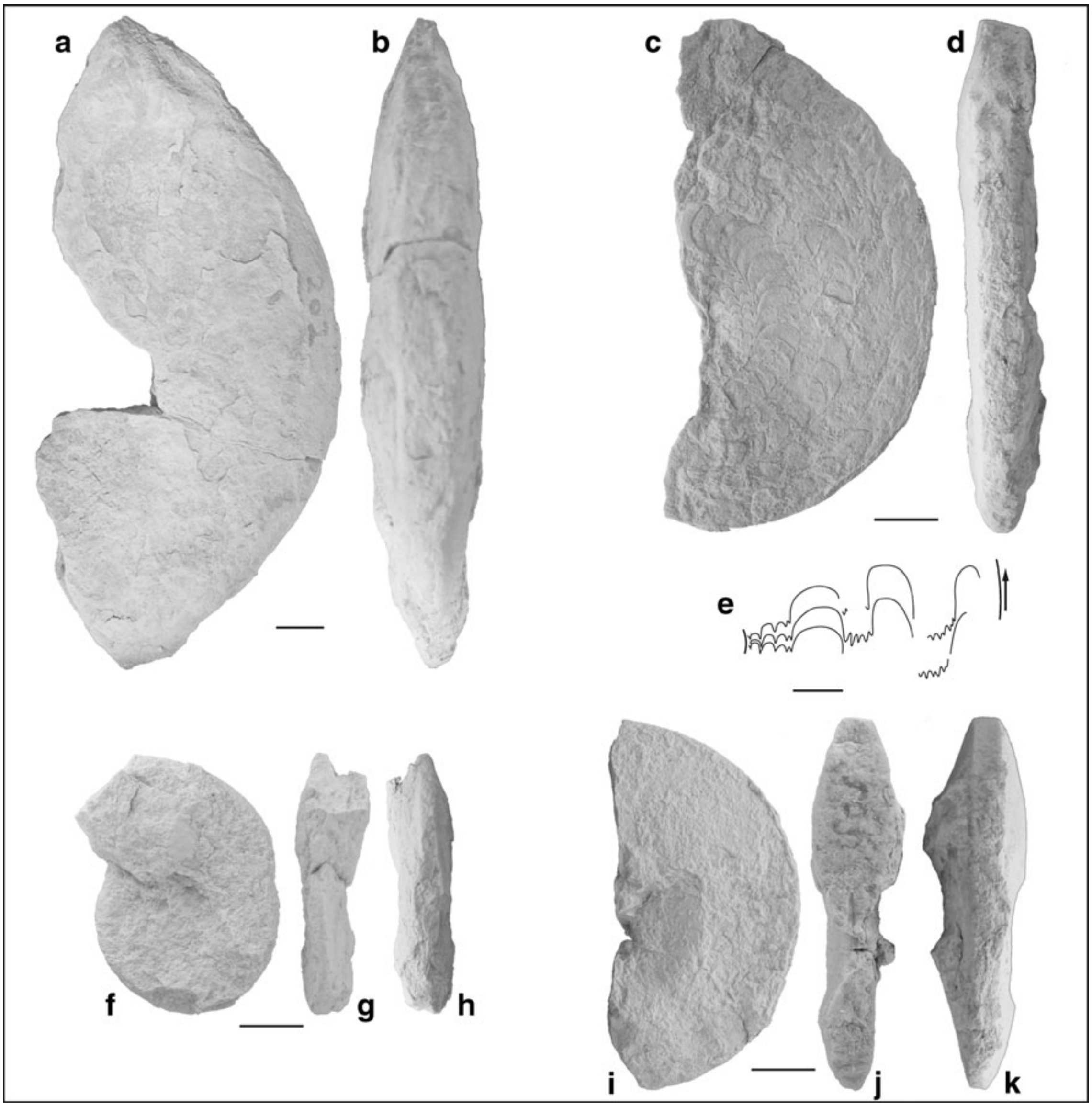

Fig. 31 **a**–**k** *Radioceras* aff. *evolvens* (Waagen 1895). All from loc. DV2-202, Pahvant Range, *Radioceras* aff. *evolvens* beds, Smithian. **a**, **b** UBGD 275036; **c**–**e** UBGD 275037; **e** *scale bar* is 5 mm ($H = 40$ mm); **f**–**h** UBGD 275038; **i**–**k** UBGD 275039

correlation with time-equivalent beds from the North Indian Margin (Brühwiler et al. 2010a, 2012c), it is likely representative of the late early Smithian (Fig. 14).

Family Proptychitidae Waagen, 1895
Genus ***Guodunites*** Brayard and Bucher, 2008
Type species Guodunites monneti Brayard and Bucher, 2008

Guodunites hooveri (Hyatt and Smith, 1905)

See Brayard et al. (2009a) for thoroughly illustrated specimens from the Confusion Range

1905 *Aspidites hooveri*; Hyatt and Smith, p. 153, pl. 17, figs. 1–12.
1932 *Clypeoceras hooveri*; Smith, p. 63, pl. 17, figs. 1–12.
v 2009a *Guodunites hooveri*; Brayard et al., p. 476, pl. 2, figs. 1–30.
v 2010 ?*Clypeoceras hooveri*; Stephen et al., figs. 6e, f, i.

Occurrence Common in Confusion Range [DH1-12, DH1-10/11, DH1-9], Pahvant Range [DV1-9, DV1-8, DV2-7, DV2-6], Mineral Mountains [MIA9, MIA8] and rare in the Torrey area [FF78-83]. Always found within the *Owenites* beds. Also within the *Meekoceras* beds, *Owenites* subzone, Union Wash (Inyo Range, California, USA).

Description For a thorough description with illustrations, reader should refer to Brayard et al. (2009a). Taxon's main characteristics are (a) involute, platycone shell with a

Fig. 32 Scatter diagrams of *H*, *W* and *U*, and *H*/*D*, *W*/*D* and *U*/*D* for *Guodunites hooveri* (all specimens from the Confusion Range and Pahvant Range, *Owenites* beds, *Inyoites oweni* horizon)

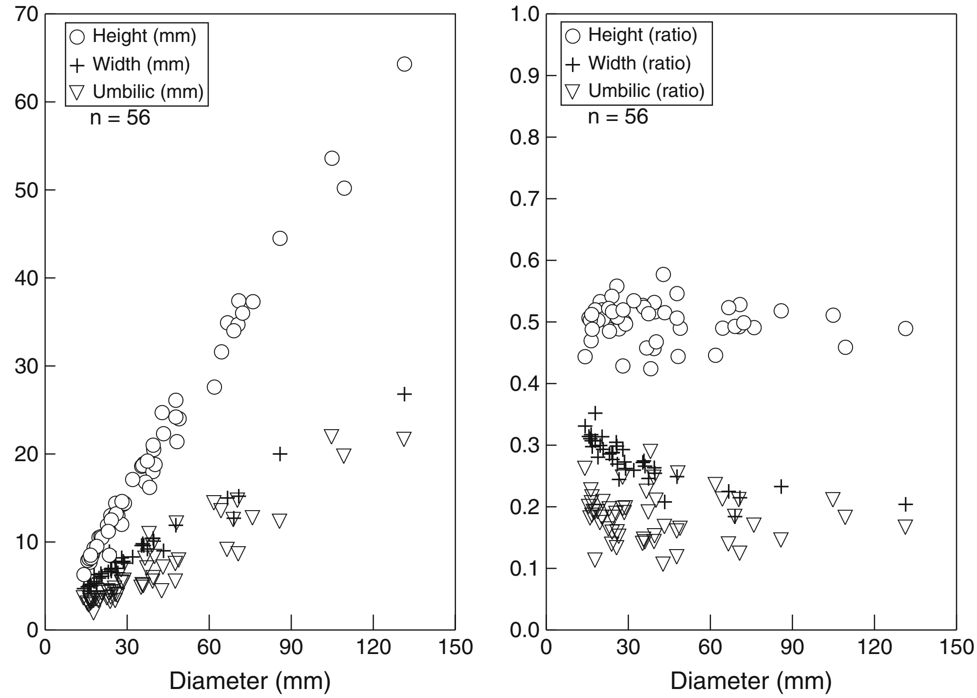

narrowly rounded venter, (b) slightly convex flanks with maximum thickness near mid-flanks, (c) egressive coiling at submature stage, (d) a deep, crateriform umbilicus, (e) projected lirae on outer shell.

On inner whorls, bundled lirae may impart weak folds on flanks. Well-preserved specimens are ornamented with a very delicate strigation (see Brayard et al. 2009a). Suture line subammonitic with delicately crenulated saddles. The architecture of the suture line is similar among species belonging to this genus, especially to that of *Guodunites monneti* from Guangxi, South China (see Brayard et al. 2009a).

Measurements See Fig. 32. Brayard et al. (2009a) estimated its maximum size to be ~20 cm. However, a maximal size about 15 cm is probably more correct.

Discussion Guodunites hooveri is distinguished from *G. monneti* from South China by its deeper umbilicus and its more involute coiling. Strong projected lirae are also visible for all ontogenic stages. In contrast with its occurrence at the relatively close Crittenden Springs (Nevada) location, *G. monneti* appears to not occur in Utah. As previously discussed by Brayard et al. (2009a), this genus is restricted to the late middle Smithian, and to date, its biogeographical distribution comprises only Oman, South China, Nevada, Utah and California thus indicating an essentially low paleolatitudinal distribution. Moreover, its paleobiogeographical distribution further strengthens the existence of significant equatorial faunal exchanges by oceanic currents between both sides of the Panthalassa at that time (Brayard et al. 2006, 2007b, 2009b; Jenks 2007; Jenks et al. 2010).

Genus ***Wailiceras*** Brayard and Bucher, 2008

Type species Wailiceras aemulus Brayard and Bucher, 2008.

Wailiceras* cf. *aemulus

Fig. 33a–e

Occurrence Very rare. Two specimens found in the Confusion Range within the *Inyoites beaverensis* sp. nov. beds [DH1-5].

Description Involute and discoidal shell with a tabulate venter and egressive coiling. Ventral shoulders are angular. Flanks are slightly convex with maximum curvature near mid-flank. Umbilical wall rather high and perpendicular with abruptly rounded shoulders. Ornamentation consists of very weak radial plications on outer whorls of one specimen. Suture line with elongated saddles and a small auxiliary series. First lateral saddle rather large.

Measurements See Fig. 34. Estimated maximum size: ~8 cm.

Discussion Brayard and Bucher (2008) thoroughly discussed and illustrated *Wailiceras aemulus* from South China. This taxon closely resembles poorly preserved specimens of *Meekoceras* species. *W. aemulus* mainly differs by its more involute coiling, its vertical umbilical wall and its suture line displaying more elongated saddles and an auxiliary series. Weak plications resembling

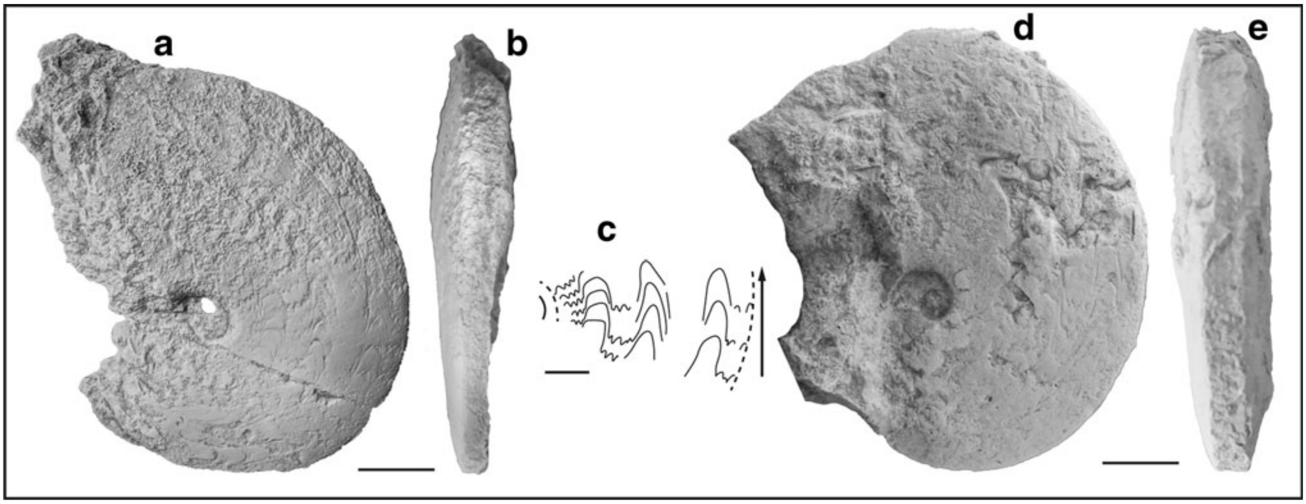

Fig. 33 **a–e** *Wailiceras* cf. *aemulus* Brayard and Bucher 2008. All from loc. DH1-5, Confusion Range, *Inyoites beaverensis* sp. nov. beds, Smithian. **a–c** UBGD 275040; **c** *scale bar* is 5 mm ($H = 23.9$ mm); **d, e** UBGD 275041

Fig. 34 Scatter diagrams of *H*, *W* and *U*, and *H*/*D*, *W*/*D* and *U*/*D* for *Wailiceras* cf. *aemulus*. Measured specimens from the Confusion Range are indicated by *white symbols* (*Inyoites beaverensis* sp. nov. beds). Other data in *grey* are from South China (“*Kashmirites kapila* beds” [$n = 11$]; Brayard and Bucher 2008)

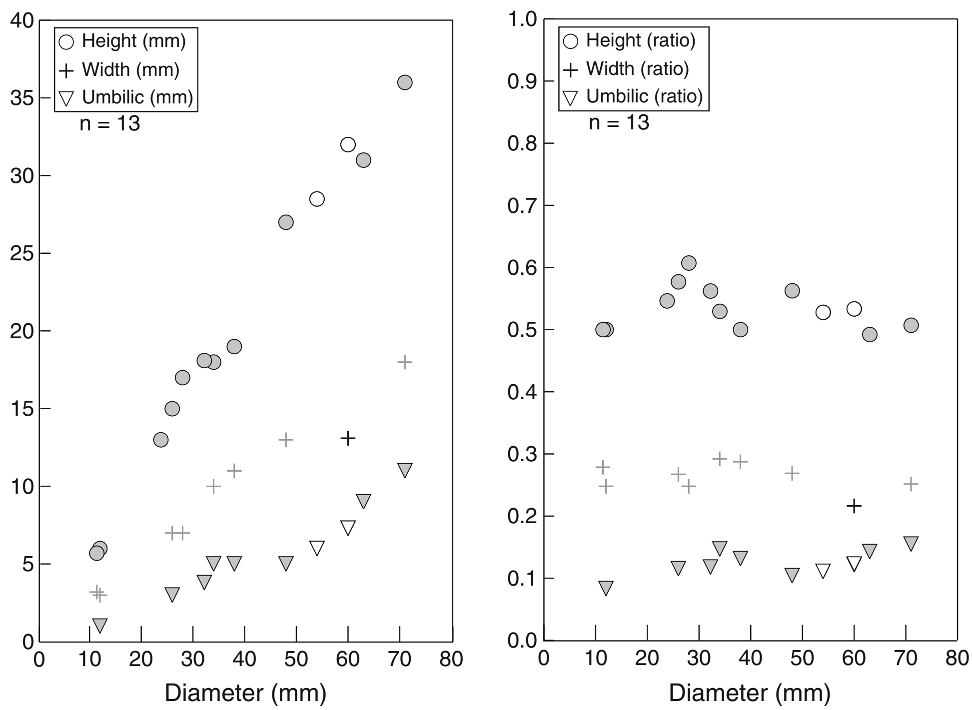

ornamentation of *W. aemulus* are visible on one specimen, thus also suggesting strong affinities with specimens from South China. However, due to the poor overall preservation and the restricted number of specimens, a definite assignment to the type species is precluded at this time. The occurrence of *W.* cf. *aemulus* in Utah is younger than in South China (“*Kashmirites kapila* beds”; Brayard and Bucher 2008).

Genus ***Xiaoqiaoceras*** Brayard and Bucher, 2008
Type species Xiaoqiaoceras involutus Brayard and Bucher, 2008

***?Xiaoqiaoceras americanum* sp. nov.**
Fig. 35a–c

Holotype UBGD 275042 (Fig. 35a–c), loc. DH1-11, Confusion Range, *Owenites* beds, *Inyoites oweni* horizons, Smithian.

Derivation of name Species name refers to its American occurrence.

Diagnosis Small moderately involute proptychitid with a characteristic suture line, but differing from the type

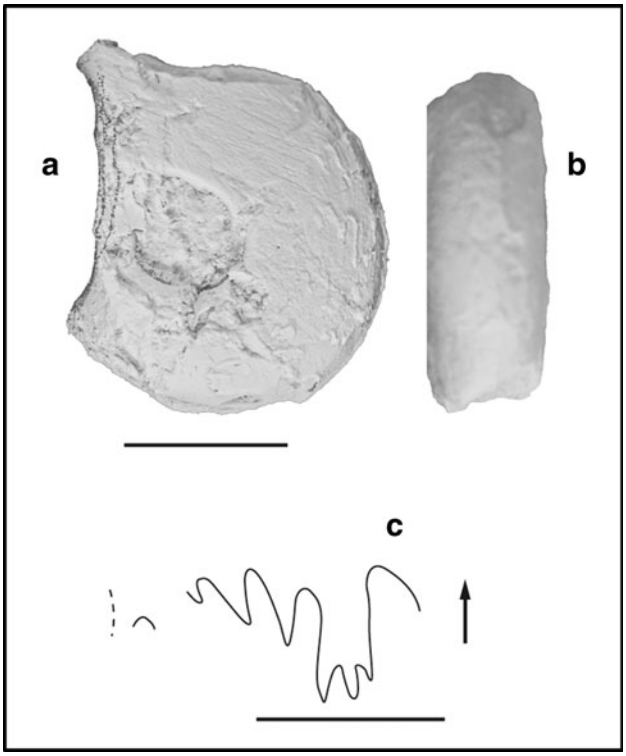

Fig. 35 **a**–**c** *?Xiaoqiaoceras americanum* sp. nov., UBGD 275042, holotype, loc. DH1-11, Confusion Range, *Owenites* beds, *Inyoites oweni* horizons, Smithian; **c** *scale bar* is 5 mm ($H = 9.8$ mm)

species by a more compressed whorl section and an almost vertical umbilical wall.

Occurrence Extremely rare. One specimen found in the Confusion Range within the *Owenites* beds, *Inyoites oweni* horizons [DH1-11].

Description Moderately involute and relatively laterally compressed shell with a rounded venter. Ventral shoulders are rounded and flanks are almost parallel. Umbilical wall almost vertical with narrowly rounded shoulders. No ornamentation displayed on our unique specimen. Simplified suture line exhibiting a structure similar to *Xiaoqiaoceras involutus* with a characteristic broad, deep and trifid lateral lobe, and an auxiliary series with numerous small saddles gently bending toward the umbilicus.

Measurements See Table 1. Estimated maximum size: ~3 cm.

Discussion Xiaoqiaoceras is a small peculiar proptychitid distinguished by its unique suture line architecture with a trifid broad and deep lateral lobe. This genus is documented from South China (Brayard and Bucher 2008) and Spiti (Brühwiler et al. 2012b) from older Smithian beds (*Flemingites rursiradiatus* and *Brayardites compressus* beds, respectively). Moreover, its attribution to proptychitids is still uncertain (see Brayard and Bucher 2008). Our specimen displays coiling features (also a laterally compressed section and a vertical umbilical wall) that differ greatly from the type species, thus possibly justifying the erection of a new genus and species. However, since our single specimen is only partly preserved and displays a suture line architecture similar to the type species we prefer here to only erect a new species. The genus assignment remains to be confirmed.

Family Dieneroceratidae Kummel, 1952
Genus ***Dieneroceras*** Spath, 1934
Type species Ophiceras dieneri Hyatt and Smith, 1905

Dieneroceras dieneri (Hyatt and Smith, 1905)
Fig. 36a–s

1905 *Ophiceras dieneri*; Hyatt and Smith, p. 118, pl. 8, figs. 16–29.
? 1905 *Xenaspsis marcoui*; Hyatt and Smith, p. 116, pl. 7, figs. 26–33.
1905 *Lecanites knechti*; Hyatt and Smith, p. 138, pl. 9, figs. 11–16.
1932 *Ophiceras dieneri*; Smith, p. 48, pl. 8, figs. 16–29.
? 1932 *Xenodiscus* (*Xenaspsis*) *marcoui*; Smith, p. 47, pl. 7, figs. 26–33.
1932 *Lecanites* (*Paralecanites*) *knechti*; Smith, p. 41, pl. 9, figs. 11-16; pl. 28, figs.1–7.
1955 *Ophiceras iwaiense*; Sakagami, p. 135, pl. 1, figs. 1–9.
1955 *Ophiceras* sp.; Sakagami, p. 136, pl. 1, figs. 10–11.
? 1959 *Kariceltites indicus*; Jeannet, p. XXX, pl. 7, figs. 10–12; pl. 8, fig. 15.
1960 *Dieneroceras iwaiense*; Kummel and Sakagami, p. 4, pl. 1, figs. 3–5; pl. 2, figs.7–9.
? 1961 *Dieneroceras dieneri*; Kiparisova, p.47, pl. 9, fig. 2.
? 1961 *Dieneroceras chaoi*; Kiparisova, p.48, pl. 9, figs. 3–6.
? 1961 *Dieneroceras caucasicum*; Popov, p. 41, pl. 6, fig. 1.
? 1965 *Dieneroceras* cf. *dieneri*; Kuenzi, p. 369, pl. 53, figs. 13–18, text-figs. 3, 4.
1968 *Dieneroceras dieneri*; Nakazawa and Bando, p. 93, pl. 4, figs. 1–6.
1968 *Dieneroceras* aff. *chaoi*; Nakazawa and Bando, p. 95, pl. 4, figs. 7, 8; pl. 5, fig.1.
? v 1973 *Dieneroceras knechti*; Collignon, p. 131, pl. 1, figs. 2, 3.
? v 1973 *Dieneroceras chaoi*; Collignon, p. 132, pl. 1, figs. 6–8.
? 1995 *Dieneroceras caucasicum*; Shevyrev, p. 25, pl. 1, figs. 3–5.
? 1995 *Dieneroceras magnum*; Shevyrev, p. 26, pl. 1, fig. 6.
2010 *Wyomingites arnoldi*; Stephen et al, fig. 5c, d.
2012a *Dieneroceras dieneri*; Brühwiler and Bucher, p. 20, pl. 8, figs. 1–4; pl. 9, figs.1–7; pl. 10, figs. 1–3.

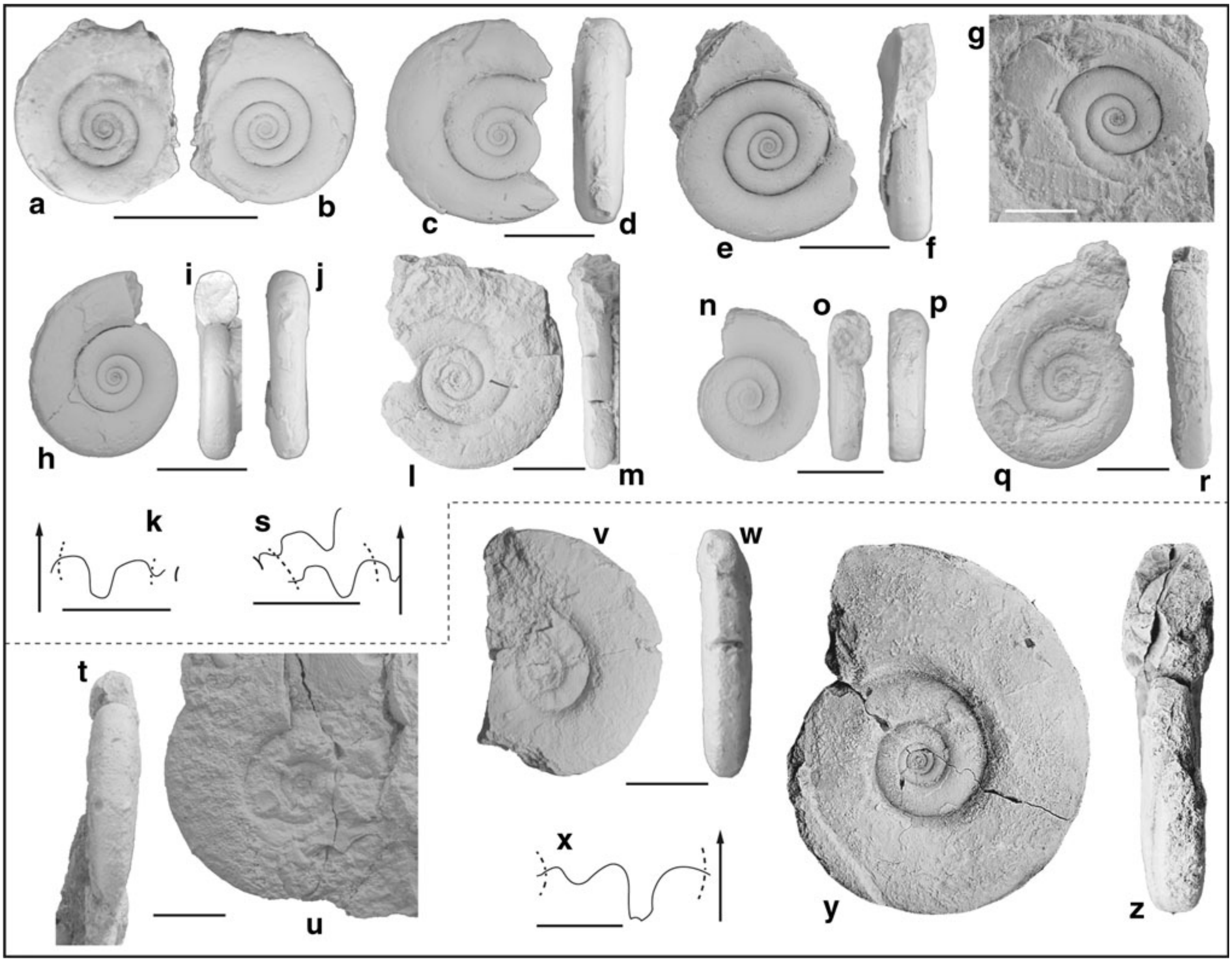

Fig. 36 **a–s** *Dieneroceras dieneri* (Hyatt and Smith 1905). All from the *Owenites* beds, *Inyoites oweni* horizons, Smithian; **a**, **b** UBGD 275043, loc. DH1-11, Confusion Range; **c**, **d** UBGD 275044, loc. DH1-11, Confusion Range; **e**, **f** UBGD 275045, loc. DH1-11, Confusion Range; **g** UBGD 275046, loc. DH1-11, Confusion Range; **h–k** UBGD 275047, loc. DH1-11, Confusion Range; **k** *scale bar* is 5 mm ($H = 4.9$ mm). **l**, **m** UBGD 275048, loc. DV1-8, Pahvant Range. **n–p** UBGD 275049, loc. DH1-11, Confusion Range; **q**, **r** UBGD 275050, loc. DH1-11, Confusion Range; **s** suture line of UBGD 275051, loc. DV1-9, Pahvant Range, *scale bar* is 5 mm ($H = 4.5$ mm). **t–z** *Wyomingites* cf. *aplanatus* (White 1879). All from loc. DH1-5, Confusion Range, *Inyoites beaverensis* sp. nov.beds, Smithian; **t**, **u** UBGD 275052; **v**, **w** UBGD 275053; **x–z** specimen from the K.G. Bylund personal collection

Occurrence Common in all studied sections within the *Owenites* beds, *Inyoites oweni* horizons except the Torrey area, where the taxon was not found [DH1-12, DH1-10/11; DV1-8; MIA9].

Description Evolute, laterally compressed shell with a subtabulate to tabulate venter and a large umbilicus. Coiling very weakly embracing preceding whorls. Broadly convex flanks with maximum thickness near umbilicus forming a slightly ovoid whorl section. Inner whorls slightly more rounded than outer whorls. Body chamber length unknown. Umbilical wall steeply inclined with rounded shoulders forming a shallow umbilicus. Ornamentation smooth with only weak folds; the spiral strigation described by Hyatt and Smith (1905) on the type specimen and on certain other species by other workers was not observed on our specimens. Classical simple ceratitic suture line with deep, but very delicately indented lobes and two main large lateral saddles. Suture line at juvenile stages is goniatitic.

Measurements See Figs. 37 and 38. Estimated maximum size: ~3.5 cm for our specimens.

Discussion Some confusion still remains not only between species included in the genus but also at higher taxonomic level. For a preliminary discussion on this issue, the reader should refer to Brayard and Bucher (2008, p. 40). Among taxa from Crittenden Springs (Nevada) attributed by Kummel and Steele (1962) to *Dieneroceras*, *D. knetchi* differs from the type species by a rounded venter and a

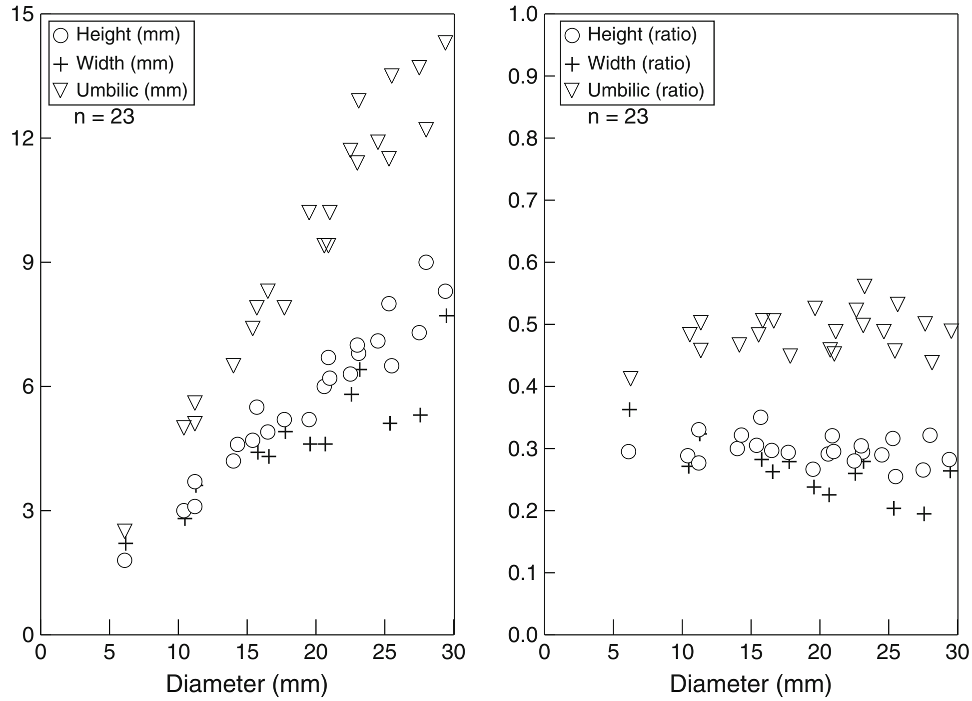

Fig. 37 Scatter diagrams of *H*, *W* and *U*, and *H*/*D*, *W*/*D* and *U*/*D* for *Dieneroceras dieneri* (all specimens from the Confusion Range and Pahvant Range, *Owenites* beds, *Inyoites oweni* horizon)

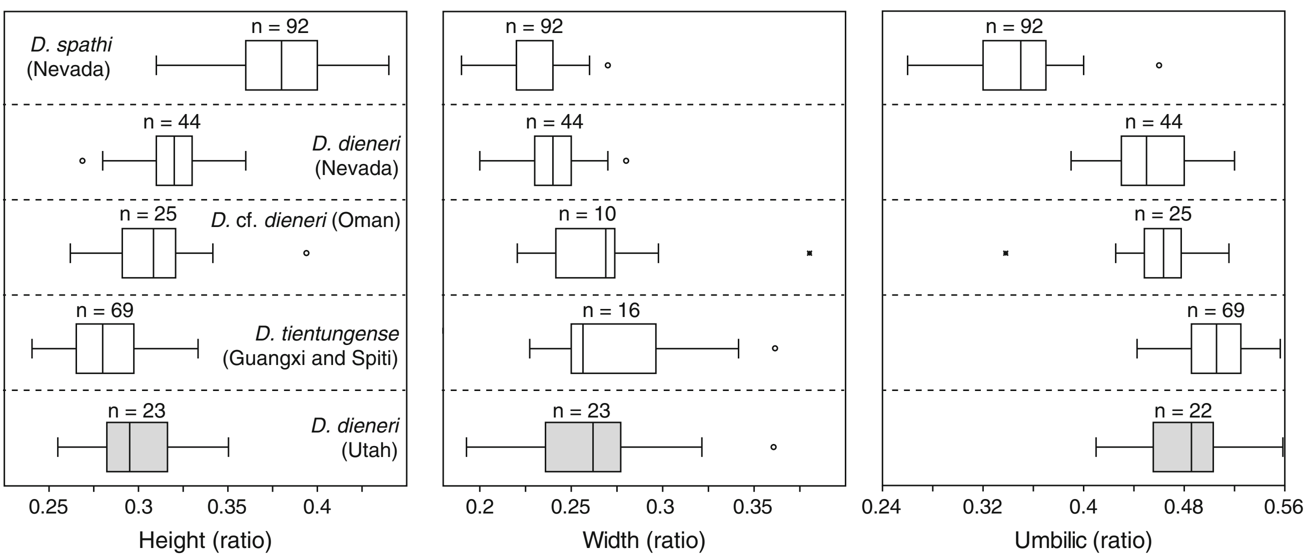

Fig. 38 Box plots of *H*/*D*, *W*/*D* and *U*/*D* for *Dieneroceras dieneri* from Utah (this work), *D.* cf. *dieneri* from Oman (Brühwiler et al. 2012a), *D. tientungense* from Guangxi and Spiti (Brayard and Bucher 2008 and Brühwiler et al. 2012b, respectively) and *D. spathi* from Crittenden Springs, Nevada (J. Jenks, ongoing work)

goniatitic suture line. Generally, the erection of a different species based only on a goniatitic suture line is not supported, especially if the goniatitic aspect results from poor preservation of some juvenile specimens. However, observed specimens from Kummel's collection and additional specimens from this locality (J. Jenks, personal observation) confirm that their suture lines are goniatitic. Our specimens of *D. dieneri* often show a goniatic suture line at juvenile stages or when poorly preserved. Thus, we regard *D. knetchi* as a valid species, but this conclusion is based only on its rounded venter. *D. spathi* erected by Kummel and Steele (1962) shows a more involute coiling and more noticeable ornamentation.

D. woondumense from Queensland (Australia) displays a coarse radial ribbing on its inner whorls, which is a unique characteristic for this genus (Runnegar 1969). *D. iwaiense* from Japan was erected only on the absence of a strigation as compared to the type species (Kummel and

Sakagami 1960, p. 5). However, American specimens of *D. dieneri* may or may not display strigation that is only seldom preserved. Thus, the absence of strigation is not useful to discriminate *Dieneroceras* species and we assign the Japanese species to *D. dieneri*. *D.* cf. *dieneri* illustrated by Kuenzi (1965) from the State of Washington (USA) appears very similar to our specimens and probably belongs to the type species. *Dieneroceras caucasicum* and *D. magnum* fall within the intraspecific variation of the type species, but their radial folding may be more obvious (e.g., Shevyrev 1995).

D. marcoui (Hyatt and Smith 1905) may also be synonymized with the type species. However, one illustrated specimen (Hyatt and Smith 1905 and Smith 1932, pl. 7, fig. 26) displays distinct radial folds that do not correspond with the diagnosis of the type species.

Dieneroceras knechti and *D. chaoi* described from Afghanistan by Collignon (1973) are fragmentary specimens and casts that impede a definitive assignment to the type species. However, the geometrical and morphological characteristics of the Afghan samples are extremely similar to *D. dieneri*.

Note that most *Dieneroceras* species discussed up till now co-occur with the middle Smithian time-marker *Owenites*.

D. tientungense from Guangxi (South China; Brayard and Bucher 2008) and *D.* cf. *tientungense* from Spiti (Brühwiler et al. 2012b) mainly differ from the type species by exhibiting a high variation in whorl section, a more perpendicular umbilical wall, strigation near the venter and weak constrictions on some large specimens. The *H*/*D*, *W*/*D* and *U*/*D* ratios between these species and *D. dieneri* are rather similar (Fig. 38) although the maximum size of American specimens is apparently much smaller. *D. tientungense* apparently also occurs earlier than the type species in Guangxi and Spiti (*Flemingites* beds; Brayard and Bucher 2008; Brühwiler et al. 2012b).

Genus ***Wyomingites*** Hyatt in Zittel, 1900
Type species Meekoceras aplanatum White, 1879

Wyomingites* cf. *aplanatus (White, 1879)
Fig. 36t–z

1879 *Meekoceras aplanatum*; White, p. 112.
1880 *Meekoceras aplanatus*; White, p. 112, pl. 31, fig. 1a, b, d.
1900 *Wyomingites aplanatus*; Hyatt, p. 556.
1902 *Ophiceras aplanatum*; Frech, p. 631.
1905 *Meekoceras* (*Gyronites*) *aplanatum*; Hyatt and Smith, p. 146, pl. 11, figs: 1-14;pl. 64, figs. 17–22; pl. 77, figs. 1-2.
1932 *Flemingites aplanatus*; Smith, p. 51, pl. 11, figs. 1–14; pl. 22, figs. 1–23; pl. 39,figs. 1, 2; pl. 64, figs. 17–32.
? 1959 *Wyomingites* cf. *aplanatus*; Kummel, p. 444, figs. 5, 6.
1962 *Wyomingites* cf. *aplanatus*; Kummel and Steele, p. 696, pl. 99, figs. 3, 4.
? 1979 *Wyomingites aplanatus*; Nichols and Silberling, pl. 1, figs. 19–21.
2008 *Wyomingites aplanatus*; Brayard and Bucher, p.42, pl. 16, figs. 1–3.
2010 *Wyomingites aplanatus*; Stephen et al., fig. 4c–e.

Occurrence Rare in the Confusion Range [DH1–5, DH1–4], *Inyoites beaverensis* sp. nov. beds. Not documented from other studied sections.

Description Evolute and laterally compressed shell with a subrectangular whorl section, a tabulate venter, rounded ventral shoulders, and nearly parallel flanks. Umbilicus with low, perpendicular wall and rounded shoulders. Typical strigation not visible on our poorly preserved specimens. Variable and wavy ribs visible. Suture line ceratitic, simple and structurally similar to *Dieneroceras*.

Measurements See Table 1. Estimated maximum size up to: ~5 cm.

Discussion See Brayard and Bucher (2008) for a discussion of the genus attribution to Dieneroceratidae. Although showing a similar overall morphology to *W. aplanatus*, our poorly preserved specimens do not display the typical strigation of this species, thus preventing a firm assignment to the type species. The occurrence of *W. aplanatus* in South China may be older (*Flemingites rursiradiatus* beds; Brayard and Bucher 2008) than in Utah.

Family Flemingitidae Hyatt in Zittel, 1900
Genus ***Flemingites*** Spath, 1934
Type species Ceratites flemingianus de Koninck, 1863

***Flemingites* sp. indet.**
Fig. 39a–d

Occurrence Very rare, one specimen was found in the Pahvant Range (*Flemingites* sp. indet. bed, DV2-5). Not found in other studied sections.

Description Moderately evolute and laterally compressed shell with a narrowly arched venter and rounded ventral shoulders. Flanks parallel near umbilicus, then gradually converge to the venter. Umbilicus wide with a deep, inclined wall and rounded margins. Ornamentation consists of a delicate, barely perceptible strigation and variable weak folds on flanks. Suture line ceratitic with rounded, deep lateral saddles and large indented lobes.

Measurements See Table 1. Estimated maximum size: ~10 cm.

Discussion Our single specimen displays the main diagnostic characters of *Flemingites* species: strigation, folds and a well-developed suture line with rounded saddle.

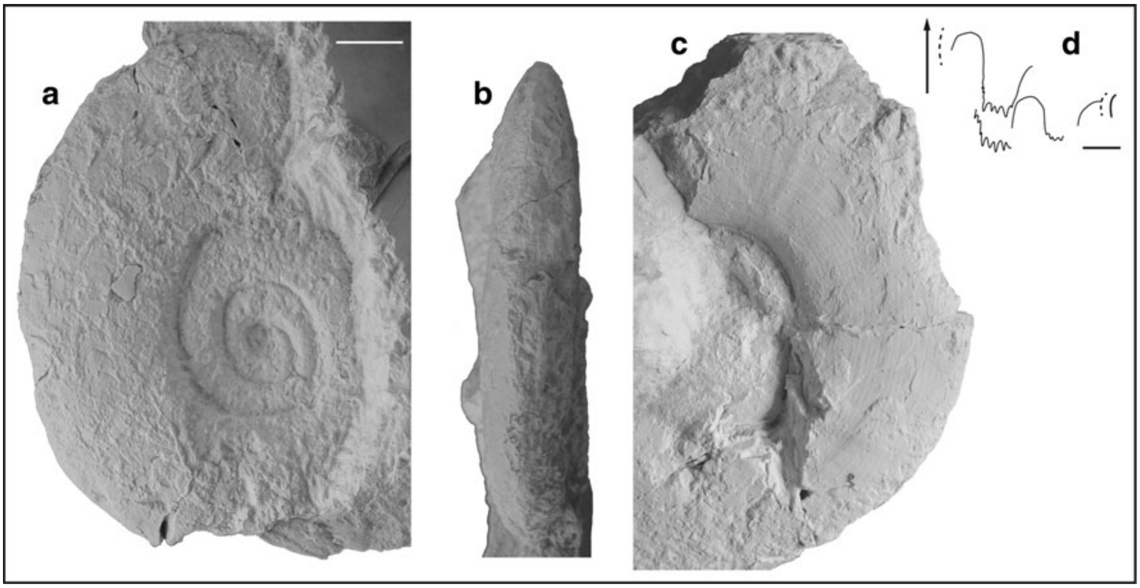

Fig. 39 **a–d** *Flemingites* sp. indet. UBGD 275054, loc. DV2-5, Pahvant Range, *Flemingites* sp. indet. beds, Smithian; **d** *scale bar* is 5 mm ($H = 24$ mm)

However, its poor preservation precludes a definite assignment to a *Flemingites* species. Surprisingly, flemingitids are much rarer in Utah than in some other known Smithian localities in the USA, such as Crittenden Springs and southeast Idaho (Nevada: e.g., Kummel and Steele 1962; Jenks et al. 2010; southeast Idaho: e.g., Smith 1932). Their rarity in Utah remains enigmatic.

Genus ***Anaflemingites*** Kummel and Steele, 1962
Type species Anaflemingites silberlingi Kummel and Steele, 1962

Anaflemingites* aff. *silberlingi
Fig. 40a–c

2000 *Anaflemingites silberlingi*; Kummel and Steele, pl. 667, pl. 102, fig. 10.

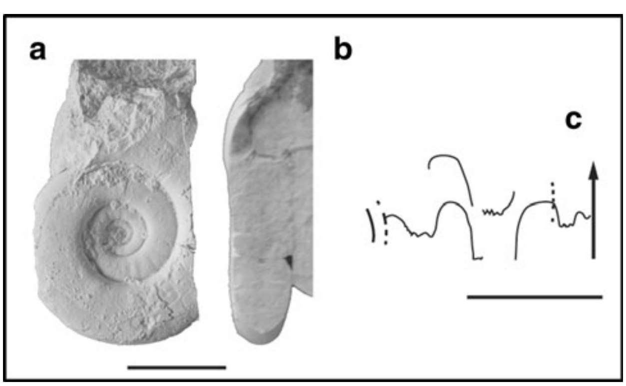

Fig. 40 **a–c** *Anaflemingites* aff. *silberlingi* Kummel and Steele 1962. UBGD 275055, loc. DV1-7, Pahvant Range, *Owenites* beds, Smithian; **c** *scale bar* is 5 mm ($H = 7.2$ mm)

v 2010 *Anaflemingites silberlingi*; Jenks et al., p. 23, figs 14, 16–18.

Occurrence Rarely occurs in the Confusion Range at the base of the *Owenites* beds (DH1-8). Also rare in the Pahvant Range, within the *Owenites* beds (DV1-7) and possibly within the *Inyoites beaverensis* sp. nov. beds (DV2-4). Not found in other studied sections.

Description Moderately evolute and laterally compressed, discoidal shell with a well-rounded venter. Flanks slightly convex with maximum curvature near mid-flank, converging to the venter without distinct ventral shoulders. Umbilicus relatively shallow with a gently sloped wall and rounded margins. Our specimens display biconcave ribs, folds and growth lines. Ribs appear more noticeable at small size. Suture line ceratitic with a broad, deep and well-indented first lateral saddle.

Measurements See Fig. 41. Estimated maximal size: ~15 cm.

Discussion Jenks et al. (2010) provided a thorough revision of the genus, based on numerous specimens from Crittenden Springs, Nevada. Our specimens are somewhat similar to the type species. However, they are small-sized and do not display the characteristic strigation, thus preventing their attribution to *A. silberlingi*. In addition, the venters of the Crittenden Springs specimens are more narrowly rounded. Moreover, the suture line of our specimens exhibits a first lateral saddle that is broader than specimens from Nevada.

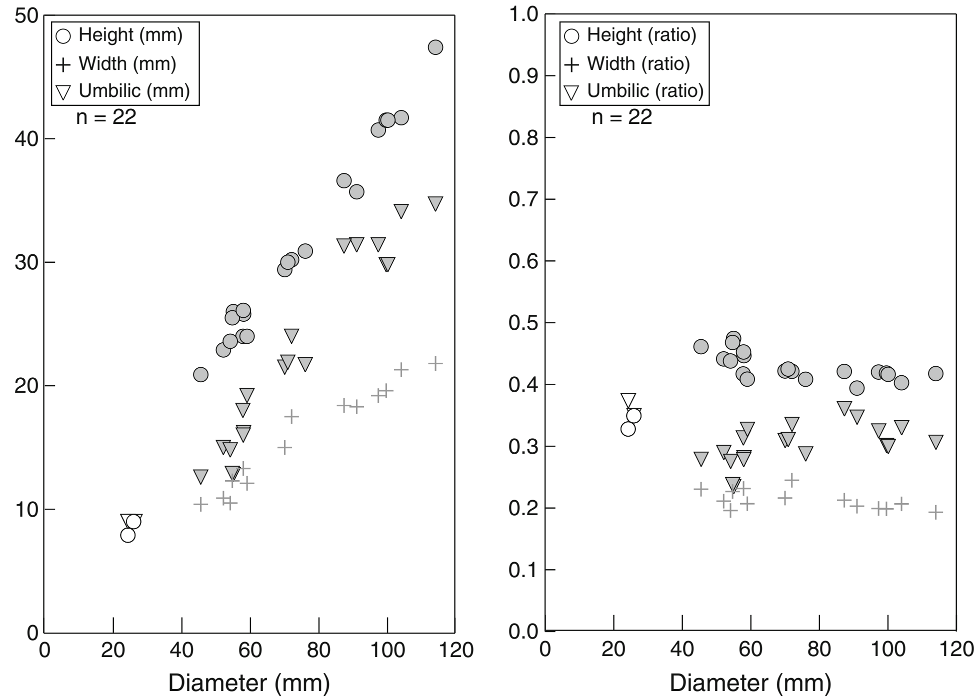

Fig. 41 Scatter diagrams of *H*, *W* and *U*, and *H*/*D*, *W*/*D* and *U*/*D* for *Anaflemingites* aff. *silberlingi* from Utah (*white symbols*; two specimens from the Confusion Range, base of the *Owenites* beds) and *Anaflemingites silberlingi* from Nevada (*grey symbols*; data from Jenks et al. 2010 [$n = 20$, *Meekoceras gracilitatis* Zone])

Family Arctoceratidae Arthaber, 1911
Genus ***Churkites*** Okuneva, 1990
Type species Churkites egregius Zharnikova and Okuneva in Okuneva 1990

Churkites noblei Jenks, 2007
Figs. 42a–f and 43a–d

2000 *Arctoceras* sp.; Gardner and Mapes, pl. 2, fig. 1.
v 2007 *Churkites noblei*; Jenks, p. 83, figs. 2, 4, 7–9.
v 2010 *Churkites noblei*; Stephen et al., figs. 5i, j.

Occurrence Common in the Confusion Range [DH1-12, DH1-10/11, DH1-9; DV1-9, DV1-8, DV2-7; MIA9] and Pahvant Range, occurs in the Mineral Mountains and rare in the Torrey area. Rare within the uppermost portion of the *Gracilitatis* Zone at Crittenden Springs, Nevada (Jenks 2007; Jenks et al. 2010). Always found within the *Owenites* beds of the studied sections.

Description Very large sized Arctoceratid with a diagnostic narrowly rounded venter on juveniles that becomes distinctively acute or angular on mature whorls. Coiling moderately evolute with compressed and relatively high whorls. Flanks gently convex forming a somewhat ovoid whorl (see Jenks 2007 for thorough description). Umbilicus wide with moderately high, inclined wall and abruptly rounded shoulders. Umbilical wall quite steep on early whorls, but gradually becoming more inclined throughout ontogeny. Ornamentation consists of weak to strong tuberculations on umbilical shoulders becoming denser and more bullate and ridge-like on adult whorls. Some slightly sinuous fold-like ribs are visible, but vary greatly in strength, width and frequency. Ribs rapidly fade away on ventral shoulders. Well-preserved shells (see specimens from Crittenden Springs; Jenks 2007) exhibit very fine, narrow, and dense radial lirae.

Suture line ceratitic, consisting of well-denticulated ventral, first lateral and second lateral lobes, as well as short auxiliary series. Width of lobes gradually decreases towards umbilicus. First lateral saddle wide and well-rounded, while second lateral saddle is somewhat narrower, but still well-rounded.

Measurements See Fig. 44. Estimated maximum size up to: ~40 cm.

Discussion Two species of *Churkites* were originally erected from the *Anasibirites nevolini* Zone of South Primorye: *C. egregius* (Zharnikova and Okuneva in Okuneva 1990) and *C. syaskoi* (Zakharov and Shigeta in Markevich and Zakharov 2004). *C. noblei* is very similar to these Russian species, but it essentially differs by its more ovoid section, more inclined umbilical wall and less dense ribs (Jenks 2007). The suture line of *C. syaskoi* also appears to be somewhat different with more denticulated lobes and more complex auxiliary series (Jenks 2007). Jenks (2007) suggested that *C. noblei*, which occurs only in the latest middle Smithian beds just below the *Anasibirites kingianus* beds, is slightly older than the Russian *Churkites* species both of which occur in the late Smithian *Anasibirites nevolini* Zone. However, since the distribution of ammonoid taxa within the *A. nevolini* Zone (and thus its

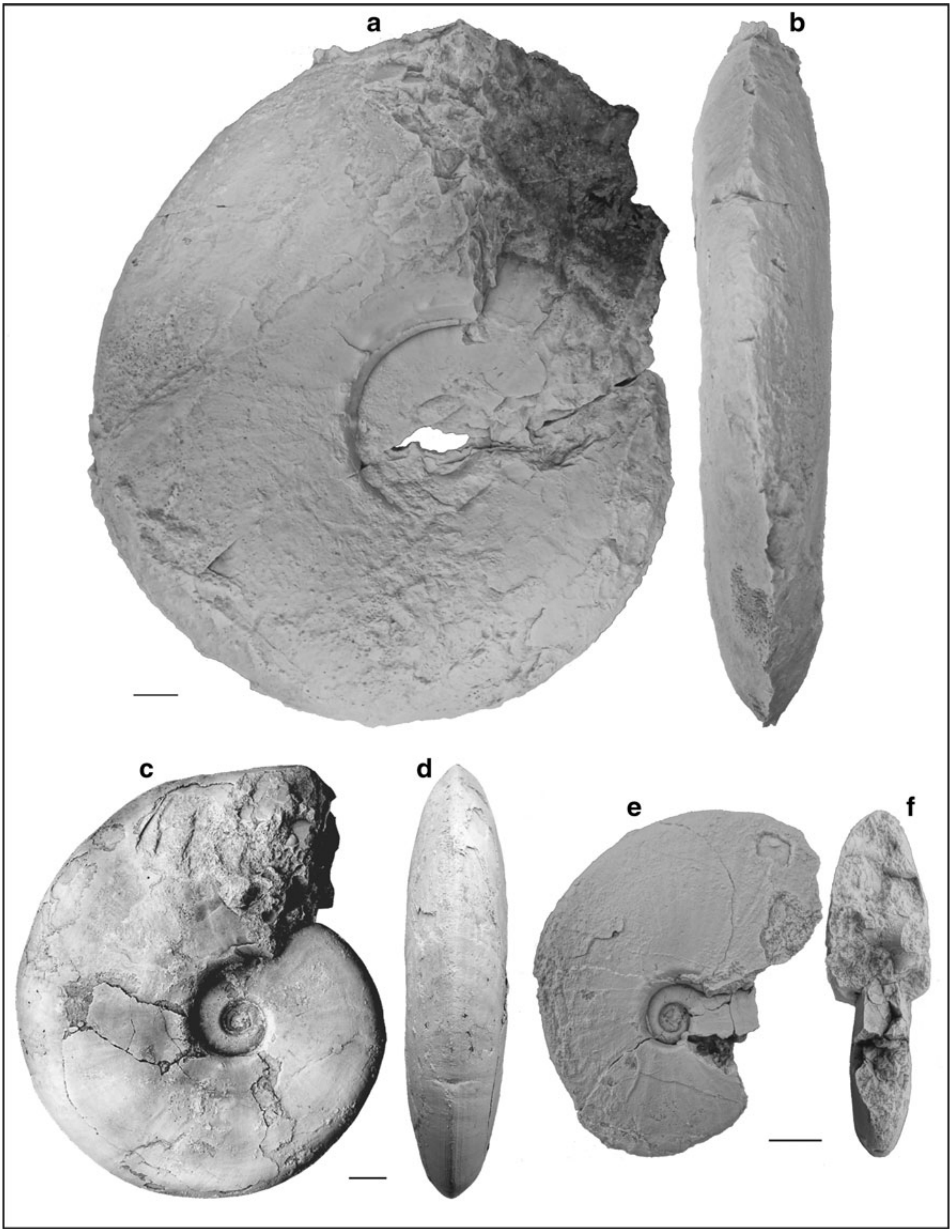

Fig. 42 **a**–**f** *Churkites noblei* Jenks 2007. All from the *Owenites* beds, Smithian; **a**–**b** UBGD 275056, loc. DV1-7, Pahvant Range; **c**–**d** specimen from the K.G. Bylund personal collection, loc. DH1-12, Confusion Range; **e**–**f** UBGD 275057, loc. DH1-12, Confusion Range

definition) is still not clear, all *Churkites* species may have temporally co-existed.

The morphology, ornamentation and suture line of *C. noblei* are closer to *Arctoceras tuberculatum* than to the Russian *Churkites* species (Jenks 2007). Consequently, it can be somewhat difficult to differentiate between juvenile and adolescent specimens of *C. noblei* and *A. tuberculatum*, especially if the particular *A. tuberculatum* specimen

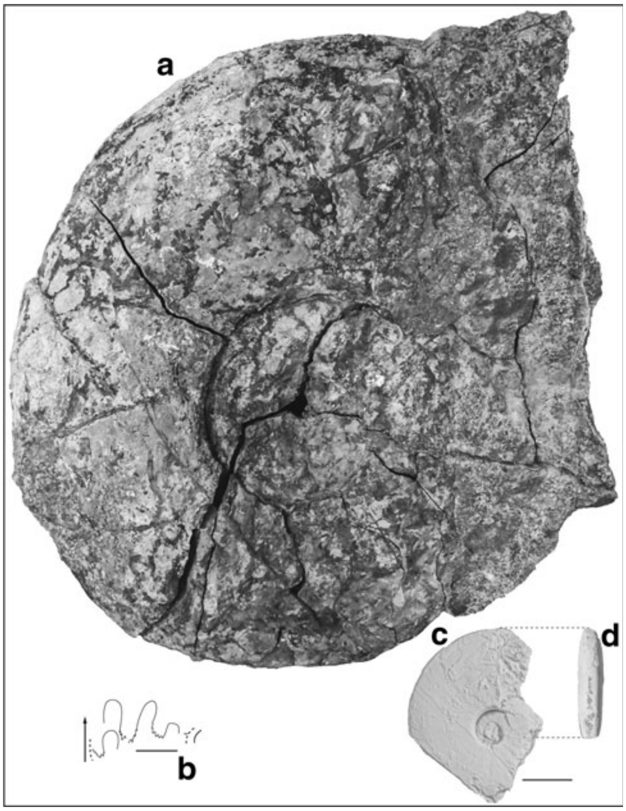

Fig. 43 *Churkites noblei* Jenks 2007. All from the *Owenites* beds, Smithian; **a** UBGD 275058, loc. DH1-12, Confusion Range (maximum diameter of this specimen is ~340 mm); **b–d** UBGD 275059, loc. DV1-9, Pahvant Range; **b** *scale bar* is 5 mm ($H = 13.5$ mm)

happens to be one of the more compressed variants. Fortunately, the whorl section of most *A. tuberculatum* shells tends to be subquadrate.

The close affinities of *Churkites* species between opposite sides of Panthalassa again underline the potential long-distance faunal exchange that occurred during the Early Triassic.

Genus ***Arctoceras*** Hyatt in Zittel, 1900
Type species Ceratites polaris Mojsisovics, 1896

Arctoceras tuberculatum (Smith, 1932)
Fig. 45a–c

1932 *Meekoceras tuberculatum*; Smith, p. 62, pl. 50, fig. 1–4.
1962 *Arctoceras tuberculatum*; Kummel and Steele, p. 697, pl. 104, figs. 1–8.
1979 *Arctoceras tuberculatum*; Nichols and Silberling, pl. 1, figs. 5–9.
? 1994 *Arctoceras gigas*; Tozer, p. 65, pl. 26, figs. 4–6.
v. 2010 *Arctoceras tuberculatum*; Jenks et al., internal frontspiece.

Occurrence Rare. A few large fragmentary specimens found within the *Preflorianites–Kashmirites* beds of the Confusion Range [DH1-1] and Pahvant Range [DV2-1 to DV2-2]. One large complete specimen found in DV2-2. Not documented from other studied sections. Abundant throughout the *Meekoceras gracilitatis* Zone, up to the

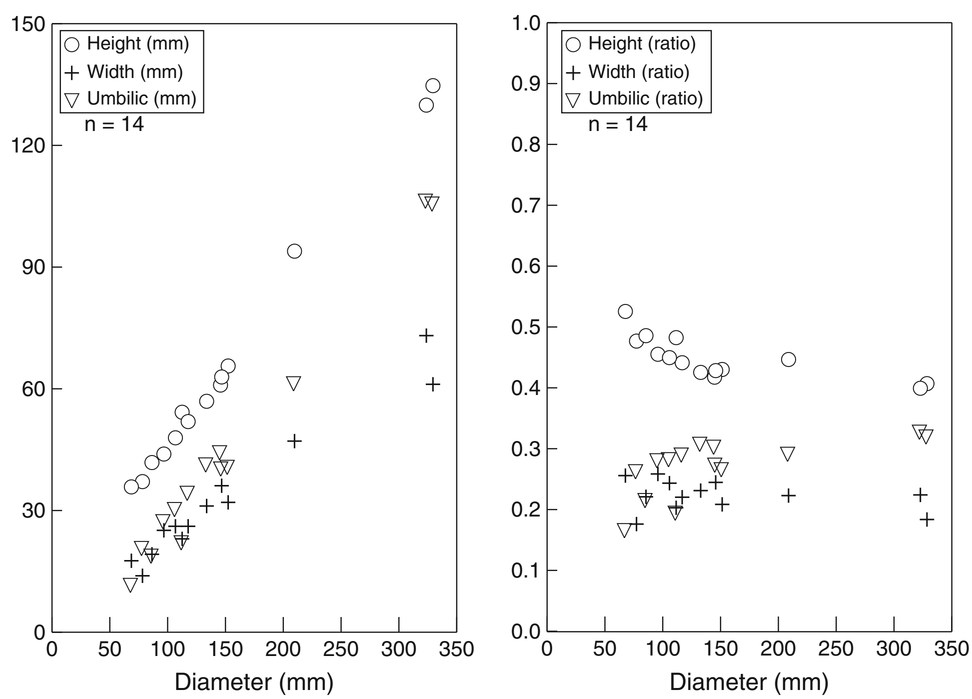

Fig. 44 Scatter diagrams of *H*, *W* and *U*, and *H*/*D*, *W*/*D* and *U*/*D* for *Churkites noblei*. Measured specimens from the Confusion Range and Pahvant Range (*Owenites* beds, *Inyoites oweni* horizons) and from Crittenden Springs, Nevada (Jenks 2007)

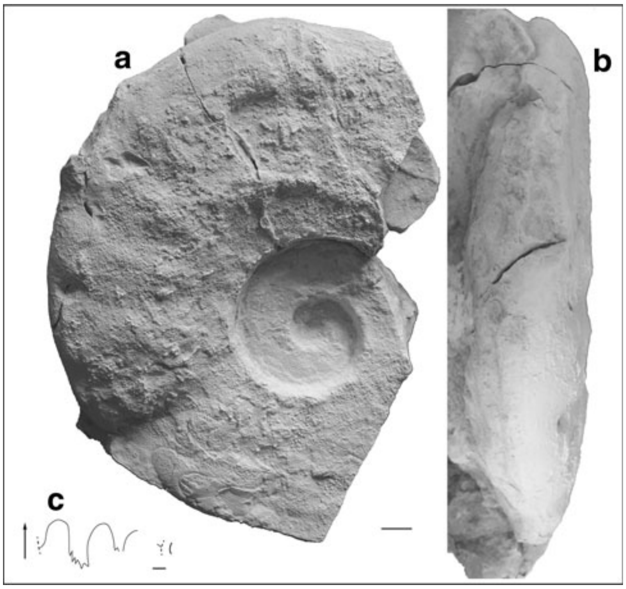

Fig. 45 **a–c** *Arctoceras tuberculatum* (Smith 1932). UBGD 275060, loc. DV2-2, Pahvant Range, *Preflorianites–Kashmirites* beds, Smithian; **c** *scale bar* is 5 mm ($H = 48.5$ mm)

Anasibirites Zone at Crittenden Springs, Nevada (Jenks et al. 2010).

Description Large-sized Arctoceratid with a moderately evolute, compressed shell. Venter varies from narrowly rounded to well-rounded on smaller specimens to well-rounded or broadly rounded on larger specimens. Flanks weakly convex, but whorl section remains subquadrate. Umbilicus rather wide with a high, nearly perpendicular wall and abruptly rounded margins. Characteristic ornamentation consists of conspicuous tubercles on umbilical shoulders often becoming denser on adult whorls. Some large radial, sinuous ribs are also visible, but they vary greatly in strength and width, and become denser at large sizes. Fine strigation is visible on well-preserved specimens from Crittenden Springs (Kummel and Steele 1962; Jenks et al. 2010), but not on our specimens. Suture line ceratitic with broad lobes and an auxiliary series. Width of lobes gradually decreases towards umbilicus.

Measurements See Figs. 46 and 47. Estimated maximum size up to: ~25 cm.

Discussion Arctoceras blomstrandi (Lindström 1865) from the Canadian Arctic (Tozer 1994) and Spitsbergen (Weitschat and Lehmann 1978) exhibits the same typical umbilical nodes, but appears slightly more involute. *A. strigatus* from South China (Brayard and Bucher 2008) differs by its conspicuous strigation and its absence of umbilical tuberculation. *Arctoceras gigas* from the Canadian Arctic (Tozer 1994) probably should be synonymized with *A. tuberculatum* due to the similar characters they share, but additional specimens of the Canadian taxon are necessary to definitively corroborate this hypothesis. *A. schalteggeri* from Pakistan (Brühwiler et al. 2011) does not have true umbilical tubercles but only weak ribs thickening at the umbilical margin. *A. septentrionale* from South Primorye (Zakharov 1968; Shigeta and Zakharov 2009) is rather similar but apparently more involute (Fig. 47).

Fig. 46 Scatter diagrams of *H*, *W* and *U*, and *H*/*D*, *W*/*D* and *U*/*D* for *Arctoceras tuberculatum.* The single complete measured specimen from the Pahvant Range is indicated by *white symbols* (*Preflorianites–Kashmirites* beds). Other data in *grey* are from Crittenden Springs, Nevada ("*Meekoceras gracilitatis* zone"; Kummel and Steele 1962)

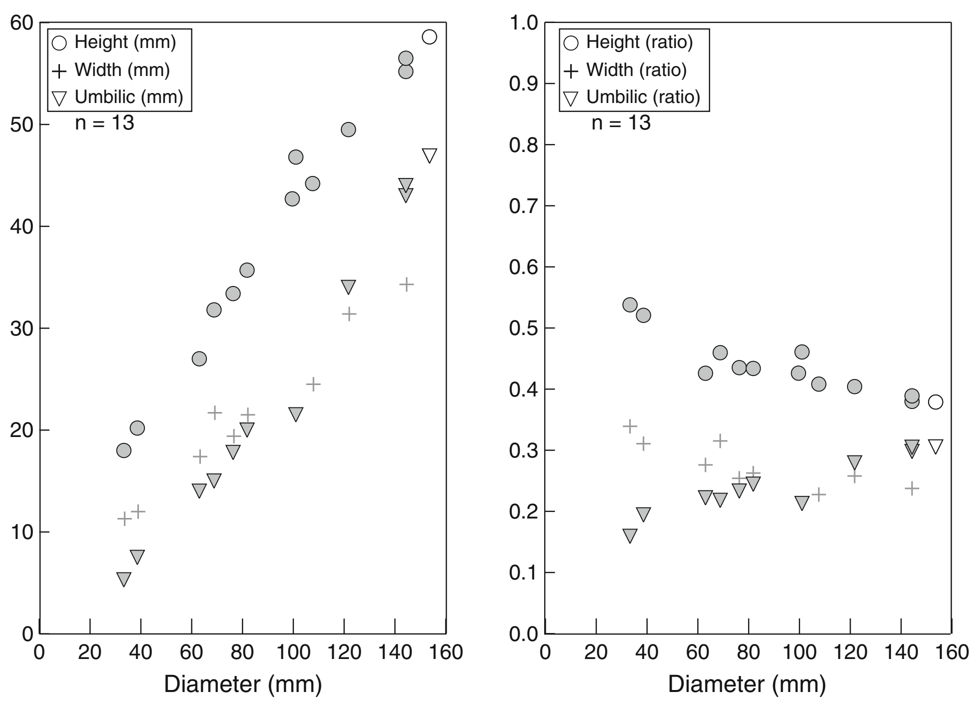

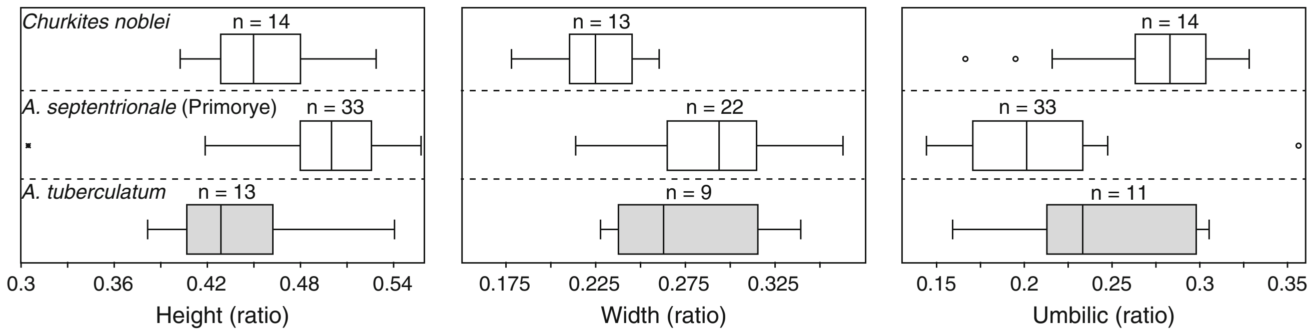

Fig. 47 Box plots of *H*/*D*, *W*/*D* and *U*/*D* for *Arctoceras tuberculatum* from Utah and Nevada (this work and Kummel and Steele 1962, respectively), *A. septentrionale* from South Primorye (Zakharov 1968) and *Churkites noblei* from Utah and Nevada (this work and Jenks 2007, respectively)

A. subhydapsis, also from South Primorye (e.g., Shigeta and Zakharov 2009), is described as more evolute than *A. tuberculatum*. Additional specimens and measurements from this Russian taxon are needed to statistically confirm the erection of a different species.

As previously discussed, *Churkites noblei* and *A. tuberculatum* are sometimes difficult to differentiate when the studied specimens are juvenile and adolescent. The adult stage of *C. noblei* can be easily distinguished by its angular venter, and it also appears to be slightly more compressed (Fig. 47). *A. tuberculatum* has definitively been documented here only from beds underlying the *Owenites* beds, but it may range up to the *Anasibirites kingianus* beds in other parts of the basin (e.g., Crittenden Springs; Jenks et al. 2010).

Genus ***Submeekoceras*** Spath, 1934
Type species *Meekoceras mushbachanum* White, 1879

Submeekoceras mushbachanum (White, 1879)
Fig. 48a, b

1879 *Meekoceras mushbachanum*; White, p. 113.
1880 *Meekoceras mushbachanum*; White, p. 114, pl. 32, fig. 1a–d.
1902 *Prionolobus mushbachanum*; Frech, p. 631: c.
1904 *Meekoceras mushbachanum*; Smith, p. 376, pl. 41, figs. 1–3; pl. 43, figs. 1, 2.
1905 *Meekoceras* (*Koninckites*) *mushbachanum*; Hyatt and Smith, p. 149, pl. 15,figs. 1–9; pl. 16, figs. 1–3; pl. 18, figs. 1–7; pl. 70, figs. 8–10.
1914 *Meekoceras mushbachanum*; Smith, p. 77, pl. 72, figs. 1, 2; pl. 73, figs. 1–6; pl.74, figs. 1–23.
1915 *Meekoceras mushbachanum*; Diener, p. 193.
non 1922 *Meekoceras mushbachanum*; Welter, p. 126.
1932 *Meekoceras* (*Koninckites*) *mushbachanum*; Smith, p. 61, pl. 15, figs. 1–9; pl.16, figs. 1–3; pl. 18, figs. 1–7; pl. 38, figs. 1; pl. 59, figs. 17–21; pl. 70, figs. 8–10; pl. 74, figs.1–23; pl. 75, figs. 1–6; pl. 76, figs. 1–3.
1932 *Meekoceras* (*Koninckites*) *mushbachanum* var. *corrugatum*; Smith, p. 61, pl.38, fig. 1.
1932 *Meekoceras* (*Koninckites*) *evansi*; Smith, p. 60, pl. 35, figs. 1–3; pl. 36, figs. 1–18.
1934 *Submeekoceras mushbachanum*; Spath, p. 255, fig. 87.
v 1959 *Paranorites ovalis*; Chao, p. 217, pl. 9, figs. 16-19, text-fig. 16b.
? 1959 *Prionolobus ophionus* var. *involutus*; Chao, p. 201, pl. 9, figs. 11–15, text-fig.11b.
v 1959 *Prionolobus hsuyuchieni*; Chao, p. 202, pl. 9, figs. 9-10, text-fig. 11c.
? 1959 *Meekoceras* (*Submeekoceras*) *tientungense*; Chao, p. 317, pl. 14, figs. 6, 7, textfig.45b.
v 1959 *Meekoceras* (*Submeekoceras*) *subquadratum*; Chao, p. 317, pl. 14, figs. 1–5; pl.39, figs. 8, 9, text-fig. 45c.
v 1959 *Meekoceras densistriatum*; Chao, p. 310, pl. 38, figs. 1–3, 19, text-fig. 43b.
v 1959 *Meekoceras yukiangense*; Chao, p. 311, pl. 39, figs. 1–7, text-fig. 44a.
v 1959 *Meekoceras kaohwaiense*; Chao, p. 311, pl. 40, figs. 16–18, text-fig. 44b.
v 1959 *Meekoceras pulchriforme*; Chao, p. 313, pl. 40, figs. 14, 15, text-fig. 44c.
? 1959 *Meekoceras jolinkense*; Chao, p. 314, pl. 14, figs. 12–15.
v 1959 *Meekoceras lativentrosum*; Chao, p. 309, pl. 38, figs. 15–18, text-fig. 43a.
v 1959 *Proptychites latumbilicutus*; Chao, p. 234, pl. 19, figs. 2, 3, text-fig. 22a.
? 1959 *Proptychites kaoyunlingensis*; Chao, p. 234, pl. 16, figs. 7, 8, text-fig. 22b.
p 1968 *Arctoceras mushbachanum*; Kummel and Erben, p. 131, pl. 21, fig. 1 only.
v 2008 *Submeekoceras mushbachanum*; Brayard and Bucher, p. 53, pl. 16, fig. 4; pl.26, figs. 1–9.
2010 *Submeekoceras mushbachanum*; Stephen et al., figs. 4a, b.

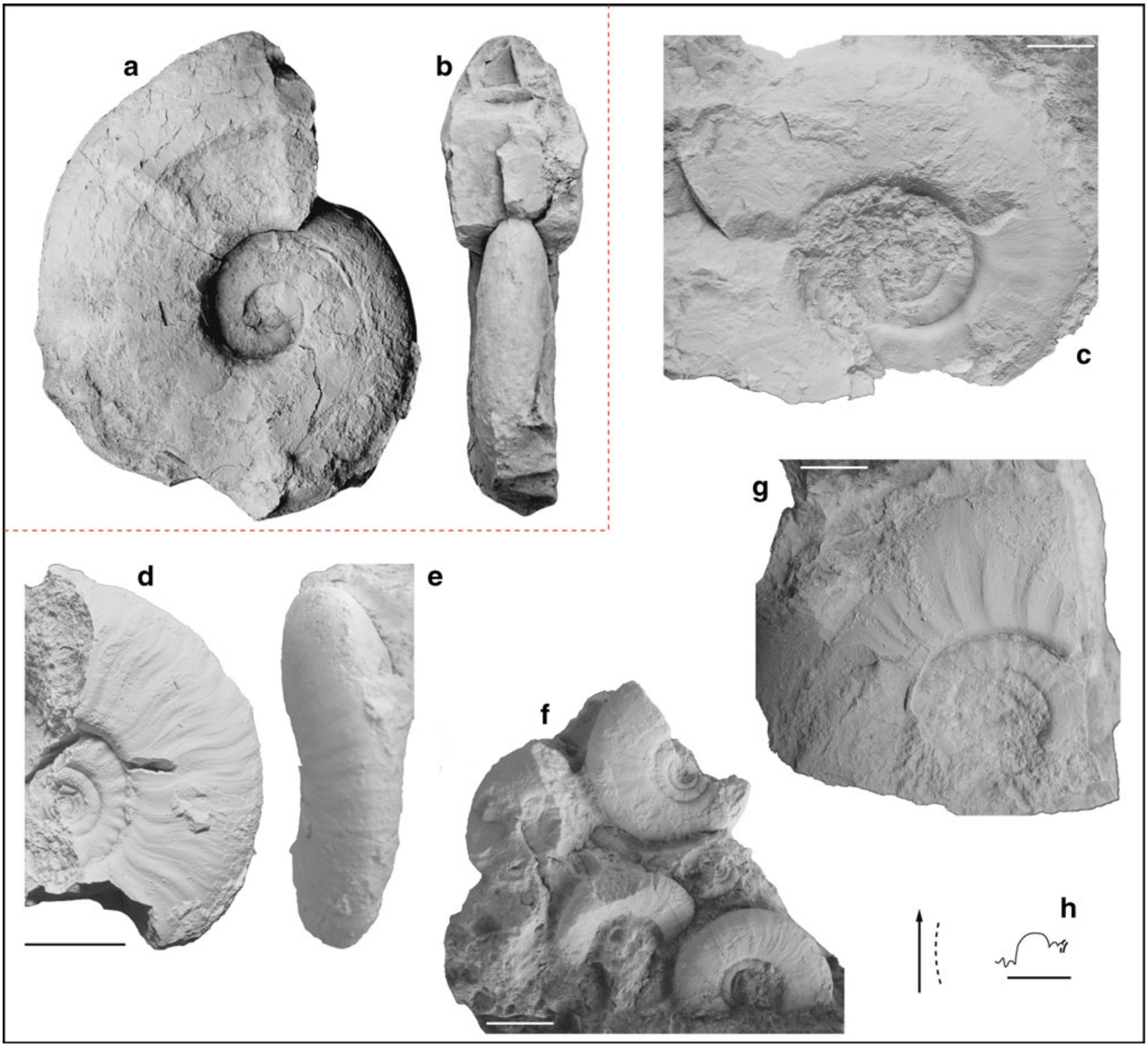

Fig. 48 **a**, **b** *Submeekoceras mushbachanum* (White 1879). Specimen from the K.G. Bylund personal collection, loc. DH1-4, Confusion Range, *Inyoites beaverensis* sp. nov. beds, Smithian. **c**–**h** *Minersvillites farai* gen. nov., sp. nov. All from loc. MIA4, Mineral Mountains, base of the *Owenites* beds, Smithian; **c** UBGD 275061, paratype; **d**, **e** UBGD 275062, paratype; **f** Group of *Minersvillites farai* gen. nov., sp. nov., UBGD 275063, paratypes; **g**, **h** UBGD 275064, holotype; **h** *scale bar* is 5 mm ($H = 8.3$ mm)

v 2012a *Submeekoceras mushbachanum*; Brühwiler and Bucher, p. 30, pl. 17, figs. 1–3.

Occurrence Occurs in the Confusion Range [DH1-5, DH1-4] within the *Inyoites beaverensis* sp. nov. beds, and rarely occurs in the Mineral Mountains [MIA4] at the base of the *Owenites* beds.

Description Slightly evolute, somewhat compressed platycone with flat, parallel flanks, a venter that varies from narrowly rounded to well-rounded on smaller specimens to well-rounded on larger specimens, with rounded ventral shoulders. Umbilicus rather deep with high, flat, perpendicular wall and abruptly rounded shoulders. Ornamentation consists of sinuous growth lines and weak, but noticeable fold-like ribs similar to *Arctoceras*. Suture line unknown on our specimens, but it is usually similar to *Arctoceras* with less indented lateral lobes.

Measurements See Table 1. Estimated maximum size: ~15 cm (see Brayard and Bucher 2008).

Discussion This taxon clearly belongs to the Arctoceratidae and juvenile specimens are hardly distinguishable from

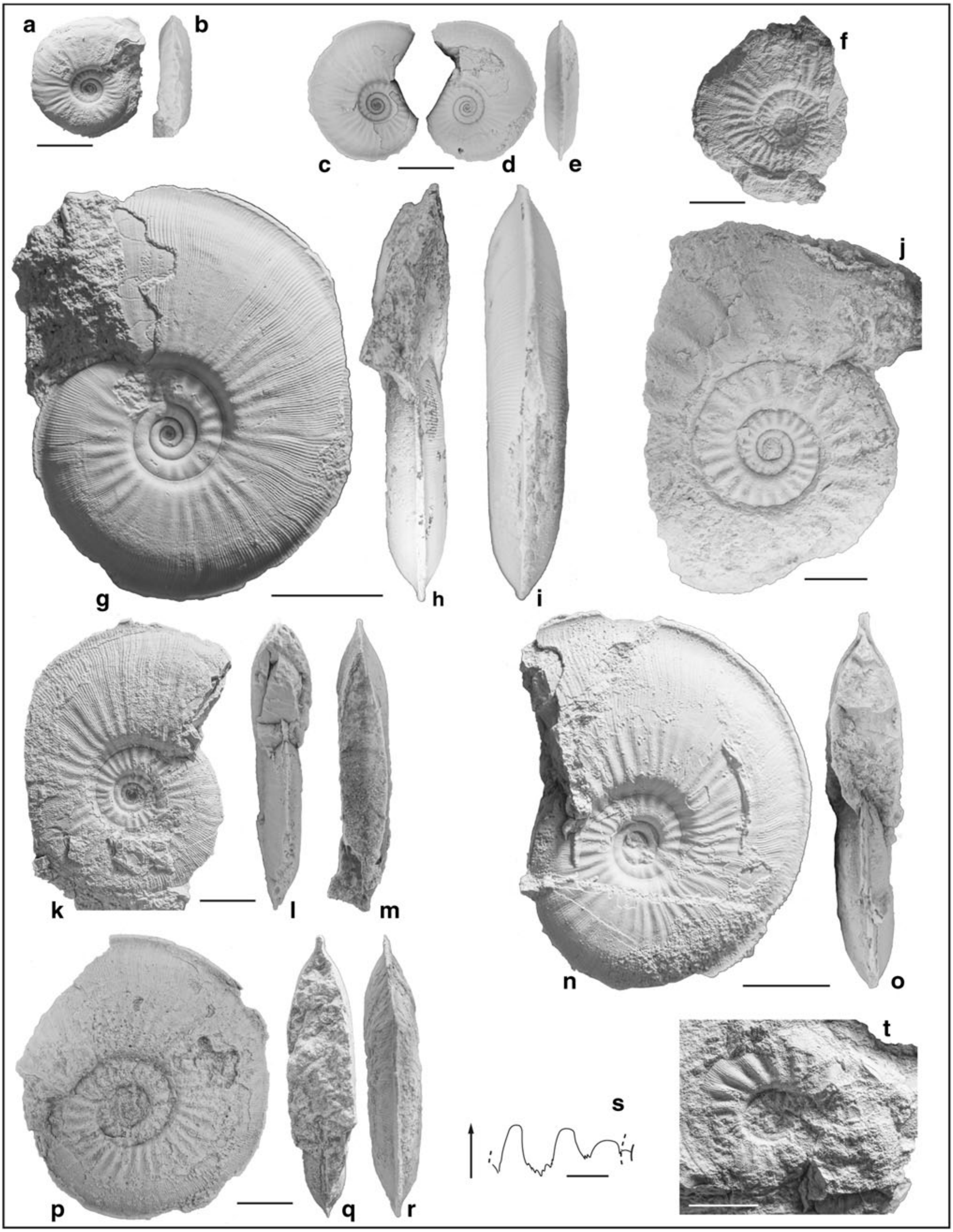
a
b
c
d
e
f
g
h
i
j
k
l
m
n
o
p
q
r
s
t

◀ **Fig. 49** *Inyoites oweni* Hyatt and Smith 1905. All from the *Owenites* beds, *Inyoites oweni* horizons, Smithian; **a**, **b** UBGD 275065, loc. DH1-10, Confusion Range; **c**–**e** UBGD 275066, loc. DH1-12, Confusion Range. **f** UBGD 275067, loc. DV1-8, Pahvant Range; **g**–**i** UBGD 275068, loc. DH1-11, Confusion Range; **j** UBGD 275069, loc. DH1-11, Confusion Range; **k**–**m** UBGD 275070, loc. DV1-9, Pahvant Range; **n**, **o** UBGD 275071, loc. DH1-12, Confusion Range; **p**–**r** UBGD 275072, loc. DH1-12, Confusion Range; **s** suture line of UBGD 275073, loc. DH1-11, Confusion Range, *scale bar* is 5 mm ($H = 21.5$ mm); **t** UBGD 275074, loc. DV1-9, Pahvant Range

Arctoceras or *Churkites*. It mainly differs from *Arctoceras tuberculatum* by the absence of umbilical tuberculation.
Genus ***Minersvillites*** **gen. nov.**

Type species Minersvillites farai gen. nov., sp. nov.
Composition of the genus Type species only.

Derivation of name Named after the small town of Minersville located just southwest of the Mineral Mountains section (Utah).

Diagnosis Evolute and compressed arctoceratid with a slightly inclined umbilical wall and sinuous, radial ribs disappearing on outer whorls.

Discussion This taxon exhibits a discoidal shape with almost parallel flanks, an arched venter, prominent ribs, a high umbilical wall and an apparently well-indented suture line with large saddles. Thus, it likely belongs to Arctoceratidae. It can be distinguished from other arctoceratids by its more evolute coiling and slightly inclined umbilical wall. Moreover, it appears to be more laterally compressed with a more ovoid whorl section. Ornamentation closely resembles that of *Submeekoceras muschbachanum* with sinuous growth lines and radial ribs fading on outer whorls. However, these ribs are more prominent near the umbilical margin, and tend to generate a small longitudinal fold at this location and thus resemble umbilical tubercles of other arctoceratids.

Minersvillites farai **gen. nov., sp. nov.**
Fig. 48c–h

Holotype UBGD 275064 (Fig. 48g, h), loc. MIA4, Mineral Mountains, base of the *Owenites* beds, Smithian.

Derivation of name Named after Emmanuel Fara (Dijon).
Diagnosis As for the genus.

Occurrence Rare in the Mineral Mountains at the base of the *Owenites* beds [MIA4; $n = 4$]. Not documented from other studied sections.

Description Evolute, laterally compressed arctoceratid with a rather narrowly arched venter. Flanks appear almost parallel near the umbilicus and become convergent towards the venter at 2/3rd of flanks. Umbilicus wide with a slightly oblique, high wall and markedly rounded shoulders. Ornamentation consists of dense, sinuous, radial growth lines and irregularly spaced ribs. Ribs are quite large and their tops sometimes become acute. Ribs fade at a large diameter and only perceptible growth lines remain. Ceratitic suture line only partly known with a broad third lateral saddle, a deeply indented lateral saddle and a short auxiliary series.

Measurements See Table 1. Estimated maximum size: ~10 cm.

Discussion As for the genus.

Family Inyoitidae Spath, 1934
Genus ***Inyoites*** Hyatt and Smith, 1905
Type species Inyoites oweni Hyatt and Smith, 1905

Inyoites oweni Hyatt and Smith, 1905
Fig. 49a–t

1905 *Inyoites oweni*; Hyatt and Smith, p. 134, pl. 6, figs. 1-16, pl. 69, figs. 1–9, pl.78, figs. 1–8.
1932 *Inyoites oweni*; Smith, p. 80, pl. 6, figs. 1–16, pl. 40, figs. 1–8, pl. 69, figs. 1–9.
1934 *Inyoites oweni*; Spath, p. 138, fig. 37.
1968 *Inyoites spicini*; Zakharov, p. 151, pl. 30, fig. 2.
v 1973 *Inyoites oweni*; Collignon, p. 12, pl. 1, fig. 9.
? 1995 *Inyoites oweni*; Shevyrev, p. 12, pl. 1, fig. 9.
v 2010 *Inyoites oweni*; Stephen et al., figs. 5a, b.
2012a *Inyoites oweni*; Brühwiler and Bucher, p. 34, pl.21, figs. 1–6.
? 2012a *Inyoites* sp. indet.; Brühwiler and Bucher, p.35, pl.21, fig. 8.

Occurrence Very abundant in the Confusion Range, Pahvant Range and Mineral Mountains within the upper part of the *Owenites* beds, *Inyoites oweni* horizons. Often co-occurs with *Guodunites hooveri* and *Churkites noblei*. Not documented from the Star Range and the Torrey area. Also found in the *Owenites* beds of Afghanistan (Collignon 1973), the Caucasus (Shevyrev 1995) and Oman (Brühwiler et al. 2012a).

Description Moderately involute, compressed shell with slightly convex flanks. Lanceolate venter with a characteristic high, pronounced keel. Ventral shoulders barely perceptible, but very gently rounded. Umbilicus shallow with a relatively high wall, becoming distinctively more and more inclined on mature whorls with abruptly rounded shoulders. Ornamentation consists of very conspicuous slightly sinuous fold-like ribs varying greatly in strength and width. Ribs rapidly fade away on outer half of the flanks where they are gradually transformed into very fine, narrow, dense and sinuous lirae. Ribs almost radial or most often slightly rursiradiate. On rare robust specimens, ribs are distinctively rursiradiate. Well-preserved specimens sometimes exhibit a faint strigation. Suture line ceratitic with rather deep lobes. Saddles elongated and rounded.

Measurements See Figs. 50 and 51. Estimated maximum size: ~8 cm.

Fig. 50 Scatter diagrams of *H*, *W* and *U*, and *H*/*D*, *W*/*D* and *U*/*D* for *Inyoites oweni* (all specimens from the Confusion Range and Pahvant Range, *Owenites* beds, *Inyoites oweni* horizons)

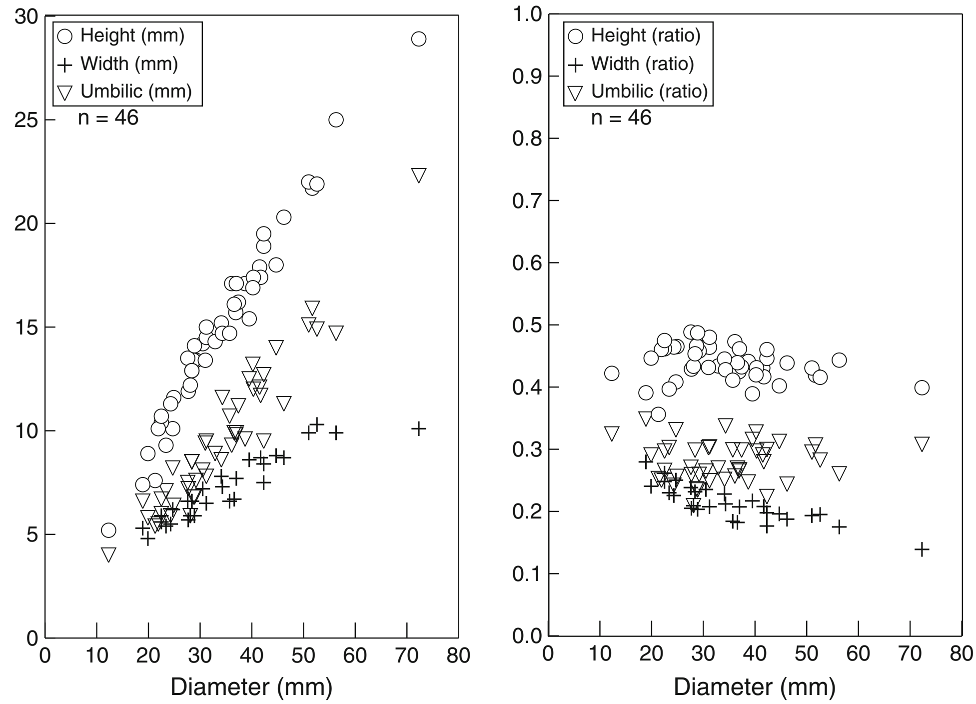

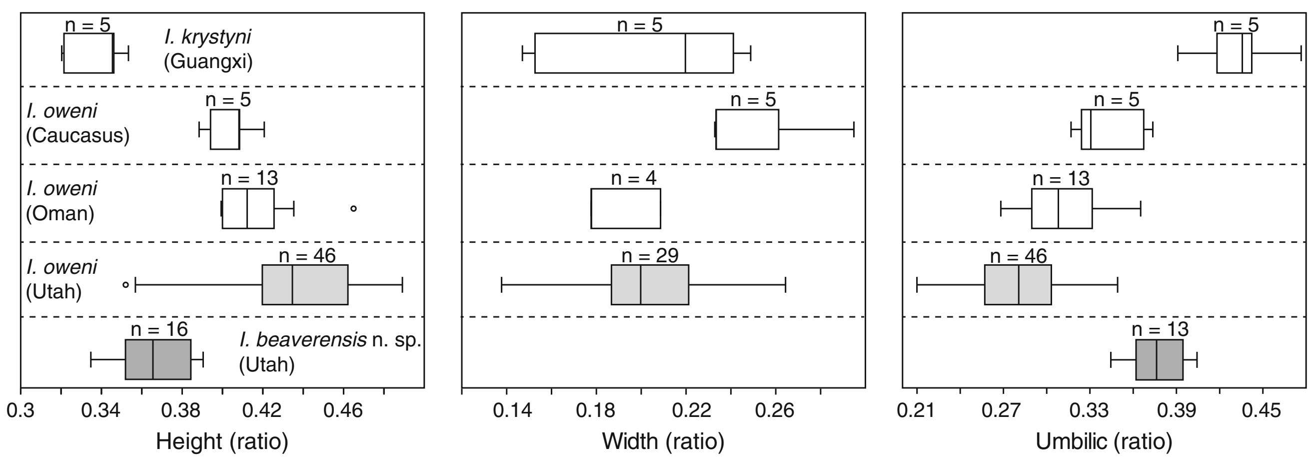

Fig. 51 Box plots of *H*/*D*, *W*/*D* and *U*/*D* for *Inyoites oweni* from Utah (this work), Oman (Brühwiler et al. 2012a) and the Caucasus (Shevyrev 1995), *I. krystyni* from Guangxi (Brayard and Bucher 2008) and *I. beaverensis* sp. nov. (this work)

Discussion Inyoites krystyni Brayard and Bucher (2008), erected from the *Owenites* beds, *Inyoites* horizon of Guangxi (South China), can be distinguished from the type species by its more evolute coiling, its larger maximum size (up to ~15 cm) and its weaker ornamentation. These two species are diagnostic of the upper part of the middle Smithian in the USA and South China, thus facilitating biostratigraphical correlation between each side of Panthalassa. *Inyoites* sp. indet. described from Oman (Brühwiler et al. 2012a) is probably conspecific with the type species, the main difference being its strong rursiradiate ribs. However, some rare *I. oweni* specimens from Utah exhibit the same type of ornamentation, and a wide range of rib variation from almost straight to rursiradiate is found. Moreover, the more slightly evolute coiling noted by Brühwiler et al. (2012a) for *Inyoites* sp. indet. may simply be due to intraspecific variation.

Inyoites oweni also occurs at Crittenden Springs (Nevada), but it is extremely rare (Jenks, ongoing work). *I. stokesi* described by Kummel and Steele (1962) probably has to be assigned to the genus *Subvishnuites* (see Brayard and Bucher 2008) due to the apparent absence of a ventral keel.

***Inyoites beaverensis* sp. nov.**

Fig. 52a–p

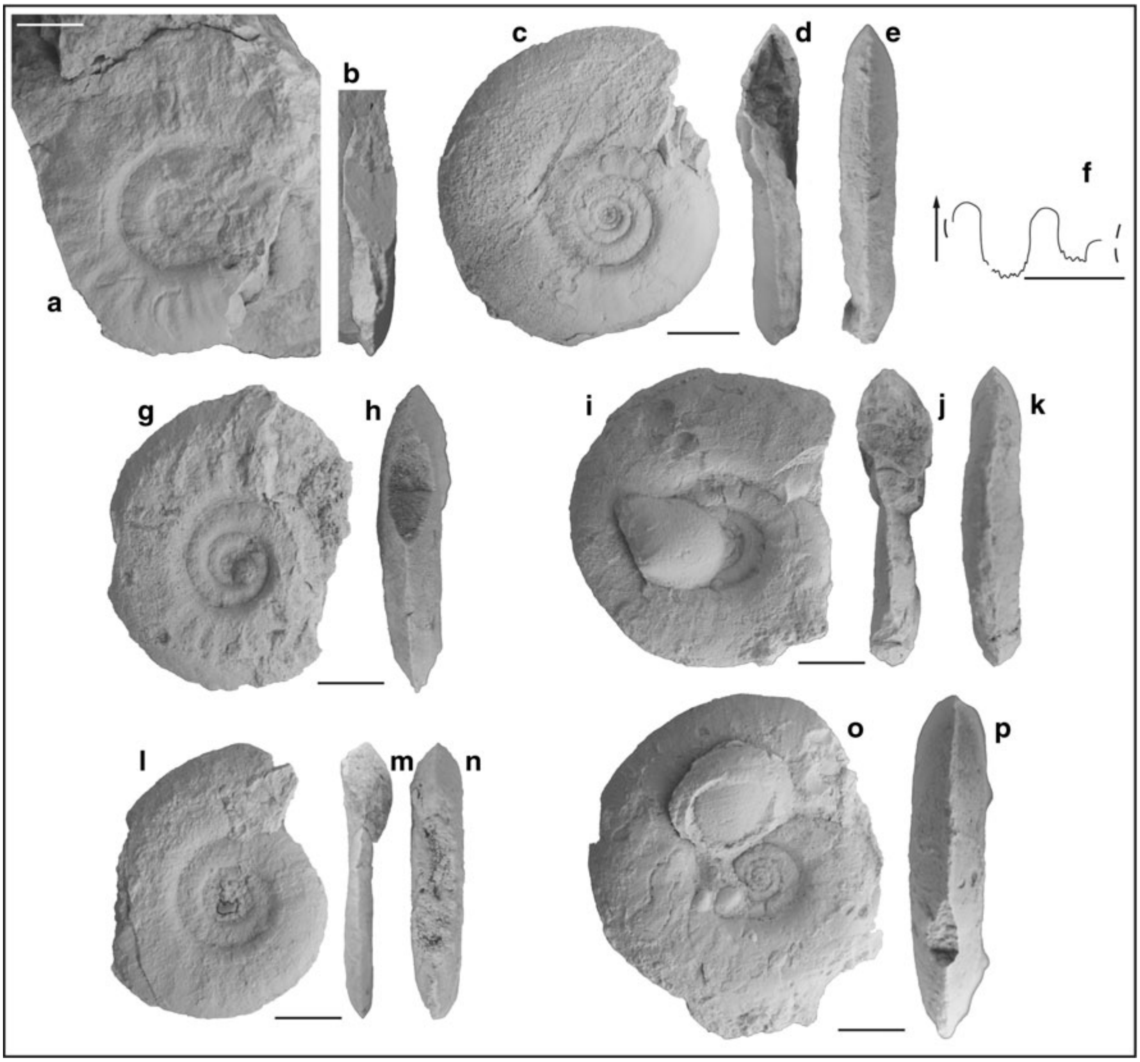

Fig. 52 *Inyoites beaverensis* sp. nov. All from loc. DH1-5, Confusion Range, *Inyoites beaverensis* sp. nov. beds, Smithian; **a**–**b** UBGD 275075, paratype; **c**–**f** UBGD 275076, holotype; **f** *scale bar* is 5 mm ($H = 9.2$ mm); **g**, **h** UBGD 275077, paratype; **i**–**k** UBGD 275078, paratype; **l**–**n** UBGD 275079, paratype; **o**, **p** UBGD 275080, paratype

Holotype UBGD 275076 (Fig. 52c–f), loc. DH1-5, Confusion Range, *Inyoites beaverensis* sp. nov. beds, Smithian.

Derivation of name Named after the city of Beaver (Utah).

Diagnosis Rather evolute inyoitidae differing from the type species by a more evolute coiling, weaker ornamentation, a less lanceolate venter and a much smaller keel.

Occurrence Abundant in the Confusion Range within the *Inyoites beaverensis* sp. nov. beds [DH1-5, DH1-4]. Rare in the Pahvant Range [DV2-4, DV2-3e, DV2-3d] and the Mineral Mountains [MIA3, MIA2]. Not documented from other studied sections.

Description Evolute, laterally compressed shell with an acute venter and a small, delicate, rarely preserved keel. Flanks parallel near the umbilicus, rapidly becoming convergent towards the venter. Umbilicus wide with rounded margins and an oblique wall. Our specimens do not display any marked ornamentation except for weak, radial folds at mid-flank. Suture line ceratitic, similar to *Inyoites oweni* with elongated saddles and deep, finely indented lateral lobes.

Measurements See Fig. 53. Estimated maximum size: ~7 cm.

Discussion Inyoites beaverensis sp. nov. differs from the type species by a near-absence of ornamentation and its more evolute coiling. It can also be distinguished from *I. krystyni* (see Brayard and Bucher 2008) by its less parallel flanks near the venter and its smaller keel. *I. krystyni* also appears more evolute (Fig. 51). *Subvishnuites stokesi* described by Kummel and Steele (1962) from Nevada exhibits a rather similar coiling ratio, but apparently does not have a ventral keel. Moreover, *S. stokesi* is more

Fig. 53 Scatter diagrams of *H*, *W* and *U*, and *H*/*D*, *W*/*D* and *U*/*D* for *Inyoites beaverensis* sp. nov. (all specimens from the Confusion Range, *Inyoites beaverensis* sp. nov. beds)

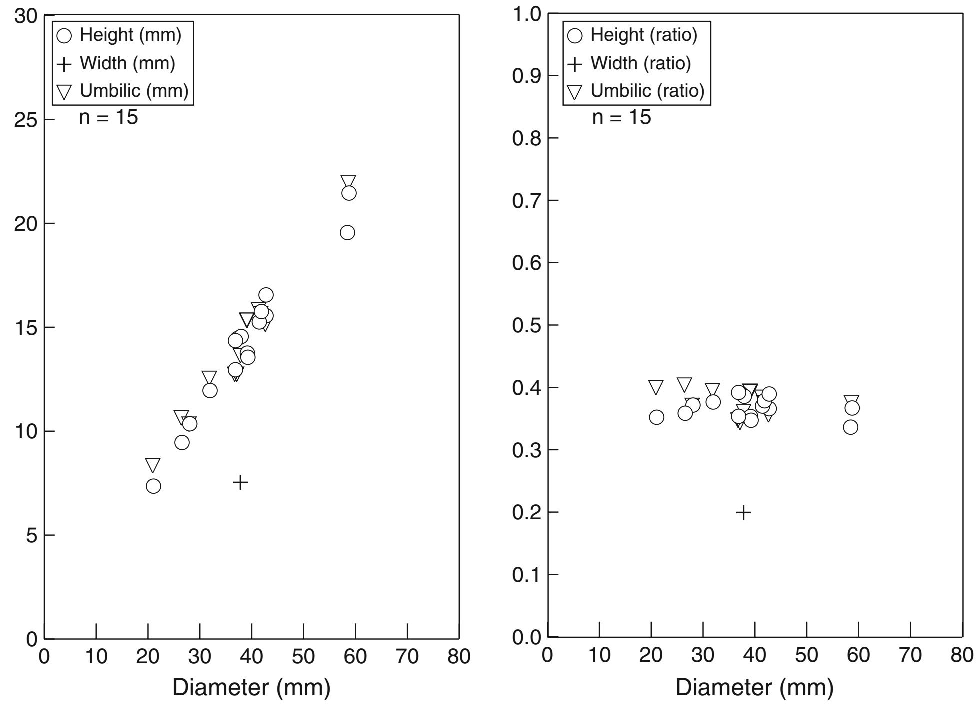

ornamented. At first sight, *I. beaverensis* sp. nov. in terms of morphology may be considered to be an "intermediate" form between *Inyoites* and *Subvishnuites* species.

Family Lanceolitidae Spath, 1934
Genus ***Lanceolites*** Hyatt and Smith, 1905
Type species Lanceolites compactus Hyatt and Smith, 1905

Discussion Lanceolites is an easily distinguishable genus, especially when its suture lines are apparent. Lucas et al. (2007a) reported a specimen of *Lanceolites* sp. from the San Rafael Swell that supposedly co-occurs with *Anasibirites* and *Wasatchites*. Although its overall shape resembles *Lanceolites*, the lack of an illustrated suture lines prevents a definite assignment to this taxon. If this attribution is confirmed in the future, it will represent the only known worldwide occurrence of this genus within the *Anasibirites kingianus* beds. Despite intensive sampling efforts in the San Rafael Swell, we failed to find this genus within these late Smithian beds.

Lanceolites compactus Hyatt and Smith, 1905
Fig. 54a–k

1905 *Lanceolites compactus*; Hyatt and Smith, p. 113, pl. 4, figs. 4-10 ; pl. 5, figs. 7–9; pl. 78, figs. 9–11.
1932 *Lanceolites compactus*; Smith, p. 90, pl. 4, figs. 4–10; pl. 5, figs. 7–9; pl. 21,figs. 21–23; pl. 28, figs. 17–20; pl. 40, figs. 9–11; pl. 60, fig. 10.
1962 *Lanceolites compactus*; Kummel and Steele, p. 692, pl. 102, figs. 6–9.
? 1979 *Lanceolites compactus*; Nichols and Silberling, pl. 2, figs. 39–43.
1995 *Lanceolites compactus*; Shevyrev, p. 39, pl. 2, figs. 1–2.
v 2008 *Lanceolites compactus*; Brayard and Bucher, p. 61, pl. 30, fig. 5, text-fig. 53.
v 2012a *Lanceolites compactus*; Brühwiler and Bucher, p. 38, pl. 20, figs. 4–6.

Occurrence Present within the upper part of the *Owenites* beds, *Inyoites oweni* horizons of the Confusion Range, Pahvant Range, Torrey area and the Mineral Mountains, but less abundant than *L. bicarinatus*. Also found within the *Owenites* beds of South China, the Caucasus and Oman.

Description Occluded discoidal shell with slightly convex flanks. Venter tabulate or slightly sulcate with angular shoulders. Maximum curvature of flanks on their inner half. Whorl height rapidly expanding. Ornamentation not present on our specimens (low folds are known to occur on some previously described specimens). Suture line typical of the genus, subammonitic with broad and strongly indented lobes. Indentations are lanceolate.

Measurements See Fig. 55. Estimated maximum size: ~10 cm.

Discussion Smith (1932) established an additional species of *Lanceolites*: *L. bicarinatus*, based on specimens with a smaller whorl width and narrower venter. Kummel and Steele (1962) questioned the validity of *L. bicarinatus* and considered it to be simply an extreme compressed variant. Brayard and Bucher (2008), Brühwiler et al. (2012a) and

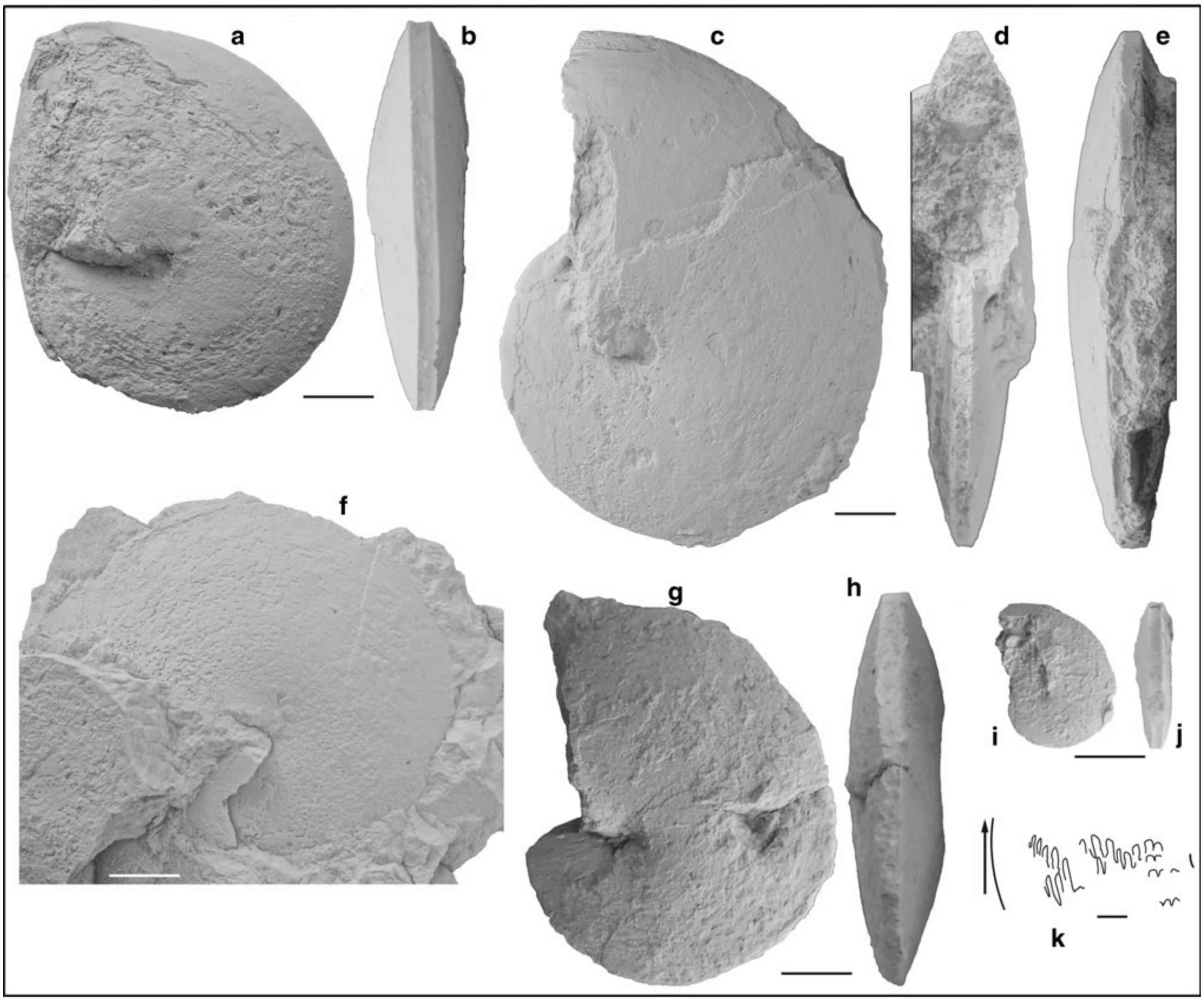

Fig. 54 *Lanceolites compactus* Hyatt and Smith 1905. All from the *Owenites* beds, *Inyoites oweni* horizons, Smithian; **a**, **b** UBGD 275081, loc. DH1-11, Confusion Range; **c–e** UBGD 275082, loc. DH1-11, Confusion Range; **f** UBGD 275083, loc. DV1-7, Pahvant Range; **g**, **h** UBGD 275084, loc. DH1-12, Confusion Range; **i**, **j** UBGD 275085, loc. DV1-8, Pahvant Range; **k** suture line of UBGD 275086, loc. DH1-11, Confusion Range, *scale bar* is 5 mm ($H = 33.4$ mm)

Shevyrev (1995) published a few measurements that indicated these two species may be valid taxa. Unfortunately, the number of previously measured specimens was not enough to resolve the issue. New measured specimens reported here from Utah indicate that any distinction between the two species is tenuous and probably not confirmed (see Fig. 55). Since the number of measured specimens from worldwide locations is still inadequate to solve this issue, we prefer to continue to discriminate the two species. Also note that the illustrated specimens of *L. compactus* from the Caucasus (Shevyrev 1995) apparently exhibit a slightly thicker whorl section at a smaller size compared to our American specimens.

Lanceolites bicarinatus Smith, 1932
Fig. 56a–f

1932 *Lanceolites bicarinatus*; Smith, p. 90, pl. 55, figs. 1–13.
1959 *Lanceolites orientalis*; Chao, p. 263, pl. 41, figs. 5–9.
1984 *Lanceolites bicarinatus*; Vu Khuc, p. 85, pl. 7, figs. 2a, b, text-fig. H18.
1995 *Lanceolites bicarinatus*; Shevyrev, p. 40, pl. 4, fig. 3.
v 2008 *Lanceolites bicarinatus*; Brayard and Bucher, p. 62, pl. 30, fig. 6, text-fig. 53.
v 2010 *Lanceolites bicarinatus*; Stephen et al., figs. 6a, b, g.

Occurrence Relatively common in the upper part of the *Owenites* beds, *Inyoites oweni* horizons of the Confusion Range, Pahvant Range and the Mineral Mountains. Also found in South China, the Caucasus, Vietnam and Oman.

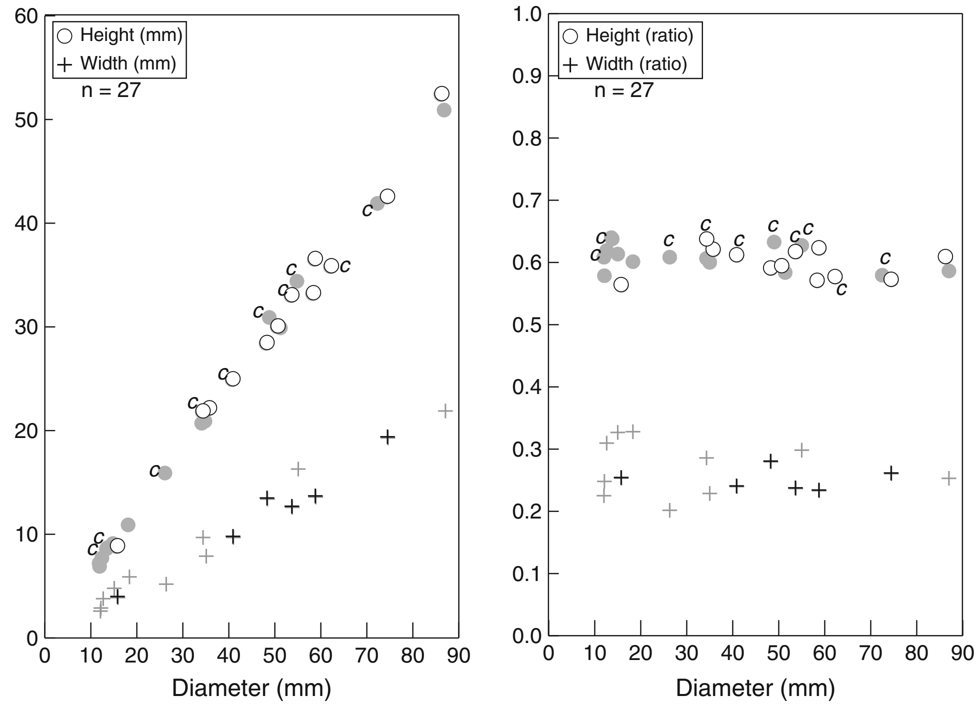

Fig. 55 Scatter diagrams of *H*, *W* and *U*, and *H*/*D*, *W*/*D* and *U*/*D* for *Lanceolites* (*open symbols* indicate specimens from the Confusion Range and Pahvant Range, *Owenites* beds, *Inyoites oweni* horizons [$n = 12$]; *grey symbols* indicate specimens from Vietnam, the Caucasus, Guangxi and Oman; data from Vu Khuc 1984, Shevyrev 1995, Brayard and Bucher 2008, Brühwiler et al. 2012a [$n = 15$]). The symbol *C* indicates specimens assigned to *L. compactus*

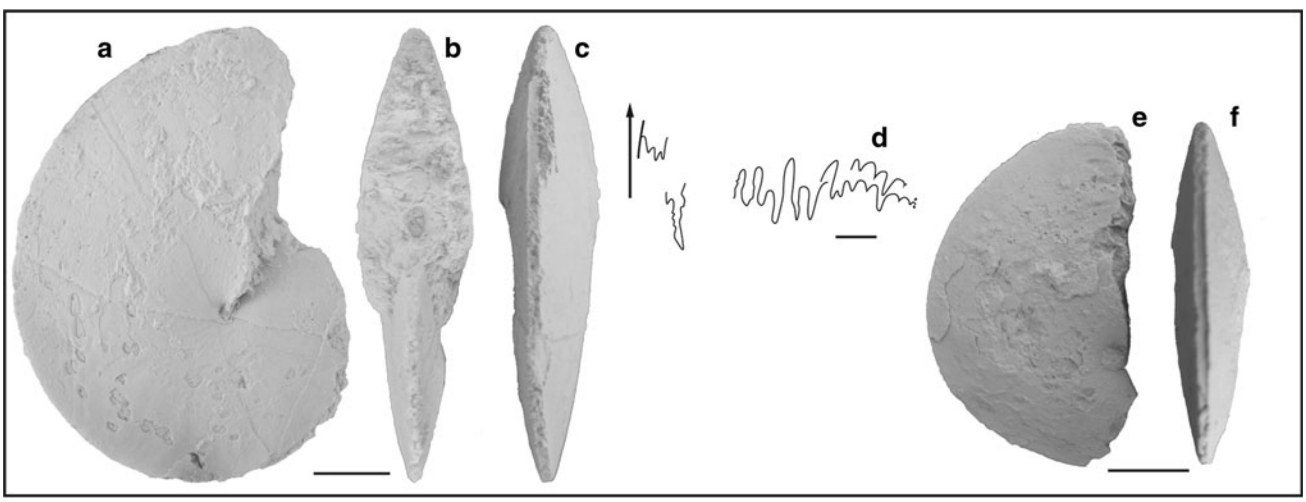

Fig. 56 *Lanceolites bicarinatus* Smith 1932. All from loc. DH1-11, Confusion Range, *Owenites* beds, *Inyoites oweni* horizons, Smithian; **a–c** UBGD 275087; **d–f** UBGD 275088; **d** *scale bar* is 5 mm ($H = 40$ mm)

Description Identical to *L. compactus*, but with a smaller whorl width and a narrower venter that appears almost bicarinate. Ventral shoulders also angular. No ornamentation visible on our specimens. Suture line identical to *L. compactus*.

Measurements See Fig. 55. Estimated maximum size: ~10 cm.

Discussion This species supposedly differs from the type species by its narrower venter (see above).

Family Ussuriidae Spath, 1930
Genus ***Parussuria*** Spath, 1934
Type species Ussuria compressa Hyatt and Smith, 1905

Discussion Scarce morphological and measurement data for ussuriids prevent a thorough revision of the different potential taxa included in the family. Indeed, it appears that the coiling parameters for *Parussuria* and *Metussuria* are extremely close based on the few available data. These genera are therefore distinguished on characters that are

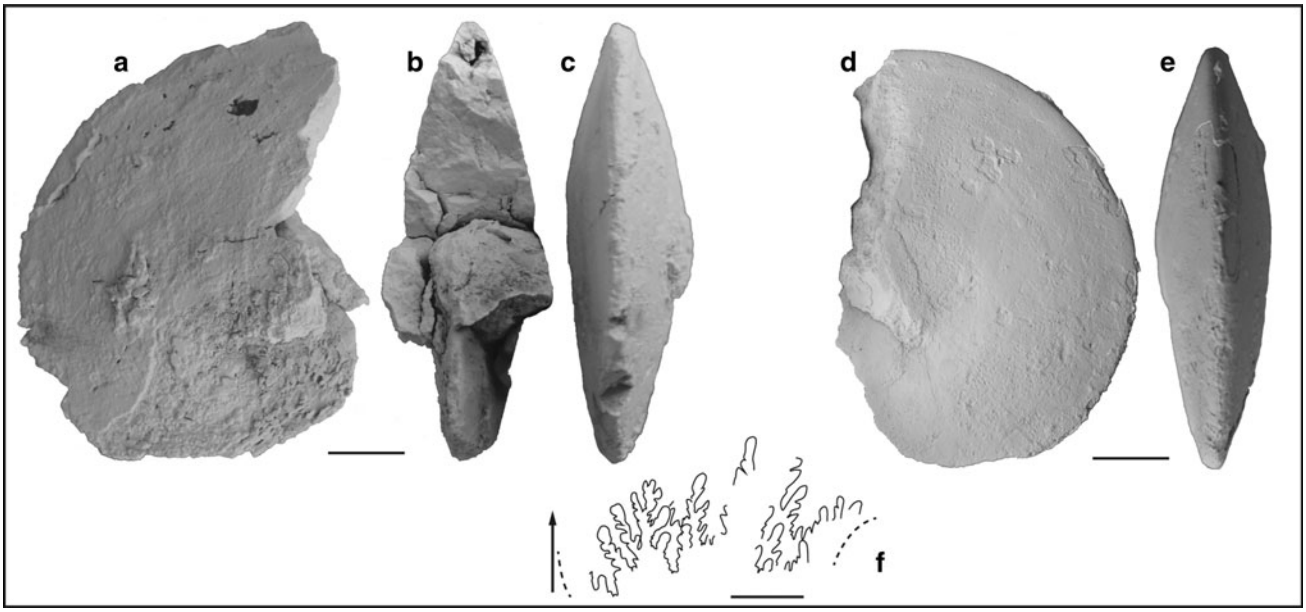

Fig. 57 *Parussuria compressa* (Hyatt and Smith 1905). All from the *Owenites* beds, *Inyoites oweni* horizons, Smithian; **a–c** UBGD 275089, loc. DV1-9, Pahvant Range; **d**, **e** UBGD 275090, loc. DH1-11, Confusion Range; **f** suture line of UBGD 275091, loc. DV1-8, Pahvant Range, *scale bar* is 5 mm ($H = 22$ mm)

subject to preservation bias such as the presence of a very weak ornamentation (*Parussuria*) or a larger juvenile whorl section (*Metussuria*). In lieu of future reported ussuriid occurrences with detailed morphological data, we thus follow the taxonomic assignments previously discussed in Brayard and Bucher (2008) and Brühwiler et al. (2012a).

Parussuria compressa (Hyatt and Smith, 1905)
Fig. 57a–f

1905 *Ussuria compressa*; Hyatt and Smith, p. 89, pl. 3, figs. 6–11.
1932 *Sturia compressa*; Smith, p. 93, pl. 3, figs. 6–11.
1934 *Parussuria compressa*; Spath, p. 213, figs. 66c, d.
1962 *Parussuria compressa*; Kummel and Steele, p. 690, pl. 99: 23; pl. 102, fig. 11.
? 1968 *Parussuria semenovi*; Zakharov, p. 59, pl.5, fig. 4.
1995 *Parussuria compressa*; Shevyrev, p. 37, pl. 4, fig. 6, text-fig. 16.
2008 *Parussuria compressa*; Brayard and Bucher, p. 56, pl. 12, fig. 17.
2012a *Parussuria compressa*; Brühwiler and Bucher, p. 31, pl. 18, figs. 8–14.

Occurrence Abundant in the Confusion Range, Pahvant Range and the Mineral Mountains, *Owenites* beds, *Inyoites oweni* horizons. Not documented from other sections.

Description Involute, compressed oxycone with a typical narrowly rounded venter. Flanks slightly convex with maximum lateral curvature near umbilicus, gradually converging to venter. Umbilicus nearly occluded, with moderately high, oblique wall and rounded shoulders. Ornamentation consists only of weak folds. Since the outer shell is not preserved on our sampled specimens, no strigation was observed. Traces of thin, radial growth lines are sometimes discernible on flanks. Suture line typical of ussuriids with highly frilled lobes and saddles.

Measurements See Fig. 58. Estimated maximum size: ~15 cm.

Discussion Metussuria waageni and *Parussuria compressa* are both reported from the Lower Triassic beds of California (e.g., Hyatt and Smith 1905). *M. waageni* mainly differs from *P. compressa* by its larger juvenile whorl section and its absence of strigation. Our specimens do not show any strigation due to their poor preservation and absence of shell material. However, the conch coiling parameters of our complete but rare specimens are compatible with other known *Parussuria compressa* data.

Family Prionitidae Hyatt, 1900
Genus ***Wasatchites*** Mathews, 1929
Type species Wasatchites perrini Mathews, 1929

Wasatchites perrini Mathews, 1929
Figs. 13d and 59a–k

1929 *Wasatchites perrini*; Mathews, p. 40, pl. 9, figs. 1–9
1929 *Wasatchites meeki*; Mathews, p. 41, pl. 7, figs. 1–3; pl. 8, figs. 11–14.
1929 *Wasatchites magnus*; Mathews, p. 41, pl. 11, figs. 1, 2.

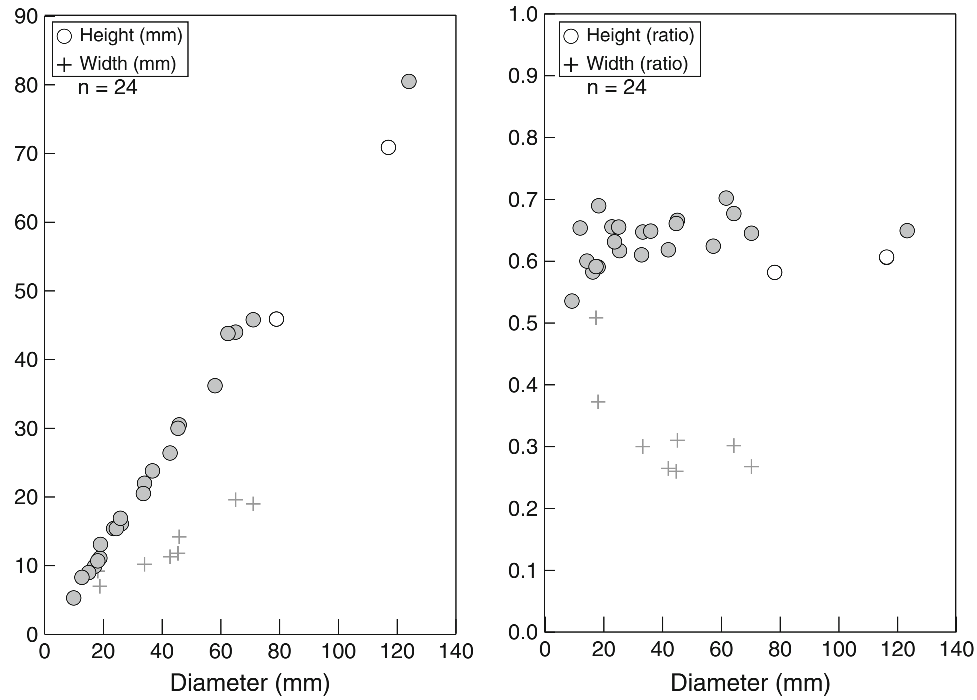

Fig. 58 Scatter diagrams of *H*, *W* and *U*, and *H*/*D*, *W*/*D* and *U*/*D* for *Parussuria compressa* (*open symbols* indicate complete specimens from the Pahvant Range [$n = 2$], *Owenites* beds, *Inyoites oweni* horizons; *grey symbols* indicate specimens from South China, California, Primorye, Oman, and the Caucasus; data from Brayard and Bucher 2008, Kummel and Steele 1962, Zakharov 1968, Brühwiler et al. 2012a, Shevyrev 1995 [$n = 22$])

1929 *Wasatchites quadratus*; Mathews, p. 42, pl. 7, figs. 23–25.
? 1929 *Kashmirites thornei*; Mathews, p. 38, pl. 6, figs. 22–25.
1929 *Kashmirites wasatchensis*; Mathews, p. 36, pl. 6, figs. 26–28.
? 1929 *Kashmirites gilberti*; Mathews, p. 38, pl. 7, figs. 4–8
1929 *Keyserlingites seerleyi*; Mathews, p. 39, pl. 8, figs. 8–10.
1932 *Kashmirites meeki*; Smith, p. 67, pl. 81, figs. 1, 2.
1932 *Kashmirites wasatchensis*; Smith, p. 69, pl. 81, figs. 3–5.
1932 *Kashmirites perrini*; Smith, p. 67, pl. 81, figs. 6–8.
1932 *Kashmirites seerleyi*; Smith, p. 68, pl. 81, figs. 11, 12.
p 1961 *Wasatchites tardus*; Tozer, p. 71, pl. 19, figs. 1a-b (only).
1994 *Wasatchites perrini*; Tozer, p. 79, pl. 29, figs. 5a-c; pl. 35, figs. 2-4.
v 2010 *Wasatchites perrini*; Stephen et al., fig. 7c.

Occurrence Present in the Confusion Range, Pahvant Range, Star Range, Cedar City, Kanarraville, Torrey and San Rafael Swell areas, *Anasibirites kingianus* beds. Not documented in Mineral Mountains.

Description Moderately involute, compressed shell with convex flanks forming a trapezoidal whorl section. Venter ranging from tabulate on some inner whorls to subtabulate or slightly arched on mature whorls, characteristic of Prionitidae, with bluntly angular ventral shoulders. Umbilicus relatively shallow with a typical oblique wall and rounded shoulders. Ornamentation very conspicuous exhibiting projected fold-like ribs varying slightly in strength and width. They typically alternate between strong and weak. Ribs are also typically fasciculate, and may stem from strong tubercles on umbilical shoulders becoming stronger and more bullate or nodate on mature whorls. Ribs do not fade away on outer half of the flanks, but instead continue onto ventral shoulders and are well visible as they cross the venter. Suture line ceratitic with rather deep lateral lobes and broad, rounded saddles, but always poorly preserved on our specimens.

Fig. 59 *Wasatchites perrini* Mathews 1929. All from the *Anasibirites kingianus* beds, Smithian; **a**, **b** UBGD 275092, loc. DH1-13, Confusion Range; **c**, **d** UBGD 275093, loc. DH1-13, Confusion Range; **e**, **f** UBGD 275094, loc. DH1-13, Confusion Range; **g**–**i** UBGD 275095, loc. RCA1, San Rafael Swell area; **j**, **k** UBGD 275096, loc. KA45/46, Kanarraville ▶

Measurements See Fig. 60. Estimated maximum size: ~15 cm.

Discussion *Wasatchites* is a cosmopolitan genus, found for instance in the USA, British Columbia, Arctic Canada, Spitsbergen, Russia, Pakistan (Salt Range), Spiti, Timor and Afghanistan. This taxon is relatively rare in central and eastern Utah compared to the famous late Smithian prionitid *Anasibirites*. However, *W. perrini* is also a typical late Smithian taxon that is helpful for biostratigraphical correlation (e.g., the *Anawasatchites tardus* Zone from British Columbia is a correlative of the *A. kingianus* beds described in this work).

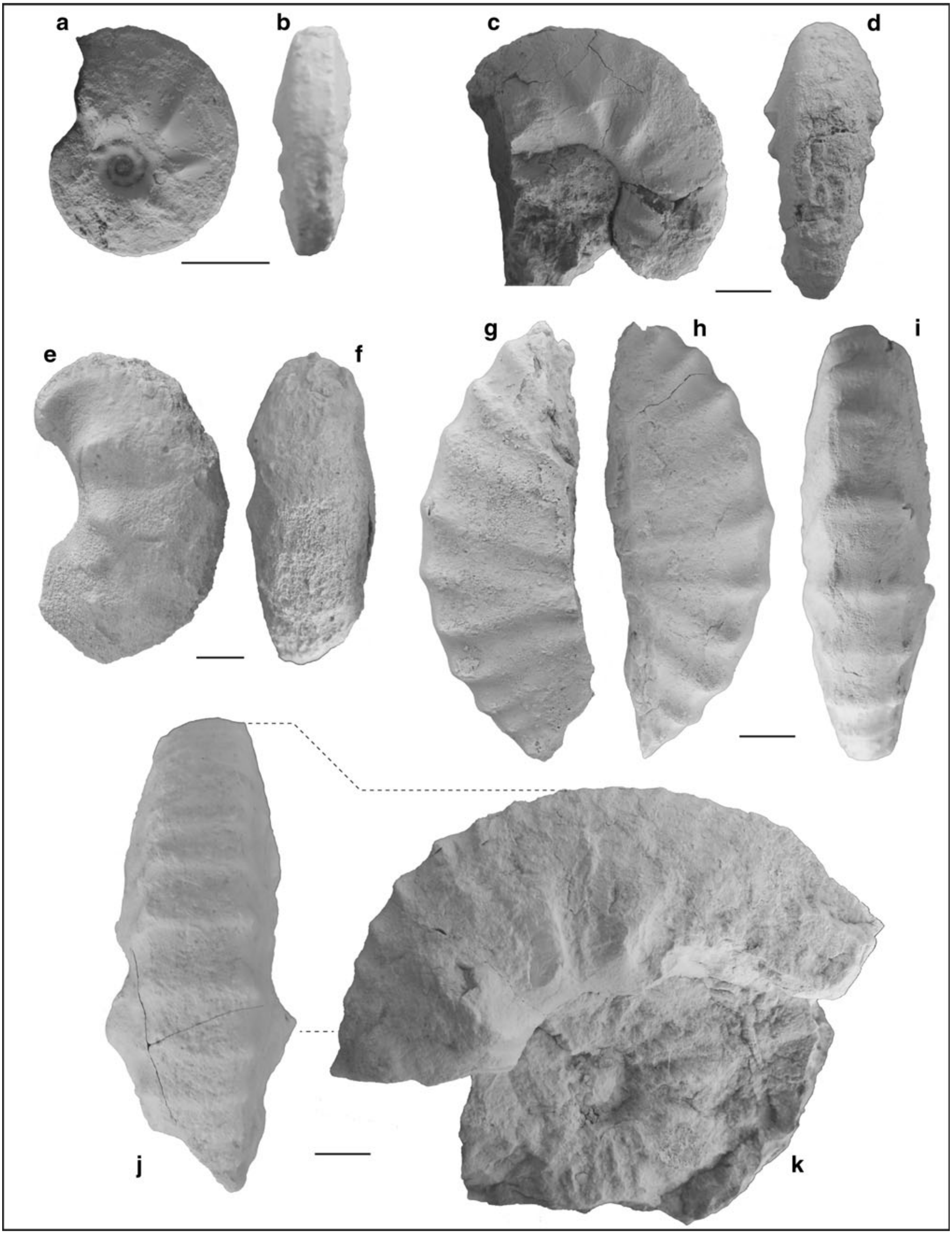
a
b
c
d
e
f
g
h
i
j
k

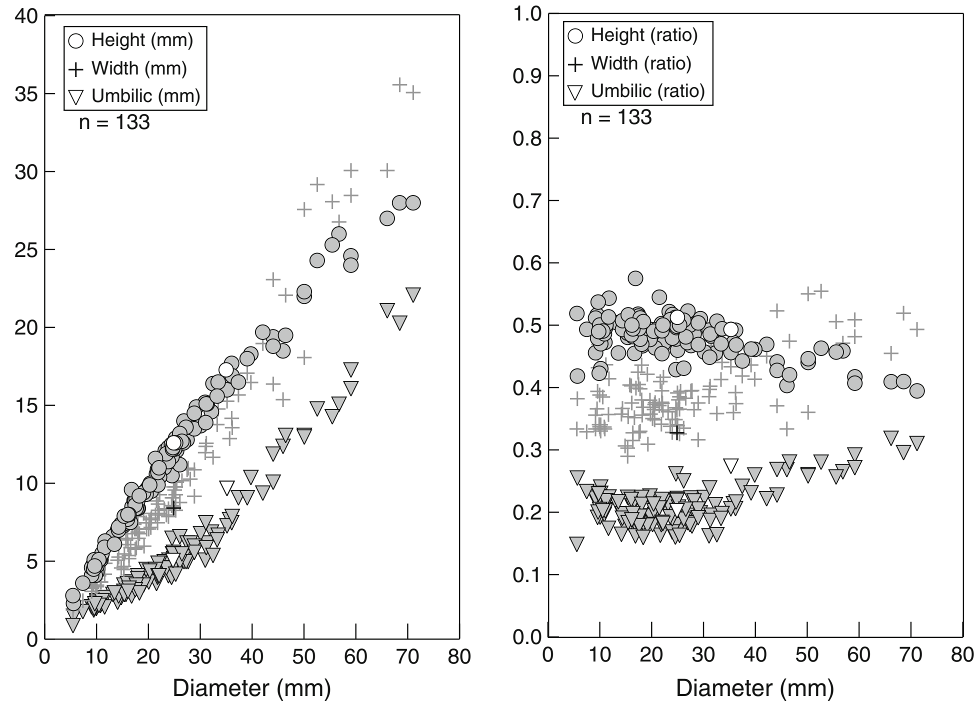

Fig. 60 Scatter diagrams of *H*, *W* and *U*, and *H*/*D*, *W*/*D* and *U*/*D* for *Wasatchites* species. Open symbols indicate complete measurable specimens of *W. perrini* from the Confusion Range, *Anasibirites kingianus* beds; *grey symbols* indicate *W. perrini* and *W. tridentinus* from British Columbia (Tozer 1994, [$n = 3$]) and *W. distractus* from the Spiti and Salt Range (Brühwiler et al. 2012b, c; [$n = 128$])

Wasatchites species may exhibit highly variable ornamentation and a very wide intraspecific variation as do almost all Prionitidae. A correct species assignment is therefore sometimes difficult. Differentiation with other prionitid genera is possible based on the associated marked tuberculation with multiple projected fasciculate or radial ribs originating from the tubercles and crossing the venter.

W. distractus (mainly documented from the Tethys area) essentially differs from the type species by the more lateral position of the spines on the flank and the more radial and conspicuous ribs that appear to diminish at maturity. *W. tridentinus* (British Columbia, Spitsbergen) displays strong bullae on only half a whorl of the body chamber (Tozer 1994). Compared to the type species, *W. deleeni* (British Columbia) presents fewer bullae on the phragmocone and a more ovoid whorl section. *W. procurvus* (British Columbia) differs from all other species by distinctive ribs crossing the venter with a conspicuous forward projected curvature.

Genus ***Anasibirites*** Mojsisovics, 1896
Type species Sibirites kingianus Waagen, 1895

Discussion Pending a thorough revision of the potentially different *Anasibirites* species, we follow the taxonomic assignments previously discussed in Brayard and Bucher (2008) and Brühwiler et al. (2012a, c). The three species illustrated below may therefore be encompassed into a single conspecific American species as previously suggested by some authors (e.g., Kummel and Erben 1968). Indeed, these species generally cannot be identified based only on their measurements (Fig. 61), and are mainly distinguished only by the strength of their ornamentation,

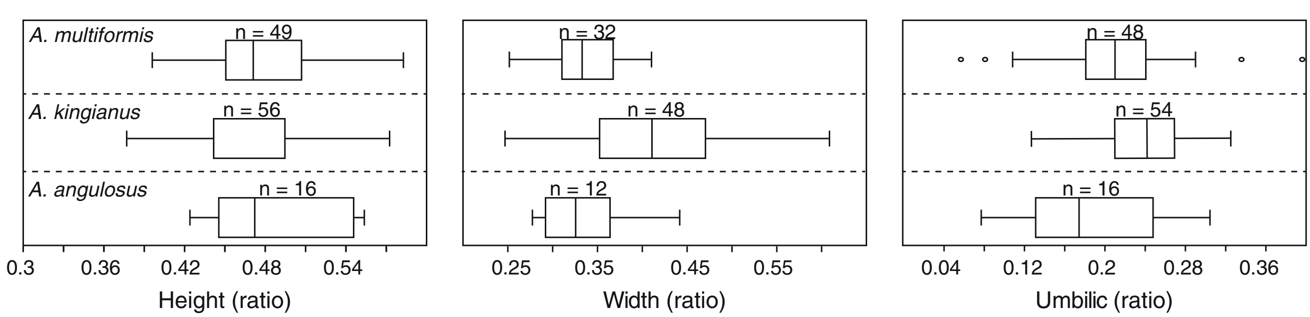

Fig. 61 Box plots of *H*/*D*, *W*/*D* and *U*/*D* for *Anasibirites* species considered in this work. Data for *A. multiformis* Utah (this work), Guangxi (Brayard and Bucher 2008), Timor and Afghanistan (Kummel and Erben 1968). Data for *A. kingianus* Utah (this work), Salt Range (Brühwiler et al. 2012c) and Tibet (Brühwiler et al. 2010b). Data for *A. angulosus* Utah (this work) and Salt Range (Brühwiler et al. 2012c)

which may conform to the Buckman's first law of covariation (Westermann 1966).

Anasibirites kingianus (Waagen, 1895)
Fig. 62a–k

1895 *Sibirites kingianus*; Waagen, p. 108, pl. 8, figs. 1, 2.
1895 *Sibirites chidruensis*; Waagen, p. 109, pl. 8, figs. 3, 4.
1895 *Sibirites inaequicostatus*; Waagen, p. 113, pl. 8, figs. 7, 8.
? 1895 *Sibirites ceratitoides*; Waagen, p. 115, pl. 8, fig. 10.
? 1905 *Sibirites noetlingi*; Hyatt and Smith, p. 49, pl. 9, figs. 1–3.
1909 *Sibirites spiniger*; Krafft and Diener, p. 131, pl. 31, figs. 2–7.
1909 *Sibirites robustus*; Krafft and Diener, p. 132, pl. 31, fig. 1.
? 1909 *Sibirites* sp. indet. ex aff. *robusto*; Krafft and Diener, p. 133, pl. 31, fig. 6.
? 1909 *Sibirites spitiensis*; Krafft and Diener, p. 136, pl. 31, fig. 8.
p 1909 *Sibirites* sp. indet.; Krafft and Diener, p. 138, pl. 31, figs. 4, 5.
1929 *Anasibirites kingianus*; Mathews, p. 8, pl. 7, figs. 14–22.
1929 *Anasibirites perrini*; Mathews, p. 18, pl. 3, figs. 34–36.
1932 *Anasibirites kingianus* var. *inaequicostatus*; Smith, p. 72, pl. 79, figs. 16, 17.
1968 *Anasibirites kingianus*; Kummel and Erben, p. 135, pl. 22, figs. 12-17; pl. 23,figs. 1–18.
? 1974 *Anasibirites kingianus*; Skwarko and Kummel, pl. 40, figs. 2–7.
1978 *Anasibirites kingianus*; Guex, pl. 3, figs. 2, 9; pl. 4, figs. 6.
1981 *Meekoceras* sp.; Dean, pl. 1, fig. 5.
? 2007a *Anasibirites kingianus*; Lucas et al., p. 104, figs. 3h-j only; figs. 4a,b, e–h, j–l.
2010 *Anasibirites kingianus*; Stephen et al., fig. 7a, b.
2012b *Anasibirites kingianus*; Brühwiler et al., p. 155, figs. 31O, 32AA–BD.
2012c *Anasibirites kingianus*; Brühwiler and Bucher, p. 101, figs. 84A–U.

Occurrence Common in all sections within the *Anasibirites kingianus* beds.

Description Moderately involute, compressed shell with convex flanks forming a trapezoidal whorl section. Venter low, arched with rounded shoulders. Umbilicus relatively shallow with an oblique to almost perpendicular wall and rounded shoulders. Well visible ornamentation consisting of an alternation of sinuous, projected fold-like ribs varying in strength and width. Ribs strongly attenuated on adult specimens. Suture line ceratitic with rather deep lateral lobes. Saddles broad and rounded.

Measurements See Figs. 61 and 63. Estimated maximum size: ~10 cm.

Anasibirites multiformis Welter, 1922
Fig. 64a–g

?p 1895 *Sibirites tenuistriatus*; Waagen, p. 124, pl. 9, figs. 2a–b.
p 1922 *Anasibirites multiformis*; Welter, p. 138, pl. 15, figs. 12, 13, 23, 24; pl. 16, figs.6–19.
? 1929 *Anasibirites welleri*; Mathews, p. 14, pl. 2, figs. 17–19.
? 1929 *Anasibirites emmonsi*; Mathews, p. 14, pl. 2, figs. 20–26.
? 2007a *Anasibirites kingianus*; Lucas et al., p. 104, figs. 3d–g only.
v 2008 *Anasibirites multiformis*; Brayard and Bucher, p. 56, pl. 28, figs. 1–6.
v 2012a *Anasibirites multiformis*; Brühwiler and Bucher, p. 33, pl. 19, figs. 1–6.

Occurrence Common in all sections within the *Anasibirites kingianus* beds.

Description Moderately involute, compressed shell with slightly convex flanks. Tabulate to subtabulate venter on inner whorls and subtabulate to arched on mature whorls, with bluntly angular ventral shoulders. Umbilicus relatively shallow with an oblique wall and rounded shoulders. Ornamentation typically consists of dense, concave, fine and projected ribs crossing the venter. Suture line ceratitic with broad and rounded saddles, similar to *A. kingianus*.

Measurements See Figs. 61 and 63. Estimated maximum size: ~10 cm.

Discussion In contrast with other *Anasibirites* species, the ribs of *A. multiformis* are not pronounced and they do not alternate with weak ribs and growth lines. Its venter is also tabulate to subtabulate.

Anasibirites* cf. *angulosus (Waagen, 1895)
Fig. 65a–g

1895 *Sibirites angulosus*; Waagen, p. 117, pl. 8, figs. 12, 13.
1895 *Sibirites ibex*; Waagen, p. 121, pl. 9, fig. 3.
1895 *Sibirites hircinus*; Waagen, p. 123, pl. 9, figs. 12, 13.
? 2007a *Meekoceras* sp.; Lucas et al., p. 104, Fig. 3a only.
2012c *Anasibirites angulosus*; Brühwiler and Bucher, p. 103, figs. 84V–AA, 86A–U,87A–P.

Occurrence Rare in the Confusion Range and San Rafael Swell area, *Anasibirites kingianus* beds.

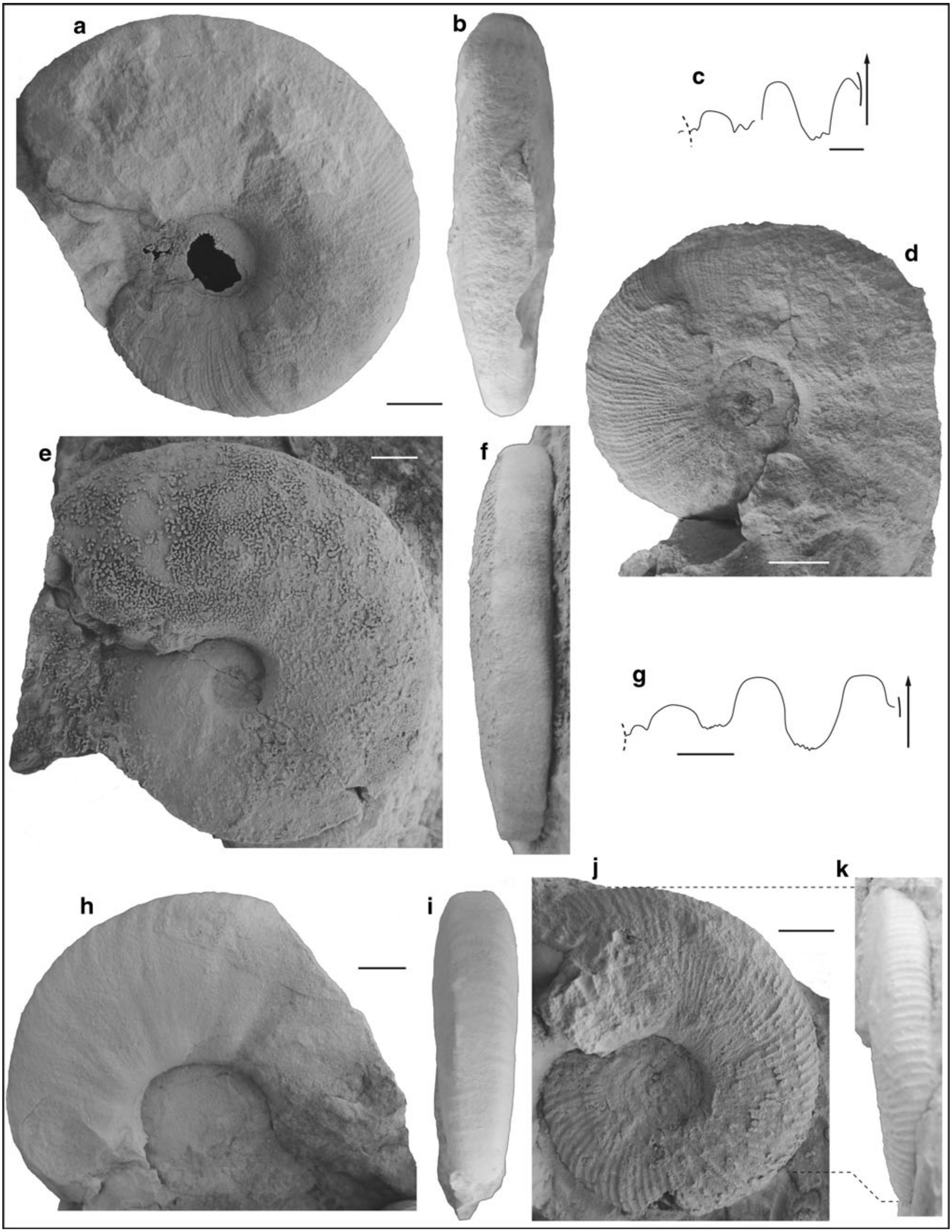
a
b
c
d
e
f
g
h
i
j
k

◀ **Fig. 62** *Anasibirites kingianus* (Waagen 1895). All from the *Anasibirites kingianus* beds, Smithian; **a–c** UBGD 275097, loc. FFA3, Torrey area; **c** *scale bar* is 5 mm ($H = 23$ mm); **d** UBGD 275098, loc. KA45/46, Kanarraville; **e–g** UBGD 275099, loc. RCA1, San Rafael Swell area; **g** *scale bar* is 5 mm ($H = 25.3$ mm); **h, i** UBGD 275100, loc. FFA3, Torrey area; **j, k** UBGD 275101, loc. RCA1, San Rafael Swell area

Description Slightly involute compressed shell with slightly convex flanks. Tabulate venter with angular shoulders. Shallow umbilicus with an oblique wall and rounded shoulders. Ornamentation consists of dense, concave, projected ribs crossing the venter. Sometimes ribs thicken forming elongated tubercles. Suture line ceratitic with broad and rounded saddles, similar to *A. kingianus*.

Measurements See Figs. 61 and 63. Estimated maximum size: ~15 cm.

Discussion A. cf. *angulosus* differs from other *Anasibirites* species by its concave ribs forming elongated tubercles. Our rare complete specimens display sparser ribs and a more compressed whorl section than specimens from the Salt Range (see Brühwiler et al. 2012c), thus preventing a definitive assignment to this species.

Genus ***Hemiprionites*** Spath, 1929
Type species Goniodiscus typus Waagen, 1895

Hemiprionites* cf. *typus (Waagen, 1895)
Fig. 66a–g

1895 *Goniodiscus typus*; Waagen, p. 128, pl. 9, figs. 7–10.
1929 *Goniodiscus typus*; Mathews, p. 31, pl. 5, figs. 12–21.
1929 *Goniodiscus americanus*; Mathews, p. 32, pl. 5, figs. 22–27.
1929 *Goniodiscus shumardi*; Mathews, p. 33, pl. 6, figs. 11–14.
? 1929 *Goniodiscus utahensis*; Mathews, p. 33, pl. 6, figs. 29–31.
? 1929 *Goniodiscus ornatus*; Mathews, p. 34, pl. 65, figs. 6–9.
1932 *Anasibirites typus*; Smith, p. 76, pl. 80, figs. 6-8.
? 1932 *Anasibirites utahensis*; Smith, p. 77, pl. 80, figs. 9, 10.
? 1932 *Anasibirites ornatus*; Smith, p. 75, pl. 80, figs. 11, 12.
1934 *Hemiprionites typus*; Spath, p. 33, figs. 114a–c.
2012c *Hemiprionites typus*; Brühwiler and Bucher, p.103, figs. 89A–AH.

Occurrence One specimen from the Pahvant Range and three fragmentary shells from the Confusion Range, *Anasibirites kingianus* beds.

Description Moderately involute, compressed shell with deeply embracing whorls and slightly egressive coiling. Flanks convex and convergent, but showing a typical depression near the ventral shoulders. Maximum curvature of the flanks near mid-flank. Venter tabulate to weakly sulcate in rare instances. Ventral shoulders bluntly angular. Umbilical shoulders broadly rounded forming a deep umbilicus with an inclined wall. Ornamentation visible on our poorly preserved specimens consists of very low radial folds that sometimes cross the venter. Flexuous growth

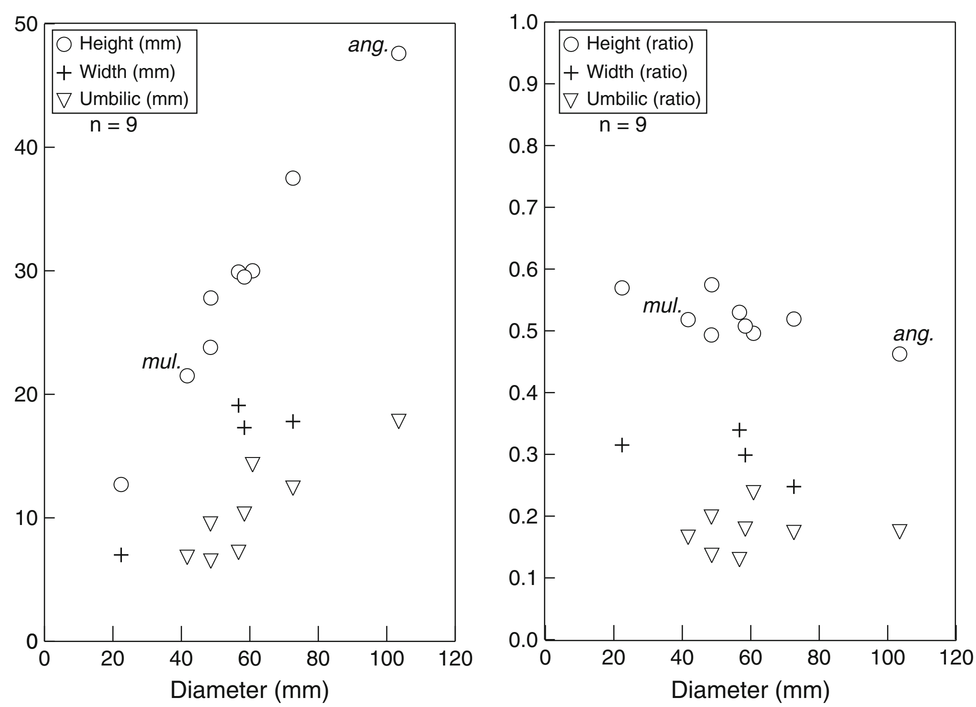

Fig. 63 Scatter diagrams of *H*, *W* and *U*, and *H*/*D*, *W*/*D* and *U*/*D* for *Anasibirites* species (complete specimens from the Confusion Range, *Anasibirites kingianus* beds [$n = 9$]). *ang.* and *mul.* indicate the *A. angulosus* and *A. multiformis* specimens

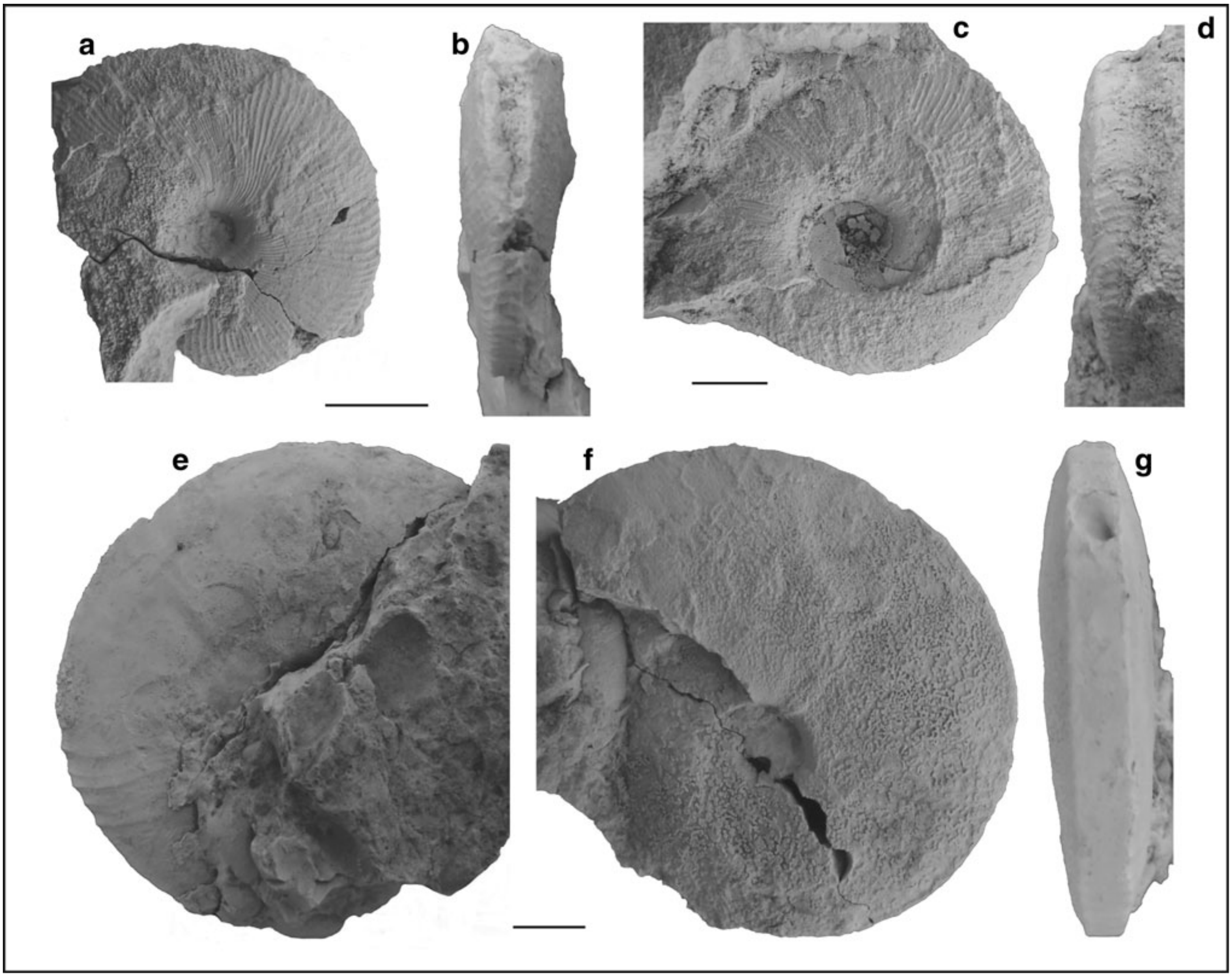

Fig. 64 *Anasibirites multiformis* Welter 1922. All from the *Anasibirites kingianus* beds, Smithian; **a**, **b** UBGD 275102, loc. DH1-13, Confusion Range; **c**, **d** UBGD 275103, loc. DH1-13, Confusion Range; **e**–**g** UBGD 275104, loc. RCA1, San Rafael Swell area

lines are superimposed onto folds. Suture line not visible on our specimens.

Measurements See Table 1.

Discussion Our specimens are similar to the type species. However, because of their poor preservation, it cannot be determined if the "keel" or weak ventral spiral lines observed respectively by Mathews (1929) and Brühwiler et al. (2012c) is present on our specimens, thus precluding their definitive assignment to the type species. They may also appear slightly more laterally compressed compared to the recently illustrated specimens from the Salt Range (Brühwiler et al. 2012c).

Nearly all *Hemiprionites* species occur in the *Anasibirites kingianus* beds (*H. roberti* is from the uppermost *Meekoceras* bed at Crittenden Springs, Nevada; Jenks et al. 2010) and most of the previously described taxa can be included within the type species variation. *H. roberti* from Crittenden Springs (Jenks et al. 2010), *H. butleri* from northern Utah (Mathews 1929) and Guangxi (Brayard and Bucher 2008) and *H. klugi* from Guangxi (Brayard and Bucher 2008) and the Salt Range (Brühwiler et al. 2012c) mainly differ from the type species by their involute coiling and funnel-like umbilicus.

Genus ***Arctoprionites*** (Frebold, 1930)
Type species Goniodiscus nodosus Frebold, 1930.

Arctoprionites resseri (Mathews, 1929)
Fig. 67a–e

1929 *Kashmirites resseri*; Matthews, p. 38, pl. 8, figs. 4–7.
1932 *Kashmirites resseri*; Smith, p. 67, pl. 81, figs. 9, 10.
1961 *Arctoprionites* sp. indet.; Tozer, pl. 20, fig. 1.
v. 1962 *Arctoprionites* sp. indet.; Kummel and Steele, p. 699, pl. 101, fig. 2.
1994 *Arctoprionites williamsi*; Tozer, p. 83, pl. 34, figs. 1–4.

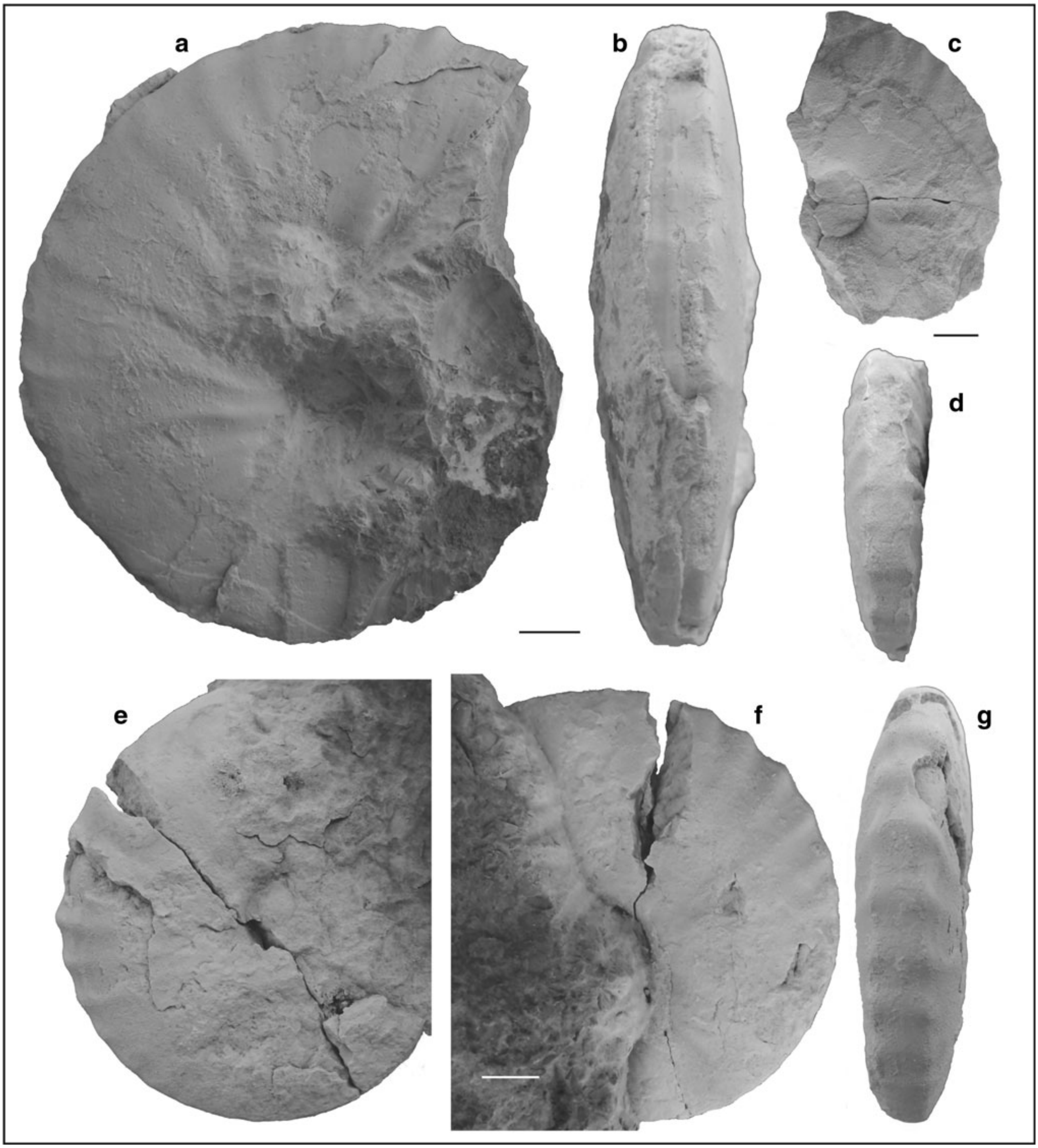

Fig. 65 *Anasibirites* cf. *angulosus* (Waagen 1895). All from the *Anasibirites kingianus* beds, Smithian; **a**, **b** UBGD 275105, loc. DH1-13, Confusion Range; **c**, **d** UBGD 275106, loc. RCA1, San Rafael Swell area; **e–g** UBGD 275107, loc. RCA1, San Rafael Swell area

Occurrence Rare in the San Rafael Swell and Kanarraville [$n = 4$]. All from the *Anasibirites kingianus* beds.

Description Moderately involute coiling similar to *Anasibirites* or *Wasatchites*. Flanks slightly convex forming a trapezoidal whorl section. On small immature whorls, a weak depression near the ventral shoulders, as in *Hemiprionites*, is discernible. Venter markedly flat with bluntly angular shoulders. Umbilical shoulders broadly rounded forming a deep umbilicus with an inclined wall. Our specimens exhibit slightly projected, angular and elongated

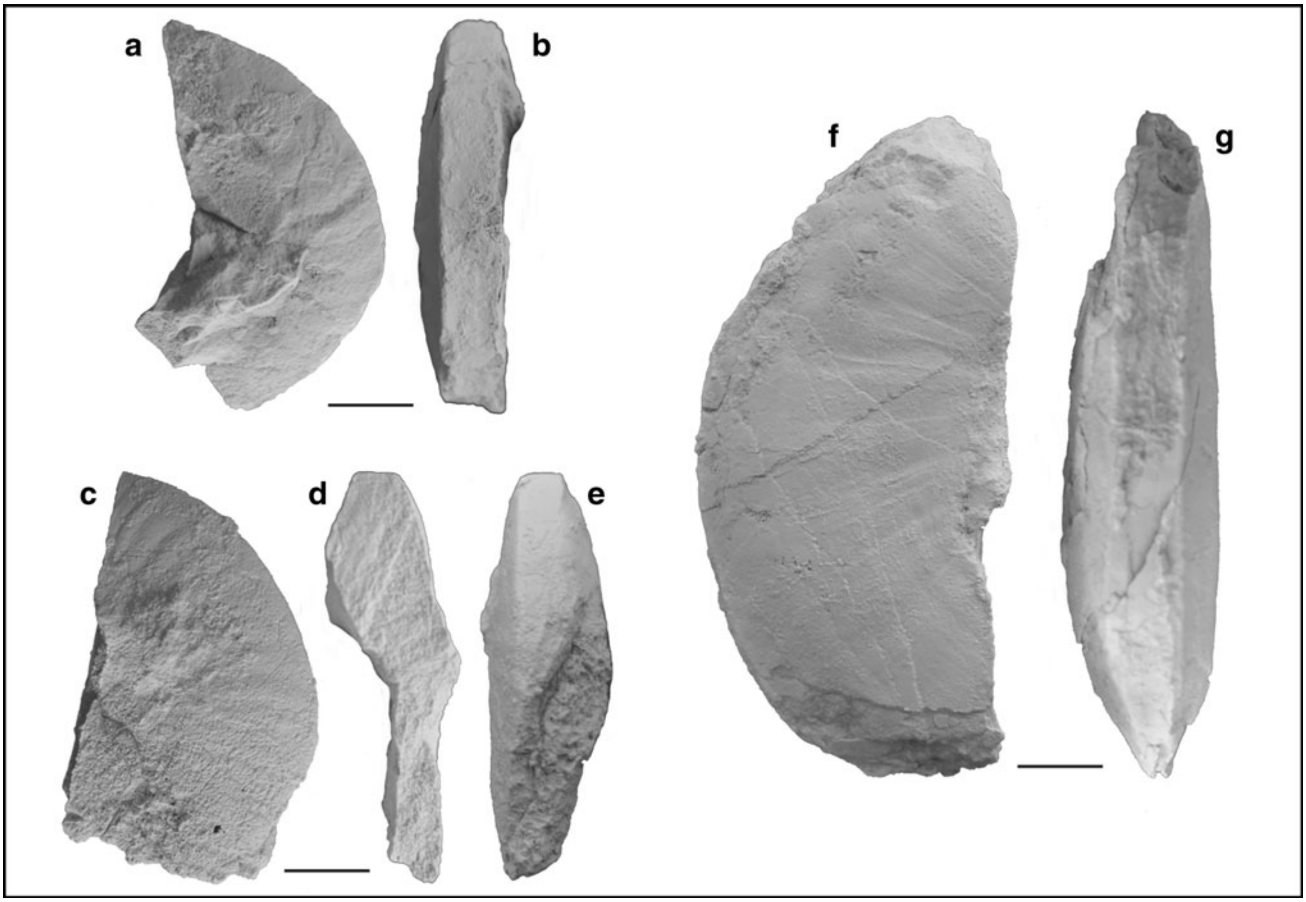

Fig. 66 *Hemiprionites* cf. *typus* (Waagen 1895). All from the *Anasibirites kingianus* beds, Smithian; **a**, **b** UBGD 275108, loc. DH1-13, Confusion Range; **c–e** UBGD 275109, loc. DH1-13, Confusion Range; **f**, **g** UBGD 275110, loc. DH1-13, Confusion Range

bullae near the umbilical margin. Bullae fade away near mid-flank but weak folds sometimes persist, forming a crenulation on the ventral shoulder on smaller specimens. Folds generally do not cross the venter, but on occasion they leave a perceptible weak trace on smaller specimens. Growth lines not visible on our specimens. Suture line ceratitic with broad rounded saddles and deep lateral lobes.

Measurements See Table 1.

Discussion This is the first report of *Arctoprionites* from Utah. *Arctoprionites* sp. indet. illustrated from Nevada by Kummel and Steele (1962) is probably conspecific with *A. resseri*. *Arctoprionites resseri* mainly differs from the Arctic species *A. nodosus* (Frebold, 1930) by its umbilical bullae. Surprisingly, the Spitsbergen specimen that Weitschat and Lehmann (1978) chose to illustrate exhibits only very weak bullae, whereas specimens originally described by Frebold (1930) as well as other specimens from Spitsbergen (J. Jenks, personal observation) exhibit quite prominent bullae. *A. williamsi* described from Arctic Canada by Tozer (1961, 1994) closely resembles *A. resseri*. The description of *A. williamsi* by Tozer (1994) with its more elevated bullae appears doubtful and thus, we consider *A. resseri* and *A. williamsi* as conspecific.

Some specimens of *Anasibirites angulosus* may exhibit similar elongated umbilical tubercules but the whorl section of this species appears more laterally compressed and the tubercles are irregularly spaced. Ribs of *Anasibirites angulosus* also cross the venter. The older prionitid, *Punjabites punjabiensis*, from the Salt Range (Brühwiler et al. 2012c) displays the same type of projected and elongated umbilical bullae, but its venter is rounded.

Genus ***Meekoceras*** Hyatt in White, 1879
Type species Meekoceras gracilitatis White, 1879

Discussion We follow herein the taxonomic assignment of Brühwiler et al. (2012c) of *Meekoceras* to the Prionitidae. Indeed, *Meekoceras* shares many of the same features as most prionitids (i.e., similar whorl shape, umbilicus and suture line), thus justifying its assignment.

Meekoceras gracilitatis White, 1879
Fig. 68a–j

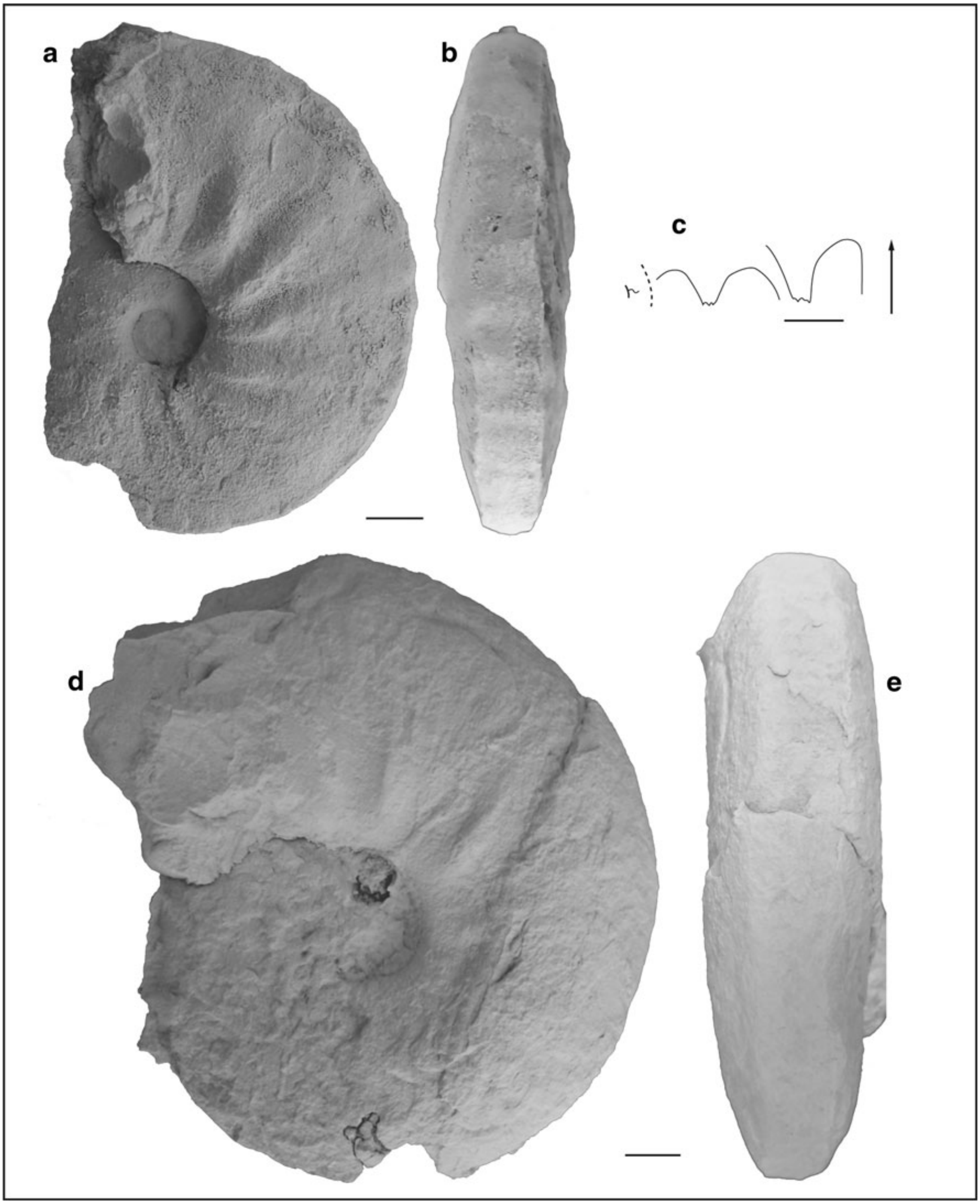

Fig. 67 *Arctoprionites resseri* (Mathews 1929). All from the *Anasibirites kingianus* beds, Smithian; **a**–**c** UBGD 275111, loc. RCA1, San Rafael Swell area; **c** *scale bar* is 5 mm ($H = 21.5$ mm); **d**, **e** UBGD 275112, loc. KA45/46, Kanarraville

1879 *Meekoceras gracilitatis*; White, p. 114.
1880 *Meekoceras gracilitatis*; White, p. 115, pl. 31, fig. 2.
1902 *Meekoceras gracilitatis*; Frech, p. 631, fig. 2.
p 1904 *Meekoceras gracilitatis*; Smith, p. 370, pl. 42, only fig. 1; pl. 43, figs. 3, 4.
1905 *Meekoceras gracilitatis*; Hyatt and Smith, p. 143, pl. 12, figs. 1–13; pl. 13, figs.1–18; pl. 14, figs. 1–8; pl. 70, figs. 4–7.
p 1932 *Meekoceras gracilitatis*; Smith, p. 57, pl. 12, figs. 1–13; pl. 13, figs. 1–18; pl.14, figs. 1–8; pl. 36, figs. 19–28; pl. 37, figs. 1–7; pl. 38, figs. 2, 3 and 5-6 only; pl. 70, figs. 4–7.
1961 *Meekoceras gracilitatis*; Tozer; p. 65, pl. 15, fig. 6; pl. 17, figs. 1-3; pl. 18,figs. 4–6.
1962 *Meekoceras gracilitatis*; Kummel and Steele, p. 693, pl. 103, figs. 1–6.

Fig. 68 *Meekoceras gracilitatis* White 1879. **a–c** UBGD 275113, loc. FFA1, Torrey area, *Owenites* beds, Smithian; **d** *scale bar* is 5 mm ($H = 31.3$ mm); **e**, **f** UBGD 275114, loc. DH1-9, Confusion Range, *Owenites* beds, Smithian; **g–j** UBGD 275115, loc. DH1-6, Confusion Range, between the *Owenites* beds and the *Inyoites beaverensis* sp. nov. beds, Smithian; **g** *scale bar* is 5 mm ($H = 30.6$ mm)

1968 *Meekoceras gracilitatis*; Kummel and Erben, p. 129, pl. 20, figs. 1–3, 8–13.
1979 *Meekoceras gracilitatis*; Nichols and Silberling, p. B3, pl. 1, figs. 1–4.
1990 *Meekoceras gracilitatis*; Dagys and Ermakova, p. 35, pl. 6, fig. 5; pl. 7, fig. 1;pl. 8, figs. 1, 2.
? 1994 *Meekoceras gracilitatis*; Tozer, p. 70, pl. 21, fig. 2.
non 1995 *Meekoceras gracilitatis*; Shevyrev, p. 29, pl. 2, fig. 3.

Occurrence Uncommon in all studied sections from the *Kashmirites–Preflorianites* beds to the *Inyoites oweni* beds. Not found in Kanarraville and San Rafael Swell areas.

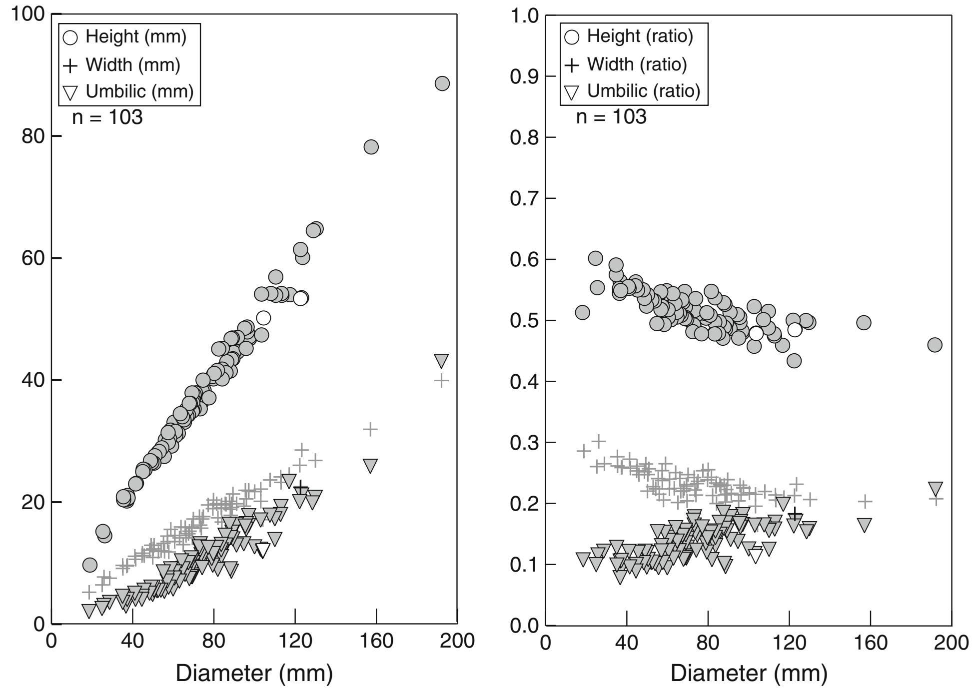

Fig. 69 Scatter diagrams of *H*, *W* and *U*, and *H*/*D*, *W*/*D* and *U*/*D* for *Meekoceras gracilitatis* (*open symbols* indicate specimens from the Confusion Range and Pahvant Range, *Owenites* beds [*n* = 2]; *grey symbols* indicate specimens from Nevada; data from Jenks et al. 2010 [*n* = 101]; Jenks et al. 2010 also described "evolute" specimens which are not illustrated here see Fig. 70)

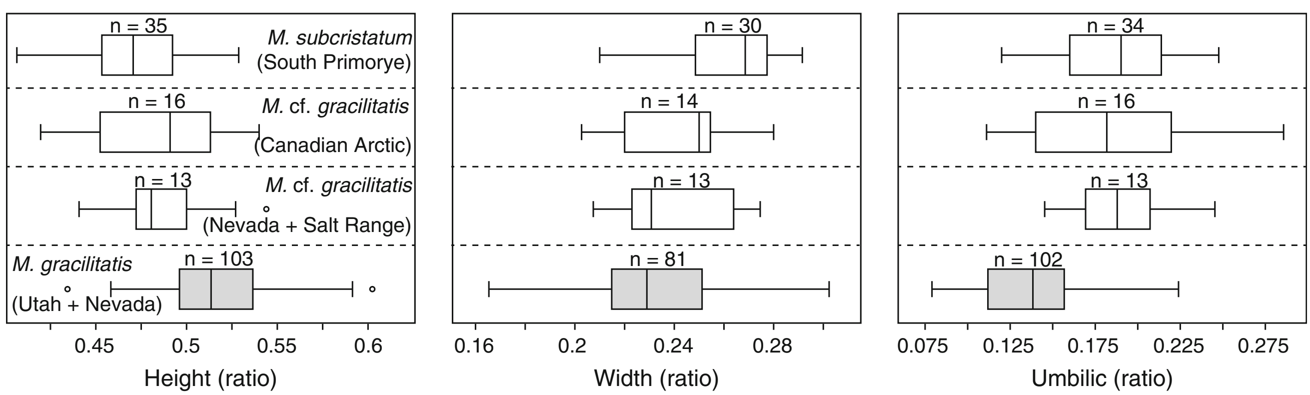

Fig. 70 Box plots of *H*/*D*, *W*/*D* and *U*/*D* for *Meekoceras gracilitatis* from Utah (this work) and Nevada (Jenks et al. 2010), "evolute" *M.* cf. *gracilitatis* from Nevada (Jenks et al. 2010) and Salt Range (Brühwiler et al. 2012c), *M.* cf. *gracilitatis* from the Canadian Arctic (Tozer 1961, 1994) and *M. subcristatum* from South Primorye (Zakharov 1968)

Description Moderately involute coiling and compressed, similar to *Anasibirites* or *Wasatchites*. Flanks slightly convex forming a trapezoidal whorl section. Venter sulcate (true bicarinate venter) on Utah specimens, especially at large size with very angular shoulders. Umbilicus with inclined wall and broadly rounded shoulders forming an intermediate deep umbilicus. Ornamentation often consists of rare barely perceptible projected folds. Folds never cross the venter. Suture line ceratitic with fairly low saddles.

Measurements See Figs. 69 and 70. Estimated maximum size: ~20 cm.

Discussion True *Meekoceras gracilitatis* specimens are relatively easy to distinguish when their preservation is rather good. Indeed, such well-preserved material often exhibits both the typical sulcate venter and the inclined umbilical wall. However, on the Utah specimens the bicarinate venter is often eroded and even becomes tabulate when the specimens are poorly preserved, which is often the case in the studied sections. Consequently, the overall shape of such specimens is extremely close to weathered specimens of *Hemiprionites* and *Anasibirites*, as well as forms of *Wasatchites* and *Arctoprionites* that display very weak ornamentation. Furthermore, the suture line is not diagnostic as is the case with most prionitids. This may explain why many authors have often reported numerous successive beds with *Meekoceras* or confused the *Anasibirites kingianus* beds with older levels where *Meekoceras* does occur. For instance, Lucas et al. (2007a) reported the co-occurrence of *Meekoceras* sp. with *Anasibirites* and

Wasatchites in the San Rafael Swell. However, this attribution is rather unlikely due to the poor preservation of the specimens, which are closer to late Smithian ornamented prionitids such as *Anasibirites*. Moreover, as far as we know, it would represent the only worldwide occurrence of this genus within the *Anasibirites kingianus* beds. We failed to find this genus within the late Smithian beds of the San Rafael Swell.

Brühwiler et al. (2012c), Jenks et al. (2010) and Tozer (1961, 1994) described respectively from the Salt Range, Nevada and southeast Idaho, and the Canadian Arctic, "more evolute" specimens of *M. gracilitatis* without showing robust statistical tests confirming this hypothesis due to the paucity of data. However, we have combined their data and compared them to *M. gracilitatis* measurements. As expected, a segregation between these two groups seems to exist, but it has not yet been statistically confirmed (see Fig. 70).

Several *Meekoceras* species described by Smith (1932; e.g., *M. arthaberi*, *M. sylvanum*) probably can be synonymized with the type species, but we need additional material from Smith's studied sections to confirm this hypothesis. *M. cristatum* is probably a distinct species characterized by its distinctive folds and ribs, which sometimes modify the venter in such a way that it becomes slightly corrugated (Smith 1932 and personal observation of the first author of specimens from southeast Idaho). Specimens from the Caucasus assigned to *M. gracilitatis* (Shevyrev 1995) are doubtful because the whorl section appears to be quadrangular and too thick, and the umbilicus is too deep. They also do not have a bicarinate venter. *M. subcristatum* from South Primorye (Zakharov 1968) mainly differs from the type species by its more conspicuous ornamentation, slightly more evolute coiling and thicker whorl section (Fig. 70).

***Meekoceras olivieri* sp. nov.**
Fig. 71a–l

Holotype UBGD 275116 (Fig. 71a, b), loc. DV2-200, Pahvant Range, *Meekoceras olivieri* sp. nov. beds, Smithian.

Derivation of name Species named after Nicolas Olivier (Lyon).

Diagnosis Very similar to the type species of *Meekoceras*, but differing by a tabulate venter that becomes arched at a large size.

Occurrence Rare (10 specimens) from the Pahvant Range within the *Meekoceras olivieri* sp. nov. beds [DV200].

Description Moderately involute coiling and compressed, similar to *M. gracilitatis*. Venter at small and medium sizes appears to be tabulate with marked rounded shoulders. Venter becomes arched at a large size and ventral shoulders become indistinct. Ornamentation on our largest specimens consists only of large folds. Suture line similar to *M. gracilitatis*.

Measurements See Fig. 72. Estimated maximum size: ~15 cm.

Discussion This taxon exhibits the same overall features as the type species. However, it can be distinguished by its arched venter at larger sizes, which contrasts with the typical sulcate venter of *M. gracilitatis*. At smaller sizes, and especially if specimens are weathered, these two species are almost indistinguishable. *M. olivieri* sp. nov. represents the oldest occurrence of *Meekoceras* in Utah.

***Meekoceras millardense* sp. nov.**
Fig. 73a–g

Holotype UBGD 275121 (Fig. 73a–d), loc. DV2-0, Pahvant Range, *Meekoceras millardense* sp. nov. bed, Smithian.

Derivation of name Name refers to its occurrence in Millard County (Utah).

Diagnosis Very similar to the type species of *Meekoceras*, but differing by its involute coiling.

Occurrence Rare (2 specimens) from the Pahvant Range within the *Meekoceras millardense* sp. nov. bed [DV2-0].
Description Involute and compressed shell with a tabulate venter. Ventral margins bluntly angular with very delicate keels when preserved. Flanks convex. Umbilicus almost occluded. No ornamentation displayed on our specimens. Suture line similar to *M. gracilitatis*, but apparently with lower saddles and delicately crenulated lobes.

Measurements See Table 1. Estimated maximal size: ~5 cm.

Discussion This taxon differs from other *Meekoceras* species by its involute coiling, but its other shell characters are extremely similar.

Family Parannanitidae Spath, 1930
Genus ***Owenites*** Hyatt and Smith, 1905
Type species Owenites koeneni Hyatt and Smith, 1905

Owenites koeneni Hyatt and Smith, 1905
Fig. 74a–i

1905 *Owenites koeneni*; Hyatt and Smith, p. 83, pl. 10, figs. 1–22.
1915 *Owenites koeneni*; Diener, p. 214.
1932 *Owenites koeneni*; Smith, p. 100, pl. 10, figs. 1–22.
1932 *Owenites egrediens*; Smith, p. 100, pl. 52, figs. 6–8.
1932 *Owenites zitteli*; Smith, p. 101, pl. 52, figs. 1–5.
1934 *Owenites koeneni*; Spath, p. 185, fig. 57.

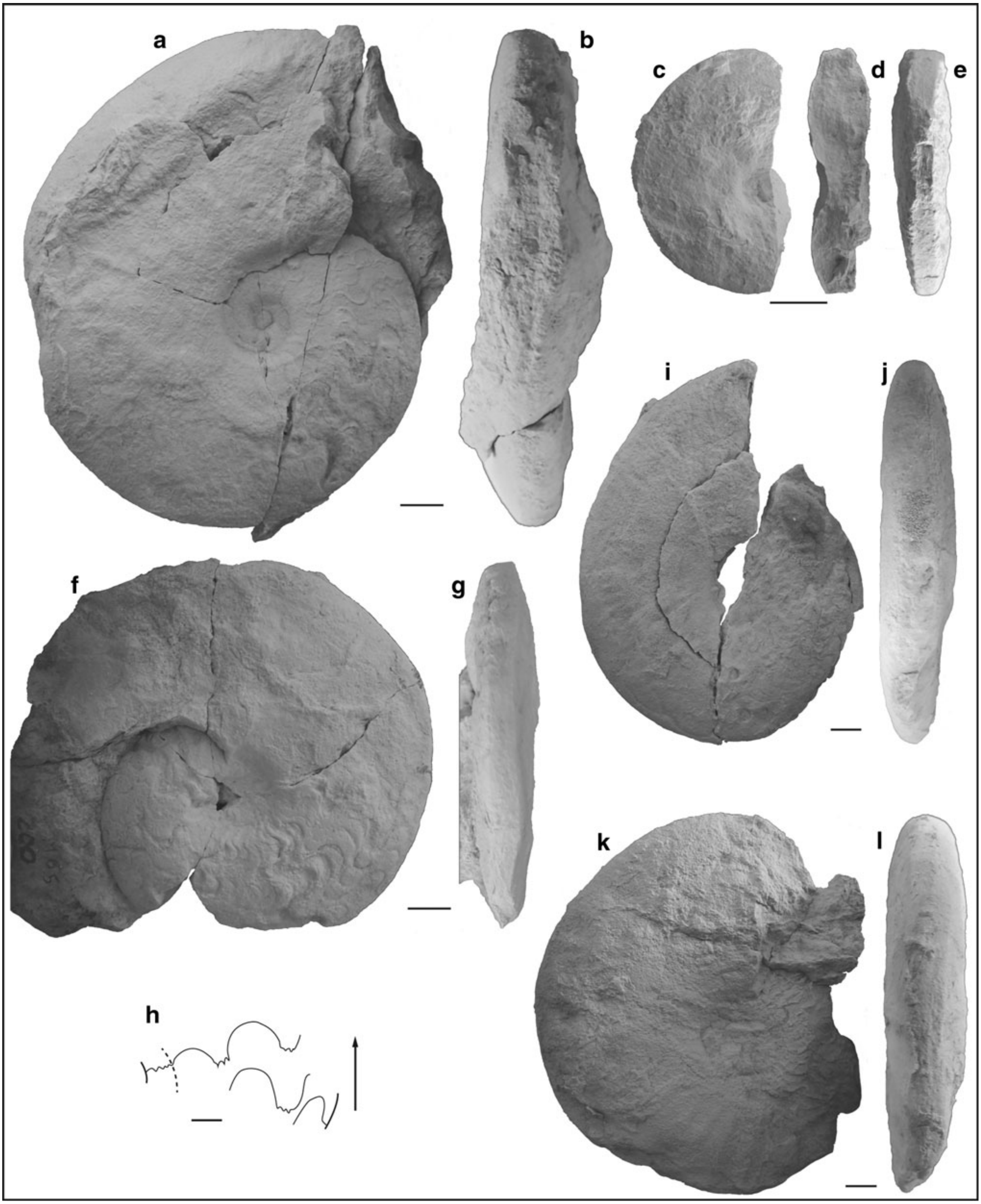

Fig. 71 *Meekoceras olivieri* sp. nov. All from the *Meekoceras olivieri* sp. nov. beds, loc. DV2-200, Pahvant Range, Smithian; **a**, **b** UBGD 275116, holotype; **c**, **e** UBGD 275117, paratype; **f**–**h** UBGD 275118, paratype; **h** *scale bar* is 5 mm ($H = 38.5$ mm); **i**, **j** UBGD 275119, paratype; **k**, **l** UBGD 275120, paratype

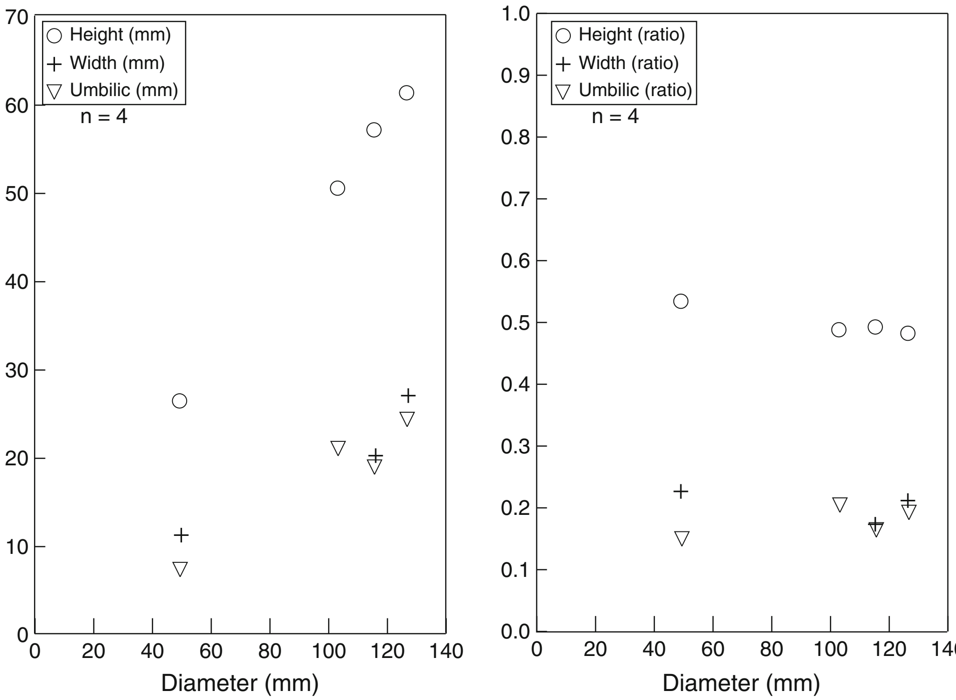

Fig. 72 Scatter diagrams of *H*, *W* and *U*, and *H*/*D*, *W*/*D* and *U*/*D* for *Meekoceras olivieri* sp. nov., *Meekoceras olivieri* sp. nov. beds

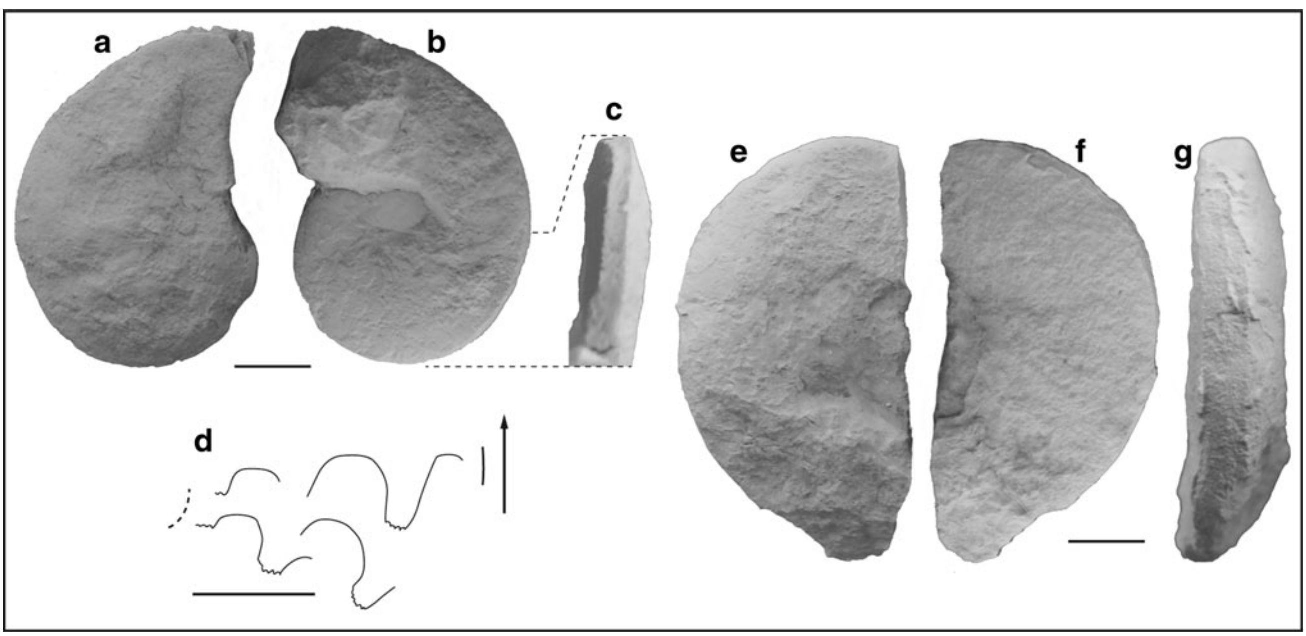

Fig. 73 *Meekoceras millardense* sp. nov. All from the *Meekoceras millardense* sp. nov. bed, loc. DV2-0, Pahvant Range, Smithian; **a–d** UBGD 275121, holotype; **d** *scale bar* is 5 mm ($H = 38.5$ mm); **e–g** UBGD 275122, paratype

1947 *Owenites* aff. *egrediens*; Kiparisova, p. 139, pl. 32, figs. 1–3.
1955 *Kingites shimizui*; Sakagami, p. 138, pl. 2, figs. 2a–c.
1957 *Owenites koeneni*; Kummel in Arkell et al., p. L138, figs. 171-8a–b.
v 1959 *Owenites costatus*; Chao, p. 249, pl. 22, figs. 10-18, 22, 23, text-fig. 26c.
v 1959 *Owenites pakungensis*; Chao, p. 248, pl. 21, figs. 6–8.
v 1959 *Owenites pakungensis* var. *compressus*; Chao, p. 248, pl. 21, figs. 4, 5.
v 1959 *Pseudowenites oxynotus*; Chao, p. 252, pl. 23, figs. 1-16, text-figs. 27a–d.
1959 *Owenites shimizui*; Kummel, p. 430.

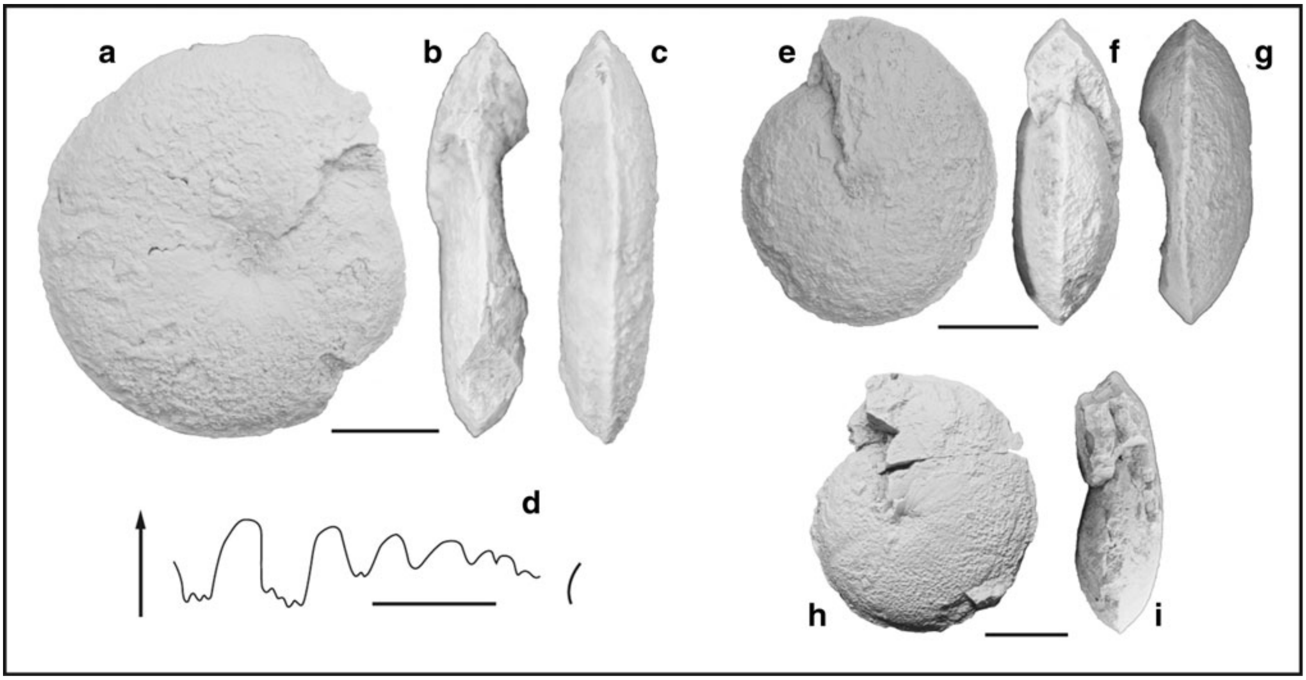

Fig. 74 *Owenites koeneni* Hyatt and Smith 1905. All from the *Owenites* beds, Smithian; **a–d** UBGD 275123, loc. DH1-9, Confusion Range; **d** *scale bar* is 5 mm ($H = 18$ mm); **e–g** UBGD 275124, loc. DH1-9, Confusion Range; **h**, **i** UBGD 275125, loc. DV1-8, Pahvant Range

1960 *Owenites shimizui*; Kummel and Sakagami, p. 6, pl. 2, figs. 5, 6.
1962 *Owenites koeneni*; Kummel and Steele, p. 674, pl. 101, figs. 3–7.
1962 *Owenites koeneni*; Popov, p. 44, pl. 6, fig. 6.
1965 *Owenites koeneni*; Kuenzi, p. 374, pl. 53, figs. 1–6, text-figs. 3d, 6.
1966 *Owenites koeneni*; Hada, p. 112, pl. 4, figs. 2–4.
1968 *Owenites koeneni*; Kummel and Erben, p. 121, figs. 12; pl. 19, figs. 10–15.
1968 *Owenites carinatus*; Shevyrev, p. 189, pl. 16, fig. 1.
1968 *Owenites koeneni*; Zakharov, p. 94, pl. 18, figs. 1–3.
1973 *Owenites koeneni*; Collignon, p. 139, pl. 4, figs. 2, 3.
1979 *Owenites koeneni*; Nichols and Silberling, pl. 1, figs. 17, 18.
1981 *Owenites koeneni*; Bando, p. 158, pl. 17, fig. 7.
1984 *Owenites carinatus*; Vu Khuc, p. 81, pl. 6, figs. 1–4, text-fig. H16.
1984 *Pseudowenites oxynotus*; Vu Khuc, p. 82, pl. 7, figs. 3, 4.
1990 *Owenites koeneni*; Shevyrev, p. 118, pl. 1, fig. 5.
1995 *Owenites koeneni*; Shevyrev, p. 51, pl. 5, figs. 1–3.
? 2004 *Owenites pakungensis*; Tong et al., p. 199, pl. 2, figs. 9-10, text-fig. 7.
v. 2008 *Owenites koeneni*; Brayard and Bucher, p. 67, pl. 36, figs. 1–8, fig. 58.
v. 2010b *Owenites koeneni*; Brühwiler et al., p. 426, fig. 15(9).
v. 2012a *Owenites koeneni*; Brühwiler and Bucher, p. 43, pl. 25, figs. 1–6.

Occurrence Rare in all sections, *Owenites* beds. Not found in the Torrey area. Common at Crittenden Springs (Nevada) and southeastern Idaho.

Description Almost involute, somewhat compressed shell with an inflated, lenticular whorl section and a typical, subangular to angular venter that may resemble a keel on mature specimens. Narrow, shallow umbilicus, with a very low, steep wall and narrowly rounded shoulders. Whorl height and umbilical diameter of *O. koeneni* display significant allometric growth (Brayard and Bucher 2008). Egressive coiling at maturity. Surface generally smooth, but may exhibit weak, forward projected constrictions and folds. Suture line ceratitic with several divided umbilical lobes.

Measurements See Table 1. Estimated maximum size: ~8 cm (see Brayard and Bucher 2008).

Discussion For a thorough discussion of *O. koeneni* systematics, please refer to Brayard and Bucher (2008). Our illustrated specimens appear somewhat more compressed than the holotype and paratypes of Hyatt and Smith (1905), and the South China specimens. Other characters appear to be similar. *Owenites* species are typical of the mid and upper parts of the middle Smithian and of the Early Triassic tropical belt.

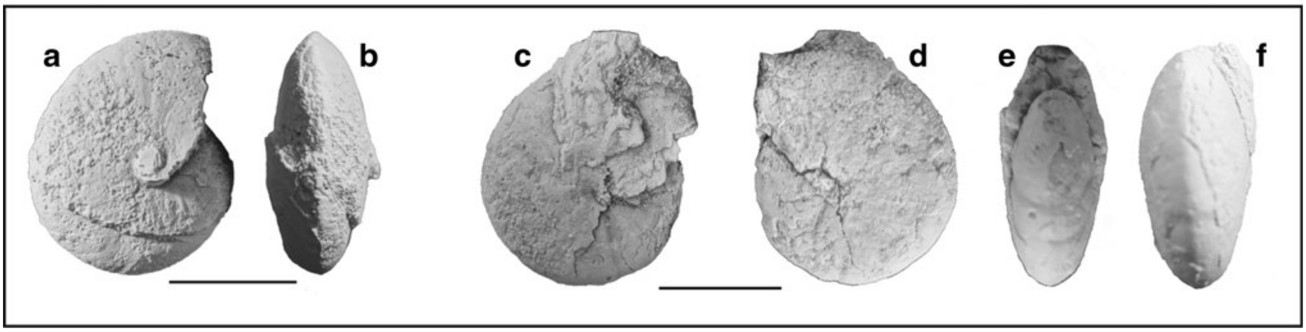

Fig. 75 *Owenites carpenteri* Smith 1932. All from the *Owenites* beds, Smithian; **a**, **b** UBGD 275126, loc. DH1-12, Confusion Range; **c**–**f** UBGD 275127, loc. DV1-8, Pahvant Range

Owenites carpenteri Smith, 1932
Fig. 75a–f

1932 *Owenites carpenteri*; Smith, p. 100, pl. 54, figs. 31–34.
1966 *Owenites carpenteri*; Hada, p. 112, pl. 4, figs. 1a–e.
1968 *Owenites costatus*; Kummel and Erben, p. 122, fig. 12l.
1973 *Owenites carpenteri*; Collignon, p. 139, pl. 4, figs. 5, 6.
v 2008 *Owenites carpenteri*; Brayard and Bucher, p. 70, pl. 43, figs. 15, 16.
2010b *Owenites carpenteri*; Brühwiler et al., p. 426, fig. 16(7, 8).
v 2012a *Owenites carpenteri*; Brühwiler and Bucher, p. 44, pl. 25, figs. 7, 8.

Occurrence Relatively rare in all sections, *Owenites* beds. Not documented from the Torrey area. Also found in northeastern Nevada (Cottonwood Canyon and Crittenden Springs), South China, Spiti and Oman.

Description Small, involute and compressed oxyconic shell. Venter subangular to narrowly rounded. Whorl section slightly inflated and lenticular. Flanks convex from the occluded umbilicus. Maximum thickness near the umbilicus. A few folds are displayed on the shell. Some distant constrictions may be present on internal mold. Suture line similar to *O. koeneni*.

Measurements See Fig. 76. Estimated maximum size: ~3.5 cm.

Discussion For a complete discussion regarding the ornamentation of this species, please refer to Brühwiler et al. (2012a). *O. carpenteri* can be easily distinguished from the type species and *O. simplex* by its occluded umbilicus and narrowly curved venter.

Family Hedenstroemiidae Waagen, 1895
Genus ***Pseudosageceras*** Diener, 1895
Type species Pseudosageceras sp. indet. Diener, 1895

Pseudosageceras multilobatum Noetling, 1905
Fig. 77a–f

1905 *Pseudosageceras multilobatum*; Noetling, pl. 25, fig. 1, pl. 26, fig. 3.
1905 *Pseudosageceras intermontanum*; Hyatt and Smith, p. 99, pl. 4, figs. 1–3; pl. 5,figs. 1–6; pl. 63, figs. 1, 2.
1909 *Pseudosageceras multilobatum*; Krafft and Diener, p. 145, pl. 21, fig. 5.
1911 *Pseudosageceras drinense*; Arthaber, p. 201, pl. 17, figs. 6, 7.
1913 *Pseudosageceras multilobatum*; Wanner, p. 181, pl. 7, fig. 4.
1922 *Pseudosageceras multilobatum*; Welter, p. 94, fig. 3.
1929 *Pseudosageceras intermontanum*; Mathews, p. 3, pl. 1, figs. 18–22.
1932 *Pseudosageceras multilobatum*; Smith, p. 87-89, pl. 4, figs. 1–3; pl. 5, figs. 1–6;pl. 25, figs. 7–16; pl. 60, fig. 32; pl. 63, figs. 1–6.
1934 *Pseudosageceras multilobatum*; Collignon, p. 56-58, pl. 11, fig. 2.
1934 *Pseudosageceras multilobatum*; Spath, p. 54, fig. 6a.
1947 *Pseudosageceras multilobatum*; Kiparisova, p. 127, pl. 25, figs. 3, 4.
1947 *Pseudosageceras multilobatum* var. *giganteum*; Kiparisova, p. 127, pl. 26, figs.2–5.
1948 *Pseudosageceras* cf. *clavisellatum*; Renz and Renz, p. 90, pl. 16, fig. 3.
1948 *Pseudosageceras drinense*; Renz and Renz, p. 92, pl. 16, fig. 6.
1948 *Pseudosageceras intermontanum*; Renz and Renz, p. 90, pl. 16, figs. 4, 7.
v 1959 *Pseudosageceras multilobatum*; Chao, p. 183, pl. 1, figs. 9, 12.
v 1959 *Pseudosageceras tsotengense*; Chao, p. 184, pl. 1, figs. 7, 8, text-fig. 5b.
v 1959 *Pseudosageceras curvatum*; Chao, p. 185, pl. 1, figs. 13, 14, text-fig. 5a.
? 1959 *Pseudosageceras multilobatum* var. nov.; Jeannet, p. 30, pl. 6, fig. 1.

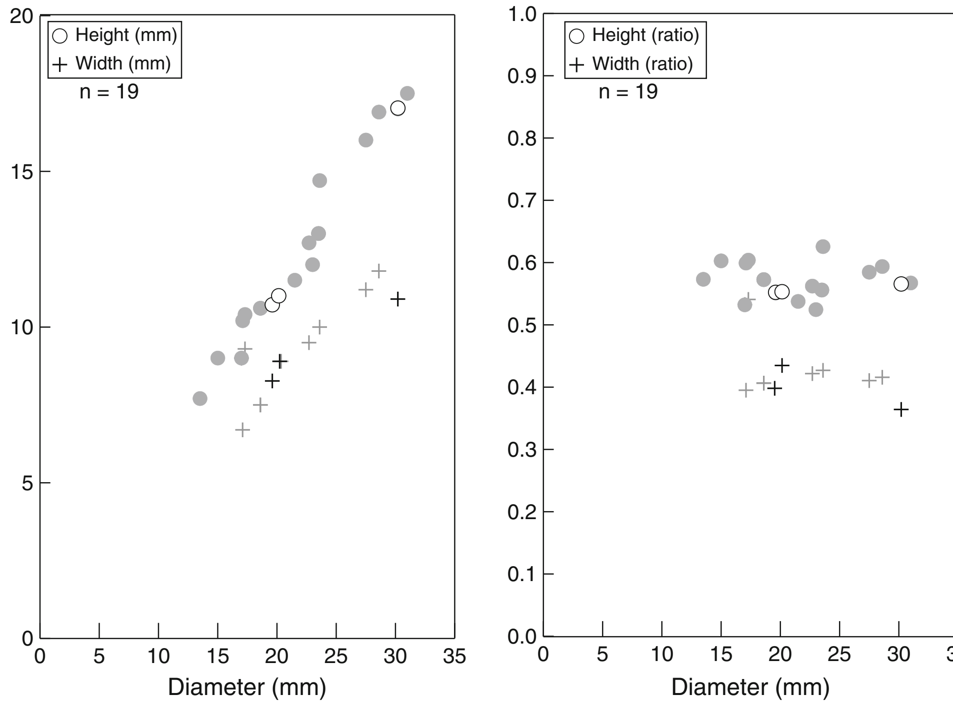

Fig. 76 Scatter diagrams of *H*, *W* and *U*, and *H*/*D*, *W*/*D* and *U*/*D* for *Owenites carpenteri* (*open symbols* indicate specimens from the Confusion Range and Pahvant Range, *Owenites* beds [$n = 3$]; *grey symbols* indicate specimens from Guangxi, Tibet, Spiti and Oman; data from Brayard and Bucher 2008, Brühwiler et al. 2010b, 2012a, b; [$n = 16$])

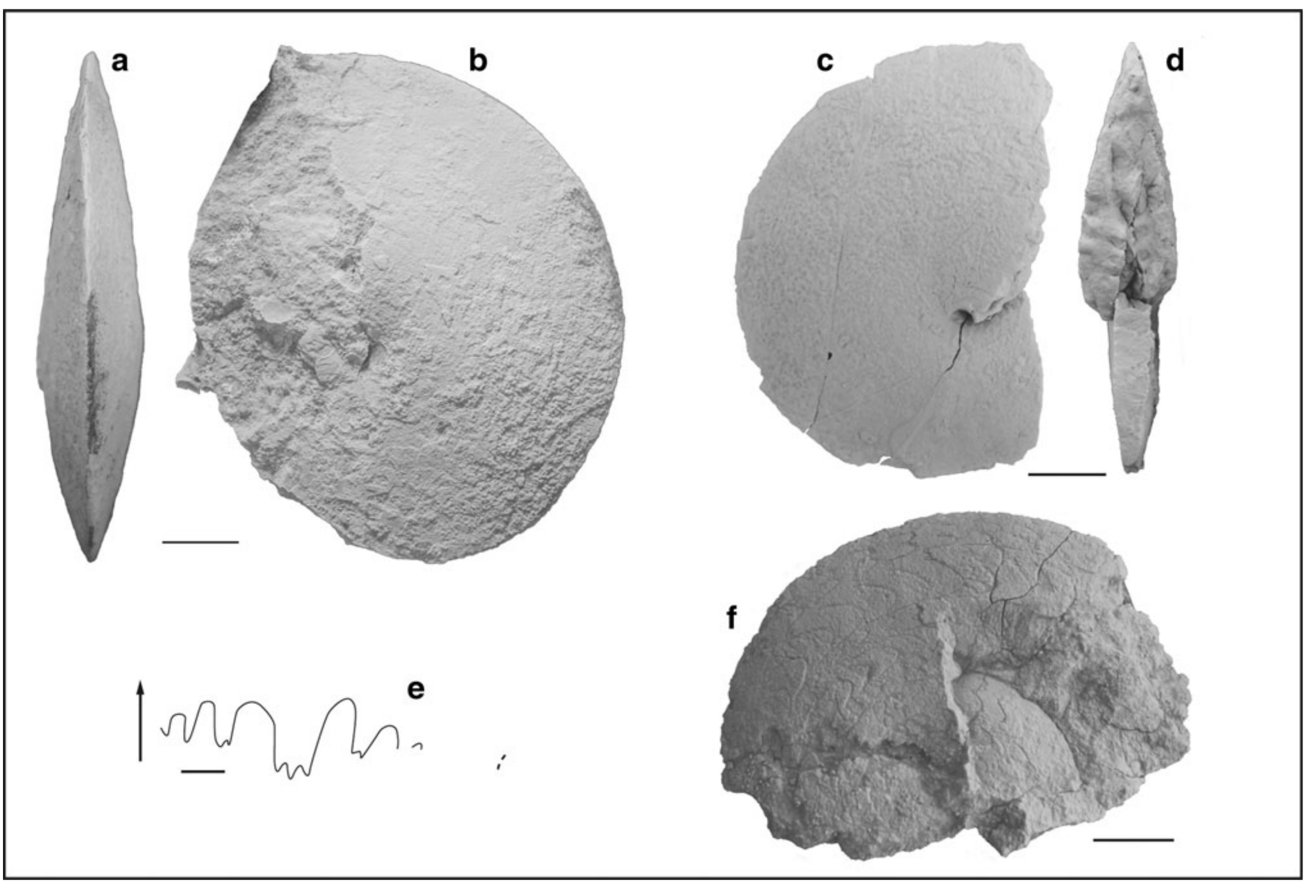

Fig. 77 *Pseudosageceras multilobatum* Noetling 1905. **a**, **b** UBGD 275128, loc. DH1-9, Confusion Range, *Owenites* beds, Smithian; **c**, **d** UBGD 275129, loc. DV2-7, Pahvant Range, *Owenites* beds, Smithian; **e** suture line of UBGD 275130, loc. DH1-2, Confusion Range, *Preflorianites–Kashmirites* beds, Smithian, *scale bar* is 5 mm ($H = 49$ mm); **f** UBGD 275140, loc. DH1-1, Confusion Range, *Preflorianites–Kashmirites* beds

1961 *Pseudosageceras schamarense*; Kiparisova, p. 31, pl. 7, fig. 3.
1961 *Pseudosageceras multilobatum* var. *gigantea*; Popov, p. 13, pl. 2, figs. 1, 2.
non 1962 *Pseudosageceras multilobatum*; Kummel and Steele, p. 701, pl. 102, figs. 1, 2.
? 1966 *Pseudosageceras multilobatum*; Hada, p. 112, pl. 4, fig. 6.
? 1968 *Pseudosageceras multilobatum*; Kummel and Erben, p. 112, pl. 19, fig. 9.
1968 *Pseudosageceras multilobatum*; Shevyrev, p. 791, pl. 1, figs. 1, 2.
? 1973 *Pseudosageceras multilobatum*; Collignon, p. 5, pl. 1, fig. 1.
1978 *Pseudosageceras multilobatum*; Weitschat and Lehmann, p. 95, pl. 10, figs. 2ab.
1984 *Pseudosageceras multilobatum*; Vu Khuc, p. 26, pl. 1, fig. 1.
1994 *Pseudosageceras multilobatum*; Tozer, p. 83, pl. 18, figs. 1a, b; p. 384, fig. 17.
v 2008 *Pseudosageceras multilobatum*; Brayard and Bucher, p. 70, pl. 37, figs. 1–5.
v 2010 *Pseudosageceras multilobatum*; Stephen et al., figs. 6c, d, h.
v 2010b *Pseudosageceras multilobatum*; Brühwiler et al., p. 429, fig. 16(14).
v 2012a *Pseudosageceras multilobatum*; Brühwiler and Bucher, p. 47, pl. 26, fig. 4.
v 2012c *Pseudosageceras multilobatum*; Brühwiler and Bucher, p. 109, figs. 95A–N.

Occurrence Long-ranging cosmopolitan species, but extremely rare in all studied sections (only one measurable complete specimen). Common in northeastern Nevada and southeastern Idaho.

Description See, e.g., Brayard and Bucher (2008) for a thorough description. Involute oxyconic shell with an occluded umbilicus. Venter extremely narrow and bicarinate. Flanks weakly convex. Surface smooth without ornamentation. Suture line complex, typical of Hedenstroemiidae with several adventitious lobes and a characteristic trifid lateral lobe. Others lobes are bifid.

Measurements See Fig. 78. Estimated maximum size: ~15 cm.

Discussion Species typical for hedenstroemiids. Easily recognizable by its compressed and involute oxyconic shell, as well as its complex suture line architecture.

Genus ***Hedenstroemia*** Waagen, 1895
Type species Ceratites hedenstroemi Keyserling, 1845

Hedenstroemia kossmati Hyatt and Smith, 1905
Fig. 79a–f

1905 *Hedenstroemia kossmati*; Hyatt and Smith, p. 101, pl. 67, figs. 3–7; pl. 84, figs.1–10.
1932 *Hedenstroemia kossmati*; Smith, p. 78, pl. 28, figs. 11–16; pl. 41, figs. 1–10; pl.67, figs. 3–7.
1932 *Hedenstroemia hyatti*; Smith, p. 78, pl. 27, figs. 13–18.
v. 2010 Proptychitid gen. et sp. indet.; Stephen et al., fig. 4g, h, i.

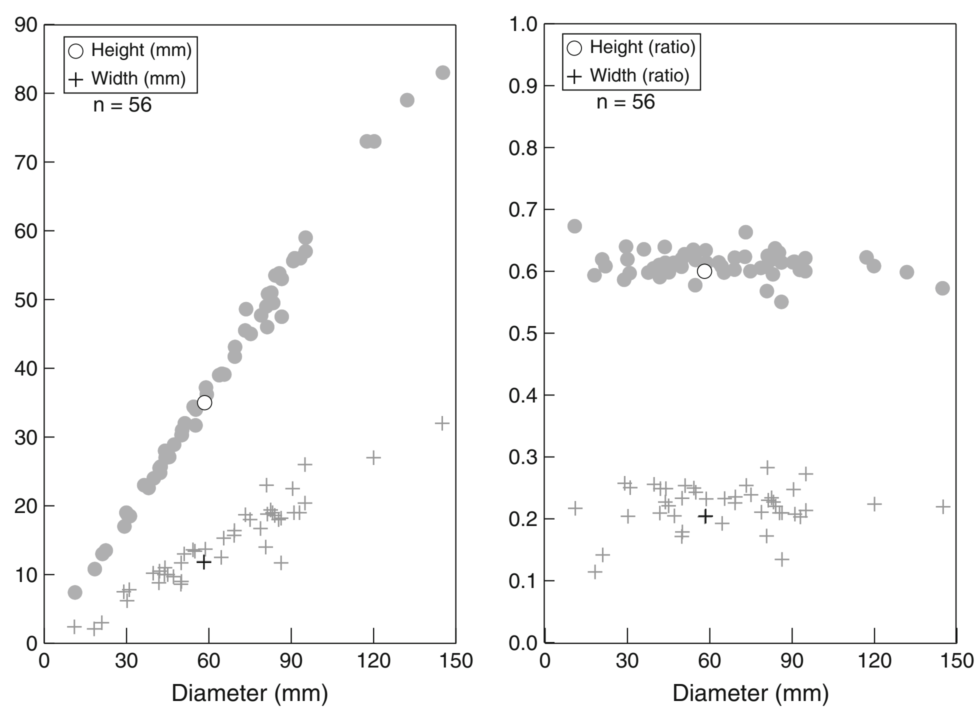

Fig. 78 Scatter diagrams of *H*, *W* and *U*, and *H*/*D*, *W*/*D* and *U*/*D* for *Pseudosageceras multilobatum* (*open symbols* indicate the one measurable specimen from the Pahvant Range, *Owenites* beds; *grey symbols* indicate specimens from Siberia, Guangxi, Nevada, Madagascar, the Caucasus, Pakistan, Tibet and Oman; data from Dagys and Ermakova 1990, Brayard and Bucher 2008, Kummel and Steele 1962, Collignon 1933, Shevyrev 1968, Brühwiler et al. 2010b, 2012a, c; [$n = 55$])

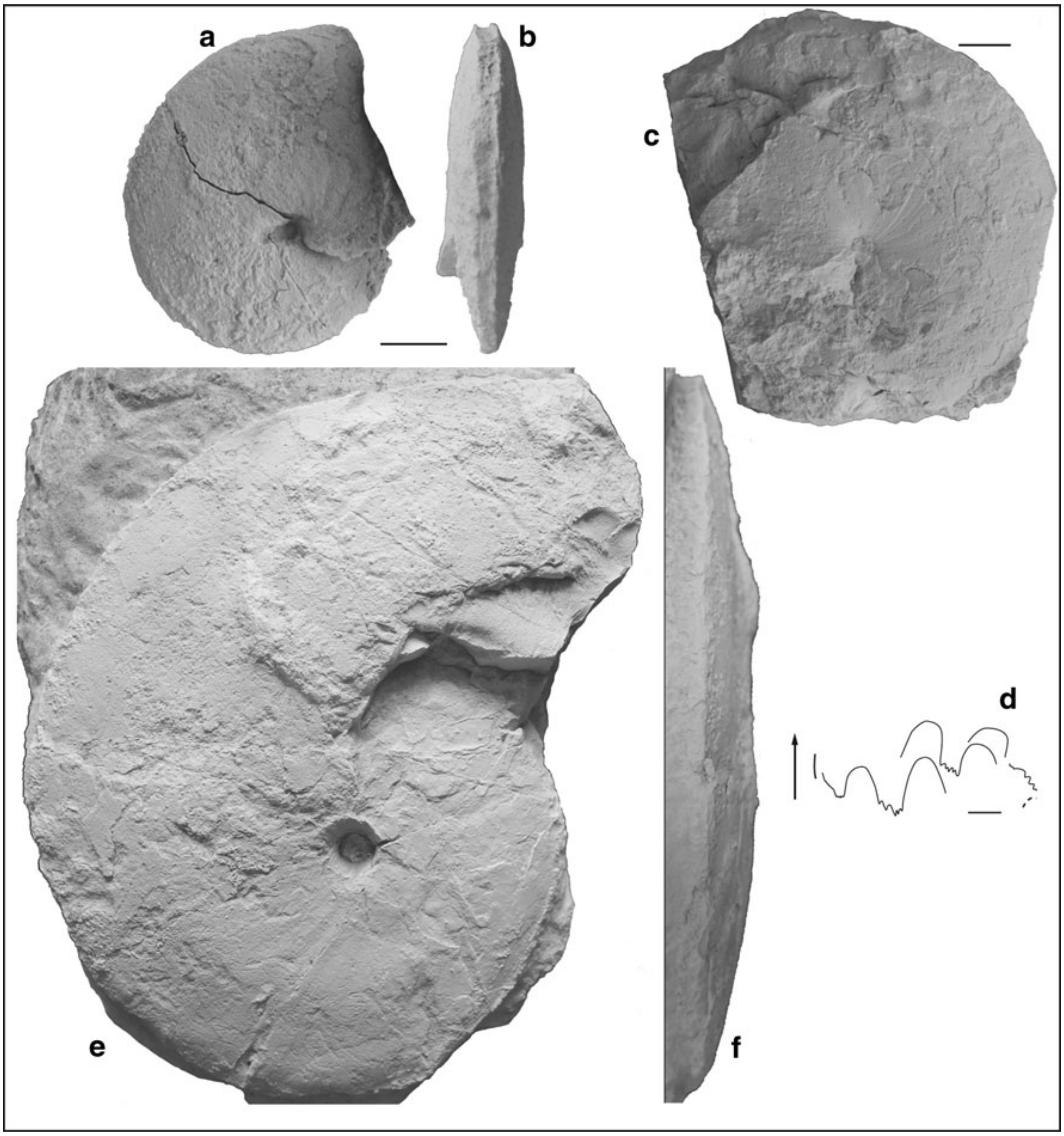

Fig. 79 *Hedenstroemia kossmati* Hyatt and Smith 1905. All from the *Owenites* beds, Smithian; **a**, **b** UBGD 275141, loc. DH1-11, Confusion Range; **c**, **d** UBGD 275142, loc. DV2-7, Pahvant Range; **d** *scale bar* is 5 mm ($H = 35$ mm); **e**, **f** UBGD 275143, loc. DV2-7, Pahvant Range

Occurrence Fairly common in *Owenites* beds and rare in the *Inyoites beaverensis* sp. nov. beds in the Confusion Range [DH1-11, DH1-9, DH1-4/5, "Gastropod shales 2"], the Pahvant Range [$n = 2$; DV1-7] and the Torrey area [$n = 1$; FFA2]. Not documented from the other studied sections.

Description Very involute, compressed shell presenting a sulcate venter at all growth stages. Ventral margins bluntly angular. Flanks convex with maximum thickness at mid-flank. Umbilicus very narrow with broadly rounded shoulders forming a rather deep funnel. Surface apparently smooth, but very small plications and growth lines are visible near the umbilicus of one specimen. Complex ceratitic suture line, typical of hedenstromiids with an adventious element and a well-developed auxiliary series bending towards the umbilicus.

Measurements See Table 1. Estimated maximum size: ~20 cm.

Discussion H. kossmati differs from the type species by its sulcate venter at all growth stages and also by its suture line, which shows a slightly more complex auxiliary series. As already discussed by Hyatt and Smith (1905) and Smith (1932), this species appears to be nearly identical to

H. mojsisovicsi Diener (1897), showing the same overall shape and complex architecture of the suture line. *H. mojsisovicsi* apparently can be distinguished only by its tabulate venter, according to Spath (1934) who assigned it a new generic and species name (*Anahedenstroemia himalayica*). However, Diener (1897) described the holotype of *H. mojsisovicsi* with "a flattened siphonal part, bordered on both sides by distinct marginal edges" (p. 63), thus suggesting persuasively that its venter was probably sulcate as observed for *H. kossmati*. Unfortunately, Diener (1897) did not illustrate the venter of his specimen or any additional material. In summary, *H. kossmati* is very likely conspecific with *H. mojsisovicsi*, and thus a junior synonym. However, the scarcity of data regarding *H. mojsisovicsi* from Spiti prevents a definitive merging of the two species. As Smith (1932) concluded, it is better to keep them separated. Without clearly visible suture lines or an exposed umbilicus, specimens of *H. kossmati* can be easily confused with *Meekoceras gracilitatis*. Another problem is that both taxa can occur within the same bed.

Noetling (1905; pl. 27, fig. 4) illustrated a specimen of *H. mojsisovicsi* from the Salt Range showing a marked egression at large size. Based on this specimen and this peculiar feature, Spath (1934) erected a new species, *H. evoluta*. Brühwiler et al. (2012c) recently illustrated additional specimens of *H. evoluta* from the Salt Range, confirming the strong egressive coiling of this species at large size.

Kummel (in Arkell et al. 1957) erected a new genus name (*Pseudohedenstroemia*) for *H. kossmati* based mainly on the tabulate aspect of its venter, compared to the type species, which shows a more acute to rounded venter at large size. However, since the type species presents a tabulate venter during early ontogenetic stages, and its suture line architecture and ornamentation are similar, we conclude that Kummel's erection of *Pseudohedenstroemia* was not justified.

Hedenstroemiidae gen. indet. A
Fig. 80a, b

Occurrence Rare in the Mineral Mountains, Xenoceltitidae gen. indet. A beds [$n = 2$; MIA11]. Not documented from the other studied sections.

Description Sampled specimens are all very poorly preserved, but coiling appears involute with a narrow, tabulate venter and almost angular ventral shoulders. Flanks probably slightly convex. Umbilicus apparently closed. Ornamentation and suture line not preserved.

Measurements Not possible due to poor preservation. Estimated maximum size: ~5 cm.

Discussion The poor preservation of our specimens precludes a taxonomic assignment. However, they more or less resemble latest Smithian *Pseudosageceras* species such as *P. augustum* from South China, Oman or Crittenden Springs (e.g., Brayard and Bucher 2008; Brühwiler et al. 2012a; Jenks et al. 2010). Another indirect indication of affiliation with the hedenstroemiid group is its stratigraphic position above the *Anasibirites kingianus* beds, which elsewhere corresponds to the *Glyptophiceras sinuatum* beds and its xenoceltitid fauna co-occurring with *P. augustum*.

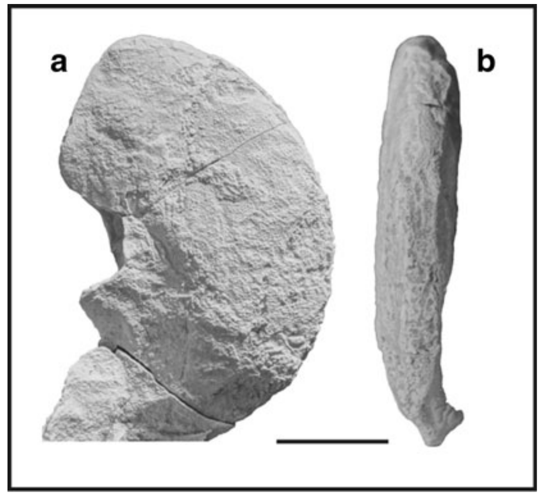

Fig. 80 **a**, **b** *Hedenstroemiidae* gen. indet. A. UBGD 275144, loc. MIA11, Mineral Mountains, Xenoceltitidae gen. indet. A beds, Smithian

Family Aspenitidae Spath, 1934
Genus ***Aspenites*** Hyatt and Smith, 1905
Type species Aspenites acutus Hyatt and Smith, 1905

Aspenites acutus Hyatt and Smith, 1905
Fig. 81a–j

1905 *Aspenites acutus*; Hyatt and Smith, 1905, p. 96, pl. 2, figs. 9-13; pl. 3, figs. 1–5.
? 1909 *Hedenstroemia acuta*; Krafft and Diener, p. 157, pl. 9, fig. 2.
1922 *Aspenites acutus*; Welter, p. 98, fig. 7.
1922 *Aspenites laevis*; Welter, p. 99, pl. 1, figs. 4, 5.
1932 *Aspenites acutus*; Smith, p. 86, pl. 2, figs. 9–13, pl. 3, figs. 1–5, pl. 30, figs. 1–26, pl. 60, figs. 4–6.
1932 *Aspenites laevis*; Smith, p. 86, pl. 28, figs. 28–33.
1932 *Aspenites obtusus*; Smith, p. 86, pl. 31, figs. 8–10.
1934 *Aspenites acutus*; Spath, p. 229, fig. 76.
? 1934 *Parahedenstroemia acuta*; Spath, p. 221, fig. 70.
1957 *Aspenites acutus*; Kummel, p. L142, fig. 173a–c.
1959 *Aspenites acutus*; Chao, p. 269, pl. 35, figs. 12–18, 23, text-fig. 34a.
1959 *Aspenites laevis*; Chao, p. 270, pl. 35, figs. 9–11, text-fig. 34b.

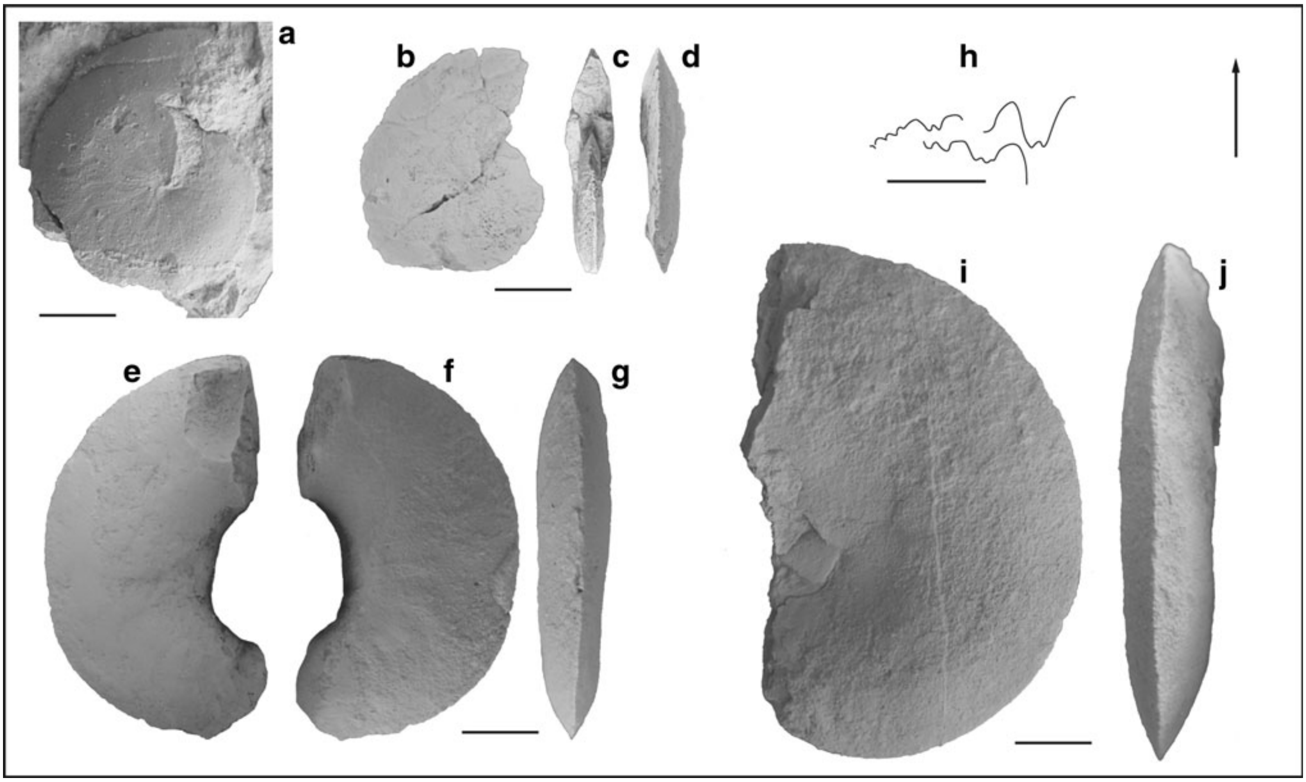

Fig. 81 *Aspenites acutus* Hyatt and Smith 1905. **a** UBGD 275145, loc. DH1-11, Confusion Range, *Owenites* beds, *Inyoites oweni* horizons, Smithian; **b–d** UBGD 275146, loc. DV1-9, Pahvant Range, *Owenites* beds, *Inyoites oweni* horizons, Smithian; **e–g** UBGD 275147, loc. DH1-5, Confusion Range, *Inyoites beaverensis* sp. nov. beds, Smithian; **h–j** UBGD 275148, loc. DH1-5, Confusion Range, *Inyoites beaverensis* sp. nov. beds, Smithian; **h** *scale bar* is 5 mm (estimated $H = 24$ mm)

1962 *Aspenites acutus*; Kummel and Steele, p. 692, pl. 99, figs. 16–17.
1962 *Hemiaspenites obtusus*; Kummel and Steele, p. 666, pl. 99, fig. 18.
1979 *Aspenites* cf. *acutus*; Nichols and Silberling, pl. 1, figs. 10–11.
1979 *Aspenites acutus*; Nichols and Silberling, pl. 1, figs. 12–14.
v 2008 *Aspenites acutus*; Brayard and Bucher, p. 77, pl. 42, figs. 1–9.
2010 *Aspenites acutus*; Stephen et al., fig. 4f.
2010b *Aspenites acutus*; Brühwiler et al., p. 429, fig. 16(12, 13).
2012a *Aspenites acutus*; Brühwiler and Bucher, p. 48, pl. 26, figs. 1, 2.
2012b *Aspenites acutus*; Brühwiler et al., p. 164, figs. 41A–M.

Occurrence Relatively rare in the Confusion Range, Pahvant Range and the Mineral Mountains (one measurable specimen), documented from the *Owenites* beds. Absent from all other studied sections. Commonly found in northeastern Nevada and southeastern Idaho. Intertropical widely distributed species (e.g., South China, Oman, Tibet).

Description Involute, very compressed oxyconic shell with slightly convex flanks and an occluded umbilicus. Maximum curvature at mid-flank. Venter with a characteristic acute keel. Umbilical region slightly depressed. Ventral shoulders may be more pronounced on some specimens. Surface nearly smooth except for fine radial folds and falcoid growth lines. Suture line basically ceratitic, but more complex with a wide curved series of small auxiliary saddles.

Measurements See Fig. 82. Estimated maximum size: ~8 cm.

Discussion Reader should refer to Brayard and Bucher (2008) for an in-depth systematic review and discussion of this species. *A. acutus* mainly differs from other aspenitid taxa (e.g., *Pseudaspenites layeriformis*) by its occluded umbilicus (see also Brayard and Bucher 2008 for a thorough comparison). Only *Parahedenstroemia acuta* (Spath 1934) from Spiti, which Spath erected based on *Hedenstroemia acuta* (Krafft and Diener 1909) as the type species, is morphologically compatible with *A. acutus*.

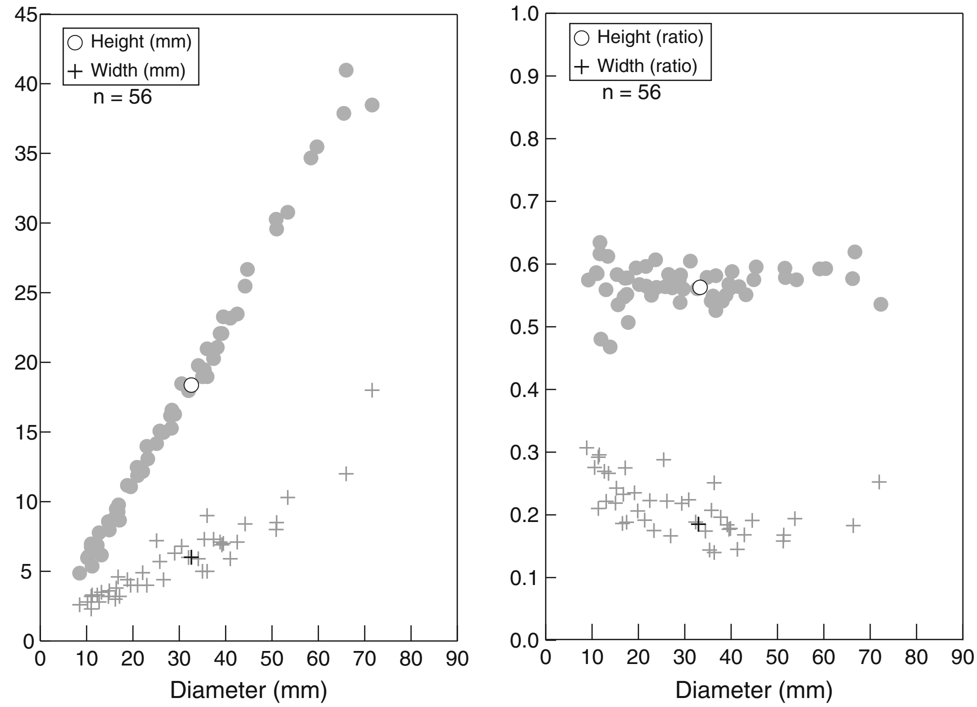

Fig. 82 Scatter diagrams of *H*, *W* and *U*, and *H*/*D*, *W*/*D* and *U*/*D* for *Aspenites acutus* (*open symbols* indicate the one measurable specimen from the Pahvant Range, *Owenites* beds; *grey symbols* indicate specimens from Guangxi, Nevada, Spiti, Tibet and Oman; data respectively from Brayard and Bucher 2008, Kummel and Steele 1962 and Brühwiler et al. 2010b, 2012a, b; [$n = 55$])

However, it appears that the suture line of this taxon is simpler. Additional material is needed to determine whether it should be placed within the *Aspenites* genus.

Family Incertae sedis

Genus **gen. indet. A**

Fig. 83a–t

Occurrence Very abundant in the Confusion Range, "Gastropod shales 2". Not found in other studied sections.

Description Small size specimens with a moderately evolute and compressed shell and a rounded venter. Flanks slightly convex with maximum curvature at two-thirds of the flank from the umbilicus. Umbilicus relatively shallow with an apparent perpendicular wall and rounded shoulders. Surface ornamented with variable strength, sinuous folds crossing the venter. On some specimens, a delicate strigation is also visible near the venter. Suture line ceratitic.

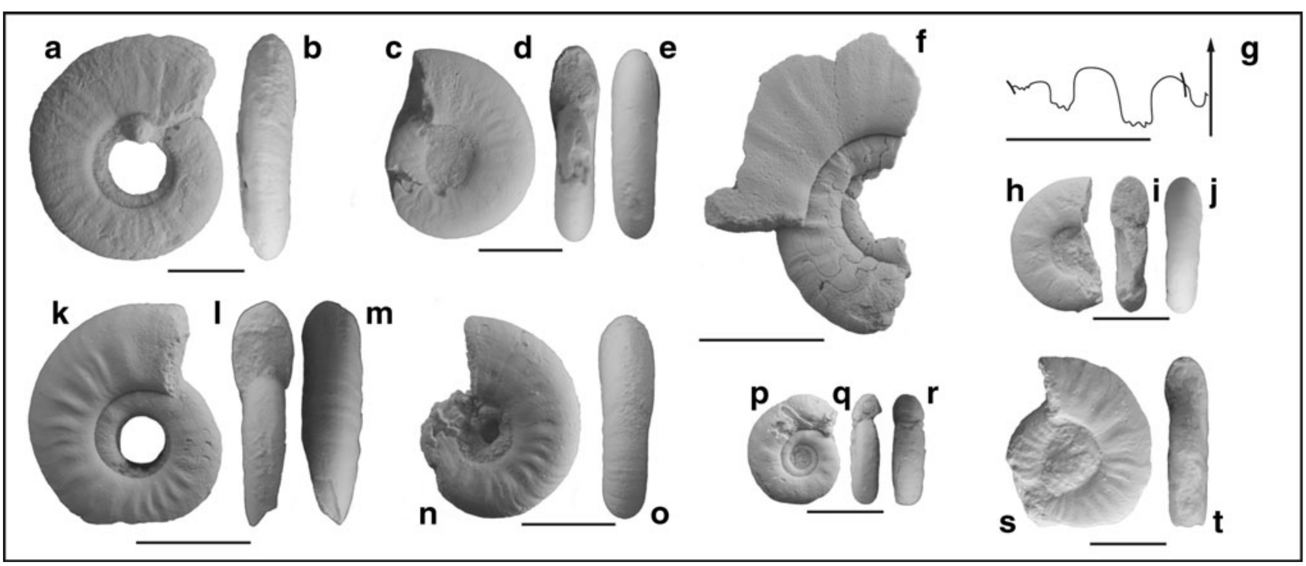

Fig. 83 Gen. indet. A. All from the loc. "Gastropod shales 2", Confusion Range, Smithian; **a**, **b** UBGD 275149; **c–e** UBGD 275150; **f**, **g** UBGD 275151; **g** *scale bar* is 5 mm ($H = 6$ mm); **h–j** UBGD 275152; **k–m** UBGD 275153; **n**, **o** UBGD 275154; **p–r** UBGD 275155; **s**, **t** UBGD 275156

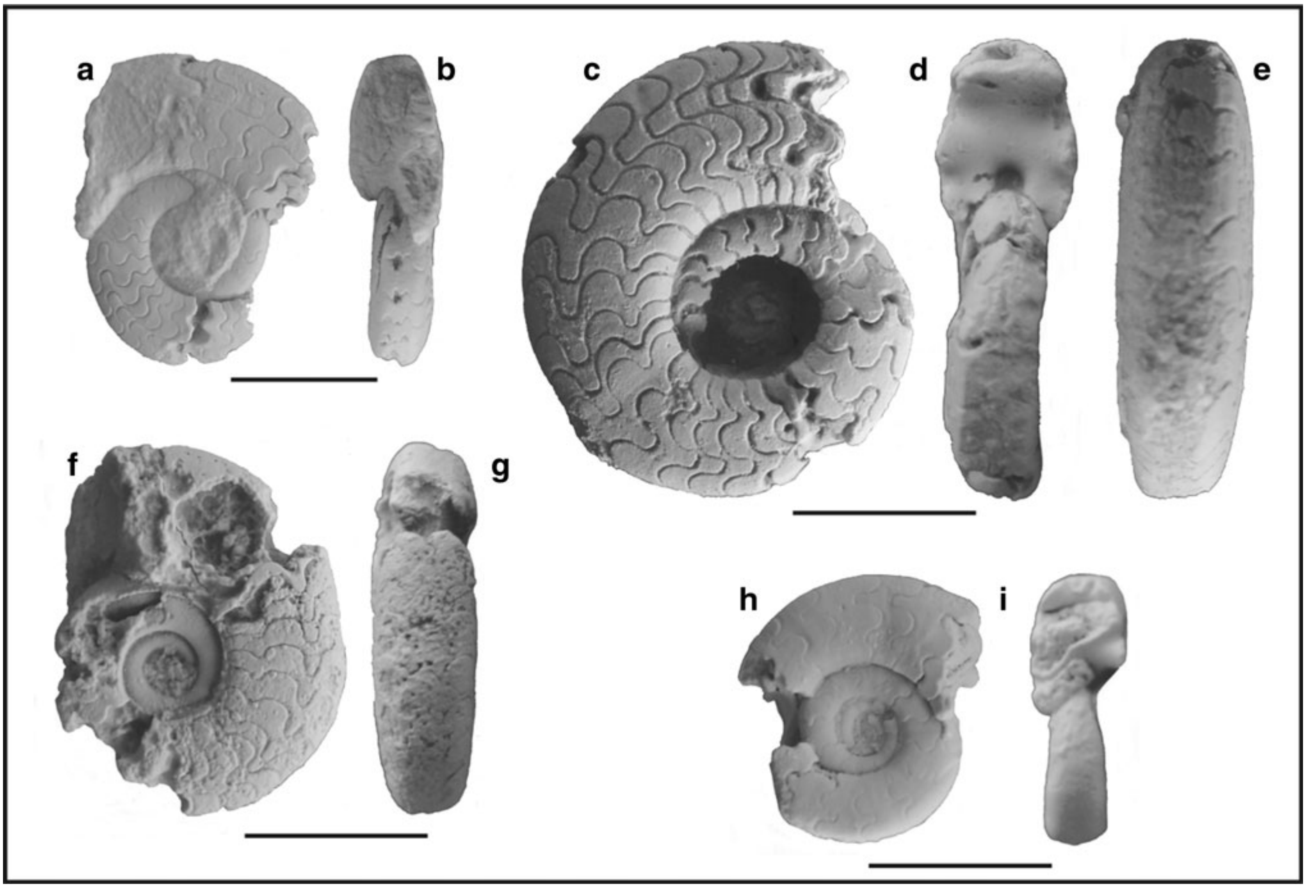

Fig. 84 Gen. indet. B. All from the loc. "Gastropod shales 2", Confusion Range, Smithian; **a**, **b** UBGD 275157; **c**–**e** UBGD 275158; **f**, **g** UBGD 275159; **h**, **i** UBGD 275160

Measurements See Table 1. Estimated maximum size: ~4 cm.

Genus **gen. indet. B**
Fig. 84a–i

Occurrence Common in the Confusion Range, "Gastropod shales 2". Not found in other studied sections.
Description Overall shell shape similar to Gen. indet. A, but with a tabulate venter. Flanks are also more convex with maximum curvature at one-third of the flank from the umbilicus. Umbilicus relatively shallow with well-rounded shoulders. Surface ornamented with very rare folds, which apparently do not cross the venter. Suture line ceratitic.

Measurements See Table 1. Estimated maximum size: ~3.5 cm.

Genus **gen. indet. C**
Fig. 85a, b

Occurrence One specimen found in the Confusion Range, *Owenites* beds, top of the *Inyoites oweni* horizons [DH1-12]. Not found in other studied sections.

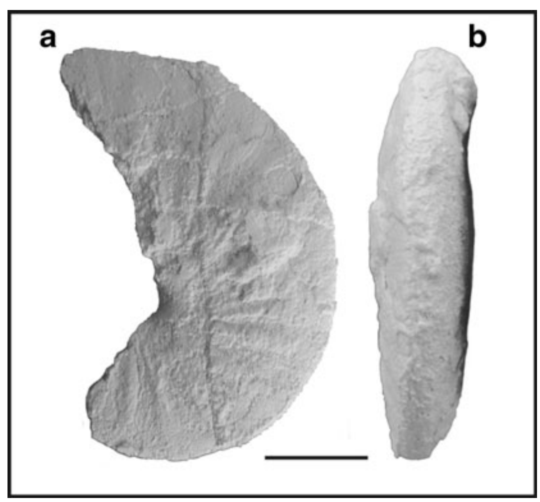

Fig. 85 **a**, **b** Gen. indet. C. UBGD 275161, loc. DH1-12, Confusion Range, *Owenites* beds, *Inyoites oweni* horizons, Smithian

Description Involute and compressed shell with a tabulate venter. Ventral shoulders angular. Flanks convex with maximum curvature near mid-flank. Umbilicus very

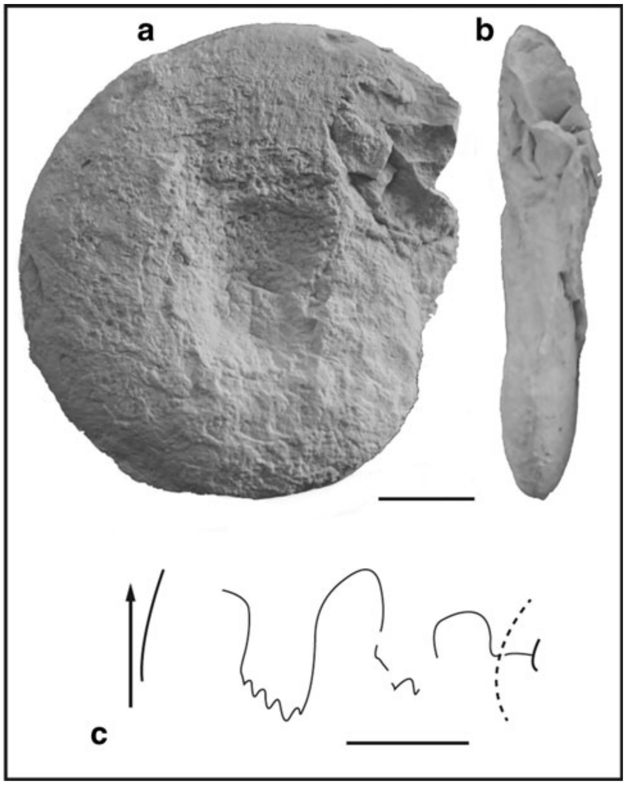

Fig. 86 **a–c** Gen. indet. *D*. UBGD 275162, loc. DV2-200, Pahvant Range, *Meekoceras olivieri* sp. nov. beds, Smithian; **c** *scale bar* is 5 mm ($H = 15.1$ mm)

narrow with broad rounded shoulders. Surface ornamented with radial ribs fading near the ventral shoulders. Suture line fragmentary, but ceratitic.

Measurements See Table 1.

Genus **gen. indet. D**
Fig. 86a–c

Occurrence One specimen found in the Pahvant Range, *Meekoceras olivieri* sp. nov. beds. Not found in other studied sections.

Description Moderately involute and compressed shell. Venter narrowly rounded. Flanks convex with maximum curvature at one-third of the flank from the umbilicus. Umbilicus relatively shallow with a prominently oblique wall and well-rounded shoulders. Surface apparently smooth. Suture line partly known with deep, well-indented lobes and elongated, pinched saddles.

Measurements See Table 1.

Discussion The suture line as well as the overall compressed shape of this specimen is similar to some flemingitids. However, the prominently inclined umbilical wall is not characteristic of flemingitids and may indicate that it belongs to another family.

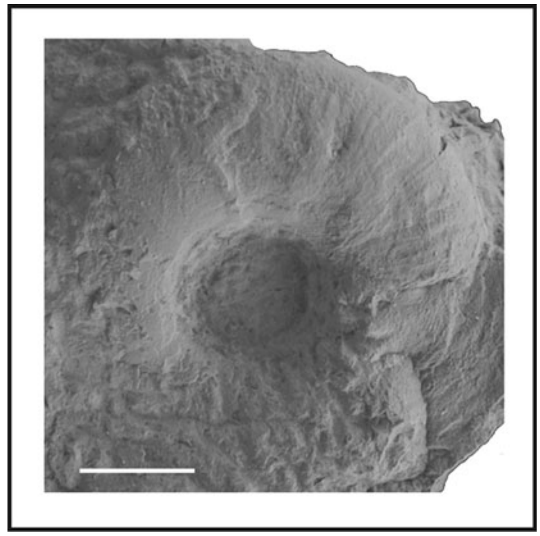

Fig. 87 Gen. indet. E. UBGD 275163, loc. DV2-5, Pahvant Range, *Flemingites* sp. indet. beds, Smithian

Genus **gen. indet. E**
Fig. 87

Occurrence One specimen found in the Pahvant Range, *Flemingites* sp. indet. bed. Not found in other studied sections.

Description Moderately involute and compressed shell with an apparent narrowly arched venter. Flanks slightly convex with maximum curvature at one-third of the flank from the umbilicus. Umbilicus appears rather deep with an inclined wall and large rounded shoulders. Surface ornamented with variable strength, radial ribs, folds and growth lines. Large ribs fade near mid-flank toward venter. Growth lines reach the venter. Suture line unknown.

Measurements Not possible.

Acknowledgments This work is a contribution to the team BioME of the UMR CNRS 6282 and to the teams "Paleoenvironments" and "Biodiversity" of the UMR CNRS 5276; it was funded by the Région Bourgogne, the FRB, and the CNRS INSU Interrvie. All fossil localities mentioned in this report are located on US public land under the stewardship of the Bureau of Land Management (BLM) of the US Department of the Interior and the US Forest Service (Fishlake National Forest) of the US Department of Agriculture; their management and access to these lands is much appreciated. C. Monnet (Lille) and an anonymous reviewer provided constructive suggestions that helped us to improve the manuscript. D. Snyder is thanked for help in the field. N. Goudemand and R. Hofmann (Zurich) kindly determined conodonts and bivalves, respectively. We also acknowledge numerous stimulating discussions with Hugo Bucher (Zurich) regarding Smithian ammonoids and biostratigraphy over the past years.

References

Arkell, W. J., Kummel, B., & Wright, C. W. (1957). Mesozoic Ammonoidea. In R. C. Moore (Ed.), *Treatise on invertebrate* *paleontology. Part L: Mollusca 4. Cephalopoda—Ammonoidea* (pp. L80–L465). Lawrence: University of Kansas Press & Geological Society of America.

Bacon, C. S. J. (1948). Geology of the confusion range, West-Central Utah. *Bulletin of the Geological Society of America, 59*, 1027–1052.

Baetcke, G. B. (1969). *Stratigraphy of the Star Range and reconnaissance of three selected mines. Triassic System*. Thesis, University of Utah.

Blakey, R. C. (1973). Stratigraphy and origin of the Moenkopi Formation (Triassic) of Southeastern Utah. *The Mountain Geologist, 10*, 1–17.

Blakey, R. C. (1974). Stratigraphic and depositional analysis of the Moenkopi Formation, Southeastern Utah. *Utah Geological and Mineral Survey Bulletin, 104*, 1–81.

Blakey, R. C. (1977). Petroliferous lithosomes in the Moenkopi Formation, Southern Utah. *Utah Geology, 4*, 67–84.

Blakey, R. C. (1979). Oil impregnated carbonate rocks of the Timpoweap Member, Moenkopi Formation, Hurricane Cliffs area, Utah and Arizona. *Utah Geology, 6*, 45–54.

Brayard, A., & Bucher, H. (2008). Smithian (Early Triassic) ammonoid faunas from northwestern Guangxi (South China): Taxonomy and biochronology. *Fossils and Strata, 55*, 1–179.

Brayard, A., Bucher, H., Escarguel, G., Fluteau, F., Bourquin, S., & Galfetti, T. (2006). The Early Triassic ammonoid recovery: Paleoclimatic significance of diversity gradients. *Palaeogeography, Palaeoclimatology, Palaeoecology, 239*, 374–395.

Brayard, A., Bucher, H., Brühwiler, T., Galfetti, T., Goudemand, N., Guodun, K., et al. (2007a). *Proharpoceras* Chao: A new ammonoid lineage surviving the end-Permian mass extinction. *Lethaia, 40*, 175–181.

Brayard, A., Escarguel, G., & Bucher, H. (2007b). The biogeography of Early Triassic ammonoid faunas: Clusters, gradients and networks. *Geobios, 40*, 749–765.

Brayard, A., Brühwiler, T., Bucher, H., & Jenks, J. (2009a). *Guodunites*, a low-palaeolatitude and trans-Panthalassic Smithian (Early Triassic) ammonoid genus. *Palaeontology, 52*, 471–481.

Brayard, A., Escarguel, G., Bucher, H., & Brühwiler, T. (2009b). Smithian and Spathian (Early Triassic) ammonoid assemblages from terranes: Paleoceanographic and paleogeographic implications. *Journal of Asian Earth Sciences, 36*, 420–433.

Brayard, A., Escarguel, G., Bucher, H., Monnet, C., Bruhwiler, T., Goudemand, N., et al. (2009c). Good genes and good luck: Ammonoid diversity and the end-Permian mass extinction. *Science, 325*, 1118–1121.

Brayard, A., Nützel, A., Stephen, D. A., Bylund, K. G., Jenks, J., & Bucher, H. (2010). Gastropod evidence against the Early Triassic Lilliput effect. *Geology, 38*, 147–150.

Brayard, A., Nützel, A., Kaim, A., Escarguel, G., Hautmann, M., Stephen, D. A., et al. (2011a). Gastropod evidence against the Early Triassic Lilliput effect: Reply. *Geology, 39*, e233.

Brayard, A., Vennin, E., Olivier, N., Bylund, K. G., Jenks, J., Stephen, D. A., et al. (2011b). Transient metazoan reefs in the aftermath of the end-Permian mass extinction. *Nature Geoscience, 4*, 693–697.

Brühwiler, T., Bucher, H., Brayard, A., & Goudemand, N. (2010a). High-resolution biochronology and diversity dynamics of the Early Triassic ammonoid recovery: The Smithian faunas of the Northern Indian Margin. *Palaeogeography, Palaeoclimatology, Palaeoecology, 297*, 491–501.

Brühwiler, T., Bucher, H., & Goudemand, N. (2010b). Smithian (Early Triassic) ammonoids from Tulong, South Tibet. *Geobios, 43*, 403–431.

Brühwiler, T., Ware, D., Bucher, H., Krystyn, L., & Goudemand, N. (2010c). New Early Triassic ammonoid faunas from the Dienerian/Smithian boundary beds at the Induan/Olenekian GSSP candidate at Mud (Spiti, Northern India). *Journal of Asian Earth Sciences, 39*, 724–739.

Brühwiler, T., Bucher, H., Roohi, G., Yaseen, A., & Rehman, K. (2011). A new Early Smithian ammonoid fauna from the Salt Range (Pakistan). *Swiss Journal of Palaeontology, 130*, 187–201.

Brühwiler, T., Bucher, H., Goudemand, N., & Galfetti, T. (2012a). Smithian (Early Triassic) ammonoid faunas from Exotic Blocks from Oman: Taxonomy and biochronology. *Palaeontographica Abteilung A, 296*, 3–107.

Brühwiler, T., Bucher, H., & Krystyn, L. (2012b). Middle and Late Smithian (Early Triassic) ammonoids from Spiti (India). *Special Papers in Palaeontology, 88*, 115–174.

Brühwiler, T., Bucher, H., Ware, D., Hermann, E., Hochuli, P. A., Roohi, G., et al. (2012c). Smithian (Early Triassic) ammonoids from the Salt Range. *Special Papers in Palaeontology, 88*, 1–114.

Carr, T. R., & Paull, R. K. (1983). Early Triassic stratigraphy and paleogeography of the Cordilleran miogeocline. In A. Reynolds & E. D. Dolly (Eds.), *Mesozoic paleogeography of the West-Central United States* (pp. 39–55). Denver: Society of Economic Paleontologists and Mineralogists, Pacific Section.

Chao, K. (1959). *Lower Triassic ammonoids from Western Kwangsi*. China: Peking Science Press.

Collignon, M. (1933). Paléontologie de Madagascar XX—Les céphalopodes du Trias inférieur. *Annales de Paléontologie, 12–13*, 151–162 & 1–43.

Collignon, M. (1973). Ammonites du Trias inférieur et moyen d'Afghanistan. *Annales de Paléontologie, 59*, 127–163.

Collinson, J. W., & Hasenmueller, W. A. (1978). Early Triassic paleogeography and biostratigraphy of the Cordilleran miogeosyncline. In A. Reynolds & E. D. Dolly (Eds.), *Mesozoic paleogeography of the West-Central United States* (pp. 175–186). Denver: Society of Economic Paleontologists and Mineralogists, Pacific Section.

Collinson, J. W., Kendall, C. G. S. C., & Marcantel, J. B. (1976). Permian–Triassic boundary in eastern Nevada and west-central Utah. *Bulletin of the Geological Society of America, 87*, 821–824.

Crosby, G. W. (1959). Geology of the South Pavant Range, Millard and Sevier Counties, Utah. *Brigham Young University Research Series, 6*, 1–59.

Dagys, A. S., & Ermakova, S. P. (1990). *Early Olenekian ammonoids of Siberia*. Moskow: Nauka.

Dagys, A. S., & Weitschat, W. (1993). Intraspecific variation in Boreal Triassic ammonoids. *Géobios, 26*, 107–109.

Davis, R. L. (1983). Geology of the Dog Valley-Red Ridge Area, Southern Pavant Mountains, Millard County, Utah. *Brigham Young University Geology Studies, 30*, 19–36.

Dean, J. S. (1981). Carbonate petrology and depositional environments of the Sinbad Limestone Member of the Moenkopi Formation in the Teasdale Dome Area, Wayne and Garfield Counties, Utah. *Brigham Young University Geology Studies, 28*, 19–51.

Dickinson, W. R. (2006). Geotectonic evolution of the Great Basin. *Geosphere, 2*, 353–368.

Diener, C. (1897). Part I: The Cephalopoda of the lower Trias. *Palaeontologia Indica. Ser. XV, Himalayan fossils, 2*, 1–181.

Ermakova, S. P. (2002). *Zonal standard of the Boreal Lower Triassic*. Moscow: Nauka.

Fraiser, M. L., & Bottjer, D. J. (2004). The non-actualistic Early Triassic gastropod fauna: A case study of the Lower Triassic Sinbad Limestone Member. *Palaios, 19*, 259–275.

Frebold, H. (1930). Die altersstellung des fischhorizontes, des grippianiveaus und des unteren saurierhorizontes in Spitzbergen. *Skrifter om Svalbard og Ishavet, 28*, 1–36.

Galfetti, T., Bucher, H., Brayard, A., Hochuli, P. A., Weissert, H., Guodun, K., et al. (2007a). Late Early Triassic climate change: Insights from carbonate carbon isotopes, sedimentary evolution and ammonoid paleobiogeography. *Palaeogeography, Palaeoclimatology, Palaeoecology, 243*, 394–411.

Galfetti, T., Bucher, H., Ovtcharova, M., Schaltegger, U., Brayard, A., Bruhwiler, T., et al. (2007b). Timing of the Early Triassic carbon cycle perturbations inferred from new U-Pb ages and ammonoid biochronozones. *Earth and Planetary Science Letters, 258*, 593–604.

Galfetti, T., Hochuli, P. A., Brayard, A., Bucher, H., Weissert, H., & Vigran, J. O. (2007c). The Smithian/Spathian boundary event: Evidence for global climatic change in the wake of the end-Permian biotic crisis. *Geology, 35*, 291–294.

Gardner, G. E., & Mapes, R. H. (2000). The relationships of color patterns and habitat for Lower Triassic ammonoids from Crittenden Springs, Elko county, Nevada. *Revue de Paléobiologie, 8*, 109–122.

Gilluly, J., & Reeside, J. B. J. (1928). Sedimentary rocks of the San Rafael Swell and some adjacent areas in eastern Utah. *USGS Professional Paper*, *150-D*, 61–110.

Goodspeed, T. H., & Lucas, S. G. (2007). Stratigraphy, sedimentology, and sequence stratigraphy of the Lower Triassic Sinbad Formation, San Rafael Swell, Utah. *New Mexico Museum of Natural History and Science Bulletin, 40*, 91–101.

Guex, J., Hungerbühler, A., Jenks, J., O'Dogherty, L., Atudorei, V., Taylor, D. G., et al. (2010). Spathian (Lower Triassic) ammonoids from western USA (Idaho, California, Utah and Nevada). *Mémoires de Géologie de Lausanne, 49*, 1–81.

Hautmann, M., & Nützel, A. (2005). First record of a heterodont bivalve (Mollusca) from the Early Triassic: Palaeocological significance and implications for the "Lazarus problem". *Palaeontology, 48*, 1131–1138.

Hermann, E., Hochuli, P. A., Bucher, H., Brühwiler, T., Hautmann, M., Ware, D., et al. (2011). Terrestrial ecosystems on North Gondwana following the end-Permian mass extinction. *Gondwana Research, 20*, 630–637.

Hintze, L. F., & Davis, F. D. (2003). Geology of Millard County, Utah. *Utah Geological Survey Bulletin, 133*, 117–121.

Hofmann, R., Hautmann, M., Wasmer, M., & Bucher, H. (2013). Palaeoecology of the Spathian Virgin Formation (Utah, USA) and its implications for the Early Triassic recovery. *Acta Palaeontologica Polonica, 58*, 149–173.

Hose, R. K., & Repenning, C. A. (1959). Stratigraphy of Pennsylvanian, Permian, and Lower Triassic rocks of Confusion Range, west-central Utah. *Bulletin of the American Association of Petroleum Geologists, 43*, 2167–2196.

Hyatt, A., & Smith, J. P. (1905). The Triassic cephalopod genera of America. *USGS Professional Paper, 40*, 1–394.

Jenks, J. (2007). Smithian (Early Triassic) ammonoid biostratigraphy at Crittenden Springs, Elko County, Nevada and a new ammonoid from the *Meekoceras gracilitatis* Zone. *New Mexico Museum of Natural History and Science Bulletin, 40*, 81–90.

Jenks, J., Brayard, A., Brühwiler, T., & Bucher, H. (2010). New Smithian (Early Triassic) ammonoids from Crittenden Springs, Elko County, Nevada: Implications for taxonomy, biostratigraphy and biogeography. *New Mexico Museum of Natural History and Science Bulletin, 48*, 1–41.

Jenks, J., Guex, J., Hungerbühler, A., Taylor, D. G., & Bucher, H. (2013). Ammonoid biostratigraphy of the Early Spathian *Columbites parisianus* Zone (Early Triassic) at Bear Lake Hot Springs, Idaho. *New Mexico Museum of Natural History and Science Bulletin, 61*, 268–283.

Kaim, A., Nützel, A., Bucher, H., Brühwiler, T., & Goudemand, N. (2010). Early Triassic (Late Griesbachian) gastropods from South China (Shanggan, Guangxi). *Swiss Journal of Geosciences, 103*, 121–128.

Kennedy, W. J., & Cobban, W. A. (1976). Aspects of ammonite biology, biogeography, and biostratigraphy. *Special Papers in Palaeontology, 17*, 1–94.

Klug, C., Brühwiler, T., Korn, D., Schweigert, G., Brayard, A., & Tilsley, J. (2007). Ammonoid shell structures of primary organic composition. *Palaeontology, 50*, 1463–1478.

Korchinskaya, M. V. (1982). *Explanatory note on the biostratigraphic scheme of the Mesozoic (Trias) of Spitsbergen* (pp. 40–99). PGO Sevmorgeologia: USSR Ministry of Geology.

Krafft, Av, & Diener, C. (1909). Lower Triassic Cephalopoda from Spiti, Malla Johar, and Byans. *Palaeontologia Indica, 6*, 1–186.

Kuenzi, W. D. (1965). Early Triassic (Scythian) ammonoids from Northeastern Washington. *Journal of Paleontology, 39*, 365–378.

Kummel, B., & Erben, H. K. (1968). Lower and Middle Triassic cephalopods from Afghanistan. *Palaeontographica, 129*, 95–148.

Kummel, B., & Sakagami, S. (1960). Mid-Scythian ammonites from Iwai formation, Japan. *Breviora, Museum of Comparative Zoology, 126*, 1–13.

Kummel, B., & Steele, G. (1962). Ammonites from the *Meekoceras gracilitatus* zone at Crittenden Spring, Elko County, Nevada. *Journal of Paleontology, 36*, 638–703.

Lindström, G. (1865). Om Trias och Juraforsteningar fran Spetsbergen. *Svenska Vetenskap-Akadamien Handlingar*, *6*, 1–20.

Lucas, S. G., Goodspeed, T. H., & Estep, J. W. (2007a). Ammonoid biostratigraphy of the Lower Triassic Sinbad Formation, East-Central Utah. *New Mexico Museum of Natural History and Science Bulletin, 40*, 103–108.

Lucas, S. G., Krainer, K., & Milner, A. R. (2007b). The type section and age of the Timpoweap Member and stratigraphic nomenclature of the Triassic Moenkopi Group in Southwestern Utah. *New Mexico Museum of Natural History and Science Bulletin, 40*, 109–117.

Markevich, P. V., & Zakharov, Y. D. (2004). *Triassic and Jurassic of the Sikhote-Alin—Book 1: Terrigenous assemblage*. Dalnauka: Vladivostok.

Mathews, A. A. L. (1929). The Lower Triassic cephalopod fauna of the Fort Douglas area, Utah. *Walker Museum Memoirs, 1*, 1–46.

McRoberts, C. A. (2010). Biochronology of Triassic bivalves. In S. G. Lucas (Ed.), The Triassic timescale (pp. 201–219). London: *The Geological Society of London*, *Special Publication*, *334*.

Monnet, C., & Bucher, H. (2005). New Middle and Late Anisian (Middle Triassic) ammonoid faunas from northwestern Nevada (USA): Taxonomy and biochronology. *Fossils and Strata, 52*, 1–121.

Monnet, C., Bucher, H., Wasmer, M., & Guex, J. (2010). Revision of the genus *Acrochordiceras* Hyatt, 1877 (Ammonoidea, Middle Triassic): Morphology, biometry, biostratigraphy and intraspecific variability. *Palaeontology, 53*, 961–996.

Newell, N. D. (1948). Key Permian section, Confusion Range, Western Utah. *Bulletin of the Geological Society of America, 59*, 1053–1058.

Nichols, K. M., & Silberling, N. J. (1979). Early Triassic (Smithian) ammonites of Paleoequatorial affinity from the Chulitna terrane, South-central Alaska. *Geological Survey Professional Paper*, *1121-B*, B1–B5.

Nielson, R. L. (1991). Petrology, sedimentology and stratigraphic implications of the Rock Canyon conglomerate, southwestern Utah. *Utah Geological Survey, Miscellaneous Publication, 91*, 1–65.

Noetling, F. (1905). Die asiatische Trias. In F. Frech (Ed.), *Lethaea geognostica* (Vol. 1, pp. 107–221). Stuttgart: Verlag der E. Schweizerbart'schen Verlagsbuchhandlung (E. Nägele).

Nützel, A. (2005). A new Early Triassic gastropod genus and the recovery of gastropods from the Permian/Triassic extinction. *Acta Palaeontologica Polonica, 50*, 19–24.

Okuneva, T. M. (1990). Triassic biostratigraphy of southern regions of the East USSR without the Primorye territory. In Y. D. Zakharov, G. V. Belyaeva & A. P. Nikitina (Eds.), *New data on Palaeozoic and Mesozoic biostratigraphy of the south Far East* (pp. 125–136). Vladivostok: Far Eastern Branch of the USSR Academy of Sciences.

Orchard, M. J. (2007). Conodont diversity and evolution through the latest Permian and Early Triassic upheavals. *Palaeogeography, Palaeoclimatology, Palaeoecology, 252*, 93–117.

Paull, R. A., & Paull, R. K. (1993). Interpretation of Early Triassic nonmarine–marine relations, Utah, U.S.A. *New Mexico Museum of Natural History and Science Bulletin, 3*, 403–409.

Romano, C., Goudemand, N., Vennemann, T. W., Ware, D., Schneebeli-Hermann, E., Hochuli, P. A., et al. (2013). Climatic and biotic upheavals following the end-Permian mass extinction. *Nature Geoscience, 6*, 57–60.

Runnegar, B. (1969). A Lower Triassic ammonoid fauna from southeast Queensland. *Journal of Paleontology, 43*, 818–828.

Shevyrev, A. A. (1968). *Triassic Ammonoidea from the southern part of the USSR*. Moscow: Nauka.

Shevyrev, A. A. (1995). Triassic ammonites of northwestern Caucasus. *Trudy Paleontologiceskogo Instituta (Akademija Nauk SSR), 264*, 1–174.

Shigeta, Y., & Zakharov, Y. D. (2009). Systematic palaeontology—cephalopods. In Y. Shigeta, Y. D. Zakharov, H. Maeda, & A. M. Popov (Eds.), *The Lower Triassic system in the Abrek Bay area, South Primorye, Russia* (pp. 44–140). Tokyo: National Museum of Nature and Science.

Silberling, N. J., & Tozer, E. T. (1968). Biostratigraphic classification of the marine Triassic in North America. *Geological Society of America Special Paper, 110*, 1–63.

Smith, J. P. (1927). Upper Triassic marine invertebrate faunas of North America. *USGS Professional Paper*, *141*, 1–262.

Smith, J. P. (1932). Lower Triassic ammonoids of North America. *USGS Professional Paper, 167*, 1–199.

Smith, J. F. J., Huff, L. C., Hinrichs, E. N., & Luedke, R. G. (1963). Geology of the Capitol Reef area, Wayne and Garfield counties, Utah. *USGS Professional Paper, 363*, 1–102.

Spath, L. F. (1934). *Part 4: The Ammonoidea of the Trias, Catalogue of the fossil cephalopoda in the British Museum (Natural History)*. London: The Trustees of the British Museum.

Stephen, D. A., Bylund, K. G., Bybee, P. J., & Ream, W. J. (2010). Ammonoid beds in the Lower Triassic Thaynes Formation of western Utah, USA. In K. Tanabe, Y. Shigeta, T. Sasaki, & H. Hirano (Eds.), *Cephalopods—present and past* (pp. 243–252). Tokyo: Tokai University Press.

Stewart, J. H., Poole, F. G., & Wilson, R. F. (1972). Stratigraphy and origin of the Triassic Moenkopi formation and related strata in the Colorado Plateau region. *Geological Survey Professional Paper, 691*, 1–195.

Tozer, E. T. (1961). The sequence of marine Triassic faunas in Western Canada. *Geologic Survey of Canada*, *61–6*, 1–20.

Tozer, E. T. (1981). Triassic Ammonoidea: Classification, evolution and relationship with Permian and Jurassic forms. In M. R. House & J. R. Senior (Eds.), *The Ammonoidea* (pp. 65–100). London: The systematics association.

Tozer, E. T. (1994). Canadian Triassic ammonoid faunas. *Geologic Survey of Canada Bulletin, 467*, 1–663.

Vu Khuc. (1984). *Triassic ammonoids in Vietnam*. Geoinform and Geodata Institute: Hanoi.

Waagen, W. (1895). Salt Range fossils. Vol 2: Fossils from the Ceratite Formation. *Palaeontologia Indica*, *13*, 1–323.

Ware, D., Jenks, J., Hautmann, M., & Bucher, H. (2011). Dienerian (Early Triassic) ammonoids from the Candelaria Hills (Nevada, USA) and their significance for palaeobiogeography and palaeoceanography. *Swiss Journal of Geosciences, 104*, 161–181.

Weitschat, W. (2008). Intraspecific variation of *Svalbardiceras spitzbergensis* (Frebold) from the Early Triassic (Spathian) of Spitzbergen. *Polar Research, 27*, 292–297.

Weitschat, W., & Lehmann, U. (1978). Biostratigraphy of the uppermost part of the Smithian stage (Lower Triassic) at the Botneheia, W-Spitsbergen. *Mitteilungen aus dem Geologischen, Paläontologisches Institut, Universität Hamburg, 48*, 85–100.

Welter, O. A. (1922). *Die ammoniten der Unteren Trias von Timor*. Stuttgart: E. Schweizerbart'sche Verlagsbuchhandlung (Erwin Nägele).

Westermann, G. E. G. (1966). Covariation and taxonomy of the Jurassic ammonite *Sonninia adicra* (Waagen). *Neues Jahrbuch für Geologie und Paläontologie Abhandlungen, 124*, 289–312.

White, C. A. (1879). Fossils of the Jura-Trias of southeastern Idaho. *Bulletin of the United States Geological and Geographical Survey of the Territories, 5*, 105–117.

Zakharov, Y. D. (1968). *Biostratiraphiya i am onoidei nizhnego triasa Yuzhnogo Primorya (Lower Triassic biostratigraphy and ammonoids of South Primorye)*. Moskva: Nauka.